UNIVERSITA' VITA-SALUTE SAN RAFFAELE

CORSO DI DOTTORATO DI RICERCA INTERNAZIONALE IN MEDICINA MOLECOLARE

CURRICULUM IN CELLULAR AND MOLECULAR BIOLOGY

CHARACTERIZING THE DYNAMIC CROSSTALK BETWEEN p53 AND NF-κB AND ITS CONSEQUENCES ON THE CANCER CELL RESPONSE TO GENOTOXIC STIMULI

DoS: Prof. Davide Mazza

Second Supervisor: Prof. Jana Wolf

Tesi di DOTTORATO di RICERCA di Emanuele Colombo

matr. 017128

Ciclo di dottorato XXVI

SSD BIO/11

Anno Accademico 2022/2023

CONSULTAZIONE TESI DI DOTTORATO DI RICERCA

Il/la sottoscritto/*I*	Emanuele Colombo
Matricola / *registration number*	017128
nato a/ *born at*	Busto Arsizio (VA)
il/*on*	03/02/1994

autore della tesi di Dottorato di ricerca dal titolo / *author of the PhD Thesis titled*

Characterizing the dynamic crosstalk between p53 and NF-κB and its consequences on the cancer cell response to genotoxic stimuli

☒ AUTORIZZA la Consultazione della tesi / AUTHORIZES *the public release of the thesis*

□ NON AUTORIZZA la Consultazione della tesi per …… mesi /DOES NOT AUTHORIZE *the publicrelease of the thesis for …… months*

a partire dalla data di conseguimento del titolo e precisamente */ from the PhD thesis date, specifically*

Dal / *from* ……/……/…… Al / *to* ……/……/……

Poiché /*because*:

□ l'intera ricerca o parti di essa sono potenzialmente soggette a brevettabilità/ *The whole project or part of it might be subject to patentability;*

□ ci sono parti di tesi che sono già state sottoposte a un editore o sono in attesa di pubblicazione/ *Parts of the thesis have been or are being submitted to a publisher or are in press;*

□ la tesi è finanziata da enti esterni che vantano dei diritti su di esse e sulla loro pubblicazione/ *the thesis project is financed by external bodies that have rights over it and on its publication.*

Data /Date .....30/10/2023..... Firma /Signature ……

DECLARATION

This thesis has been:

- composed by myself and has not been used in any previous application for a degree. Throughout the text I use both 'I' and 'We' interchangeably.
- has been written according to the editing guidelines approved by the University.

Permission to use images and other material covered by copyright has been sought. For the following image/s (Figure 1.6, Figure 1.7), it was not possible to obtain permission and is/are therefore included in thesis under the "fair use" exception (Italian legislative Decree no. 68/2003).

All the results presented here were obtained by myself, except for:

- **generation of MCF-7-p53GFP clone and its validation** through RT-qPCR and Western Blot (Figure 3.2) were performed by Alessia Loffreda, Experimental Imaging Center, San Raffaele Scientific Institute, Milan, Italy.

- **python codes for automatic detection of region of interest (ROI) from FISH images** were written by Tom Fillot, Experimental Imaging Center, San Raffaele Scientific Institute, Milan, Italy.

All sources of information are acknowledged by means of references.

AKNOWLEDGEMENTS

Scrissi una pagina di ringraziamenti ormai 4 anni fa per la tesi di laurea e sebbene 4 anni sembrino pochi, ciò che è successo e le persone con cui ho condiviso questo intenso PhD meritano il giusto spazio.

In primis, grazie al mio DoS, Davide: tutta l'energia e la passione che mi hai trasmesso, da quando sono arrivato nel tuo gruppo fino ad oggi, mi hanno sempre spronato a impegnarmi e a mettermi in gioco e mi hanno sempre ricaricato le batterie, anche quando questo oscuro mondo della biologia mi faceva impazzire. Grazie Samuel, per il tuo entusiasmo e instancabilità sin dal primo giorno del progetto fino alle simulazioni dell'ultim'ora; grazie per la pazienza e la dedizione che mi hai trasmesso a ogni nostro meeting. Thank to prof. Jana Wolf, for being my second supervisor during these years, for the high-level scientific conversations we had during my PhD seminars and at the "Biological Oscillators" conference.

A sentire altri PhD students, mi sono sempre sentito fortunato di esser capitato nel mio gruppo di ricerca, per cui grazie di cuore a tutti voi. Matteo, sei stato una sorta di "fratello maggiore" nel dottorato: grazie per aver condiviso con me ricerca scientifica, viaggi e conferenze, conversazioni sia serie che mondane, momenti di sconforto, dubbio, rassegnazione, ma anche di gioia, emozione e crescita. Alessia, sei sempre stata pronta e disponibile per qualunque mia incertezza o incapacità, anche quando ti facevo perdere tempo o mi dimenticavo cose che mi avevi detto 5 minuti prima (è l'età che avanza). Grazie per la tua onnipresenza e per essere stata una "sicurezza" quando avevo bisogno, per il rito degli ovetti del giovedì post CIS meeting, per aver ascoltato i miei dubbi, i miei sfoghi e le mie piccole gioie, per gli sguardi d'intesa (e di fuoco) quando la signora della mensa chiama me "Giovanotto" e te "Signora", per i mille meme che curiosamente descrivevano ogni cosa che succede in laboratorio, per le immagini di cuccioli di animali nei giorni di presentazioni importanti, per gli innumerevoli bigliettini e messaggini scritti e sparsi sulle nostre scrivanie: senza tutto questo non sarei arrivato fino in fondo. Daniela, Tom e Fulvio: vi ringrazio per avermi sempre supportato negli esperimenti, nelle discussioni scientifiche e nella vita quotidiana di laboratorio; grazie per i preziosi consigli e per i momenti più "spensierati" che abbiamo vissuto insieme. Non ho dubbi che, senza di voi, questi 3 anni sarebbero stati molto più pesanti e difficili.

Sono grato a tutti i membri, passati e presenti, dell'Experimental Imaging Center, che, dall'ottobre 2018, momento del mio arrivo tra loro, mi hanno accolto, supportato e visto crescere. Grazie Zeno, per le ore passate a urlare contro a microscopi, specchi e laser; Paola, per gli infiniti spunti/spuntini post CIS meeting; Tiziana, per avermi affibbiato l'epiteto di "aspirante biologo", e che rimarrà inalterato; Amleto, per gli innumerevoli pareri su film e serie; Serenella (per la ginnastica fatta nell'aiutarla col magazzino; grazie

Cecilia, Martina, Andrea, Camilla, Clara, Nicoletta, Giulia, Stefano, Ivana, per aver condiviso e smezzato giornate stressanti e per avermi strappato un sorriso anche nei momenti più faticosi. Grazie anche ai colleghi PhD students del gruppo CMB con cui ho condiviso corsi, seminari, gioie e dolori: Adriana, Marco, Elisa, Lucrezia, Anne.

Grazie al sostegno e all'affetto della mia famiglia, ai miei genitori Angela e Marco, Asia e Sara, Laura ed Enzo, Arianna e Riccardo, Giulia e Matteo, agli zii e ai nonni: a voi tutti vorrei esprimere la mia profonda gratitudine. Grazie per avermi guidato, sostenuto, incoraggiato e amato in ogni momento della vita.

Grazie ai miei amici, la mia seconda famiglia con cui condivido le cose belle della vita, ma su cui posso sempre contare nei momenti più duri. Luca, Eleonora, Camilla, Antonella, Valentina, Davide, Luana, Elena, Matteo, Matteo, Sara: grazie per essere miei amici, grazie per la vostra costante presenza nella mia vita che da sapore e un senso a tutto. Grazie di cuore anche a don Luca, Filippo, Kiddu, Elia, Niccolò, al gruppo dei "Cervelli", il gruppo GMG e a quello dei 18/19enni che mi fanno sempre sentire un po' meno vecchio di quel che sono (solo fisicamente però!).

Infine, Puffo. Mentre scrivevo la tesi, in questi mesi di dolore dopo l'11 agosto, continuavo a pensare e pensare, rivivendo quegli ultimi momenti insieme in Portogallo. E mi dicevo: chi se ne frega di p53, di NF-κB, del PhD, di tutto, perché non ho fatto abbastanza per te in quei giorni e non ho più la possibilità di rimediare, perché tu ora non ci sei più. La tua morte mi ha sbattuto in faccia la realtà e continua a farlo ancora oggi, a me che tento sempre di fuggirla, per evitare le fatiche e le responsabilità che comporta. Eppure, in questa dolorosa realtà convive anche l'inspiegabilità di quello che ti è successo, perché è qualcosa che ne biologia ne statistica sembrano spiegare. Qualcosa che sembra volermi dire che in questa realtà che vivo, sebbene con tutte le fatiche e le delusioni, c'è qualcosa di più Bello e di più Grande, che ho ancora da scoprire e vivere: questo non mi toglie la tua mancanza, ma mi dà un po' di speranza. Ti ringrazio Puffo per l'amicizia che abbiamo vissuto, per i momenti che hai condiviso con me, le abbuffate, i consigli su cinema e serie da vedere, le vacanze, le colazioni, i meme e le foto di dolci al pistacchio, i discorsi seri sul futuro, l'essere stati educatori insieme per tanti anni. Porto nel cuore e nella mente questi momenti e mi fa male sapere che non ne vivremo più insieme. Ora sta a me diventare grande in questa nuova realtà e ripartire per rendere più bella la mia vita: ti prometto che mi impegnerò in questo, per raccontartelo quando ci rivedremo.

ABSTRACT

Transcription factors (TFs) play a pivotal role in orchestrating the cellular response to various environmental stresses. These specialized proteins can activate or inhibit the expression of specific genes, enabling cells to adapt and survive in challenging conditions. p53 and NF-κB are two key TFs that mediate cell life/death decisions with opposite roles in cancer: p53 acts as a tumour suppressor, regulating cell fate after genotoxic stress, while NF-κB promotes inflammation, survival, and chemo-resistance. Different works show that these two TFs influence each other, and this crosstalk has been previously described in different cellular processes and phenotypes, but its precise mechanism remains unclear. Moreover, both TFs display a dynamic behaviour, key in regulating transcriptional programs and cell fate. The potential temporal dimension in their crosstalk remains largely unexplored, thus limiting our ability to reproduce an *in vivo* cancer scenario where both pathways are activated dynamically.

In this work, we studied how p53 and NF-κB dynamics affect each other in breast cancer cells using molecular biology techniques and live-cell microscopy. Our results support the idea of a "dynamic crosstalk" between p53 and NF-κB. We found that triggering NF-κB with pro-inflammatory cytokines perturbs both p53 oscillations after DNA damage and progressive nuclear accumulation after Nutlin treatment, leading to higher p53 levels in both cases. This perturbation is abolished if we knock-out NF-κB's key monomer p65 and is functional, since p53 target genes are transcribed more upon NF-κB co-activation. A combination of smFISH experiments and mathematical modelling suggest that the perturbation of p53 dynamics is caused by NF-κB-mediated upregulation of the *TP53* gene. This perturbation impinges DNA damage repair efficiency: while p53 oscillations are capable of resolving DNA damage, its NF-κB-perturbed oscillations are less efficient, thus leading to a prolonged state of DNA injury.

Our characterization highlights the relevance of studying the crosstalk of transcriptional pathways from a dynamic perspective. It provides novel insights on how these two TFs mutually influence each other, and in particular, chemotherapeutic treatments and tumour micro-environmental cues can co-participate in cancer cell fate decisions.

Table of content

<

ACRONYMS AND ABBREVIATIONS

AUC	Area under the curve
Chip	Chromatin Immunoprecipitation
CRC	Colorectal cancer cells
DDR	DNA damage response
DSB	Double-strand break
GFP	Green Fluorescent Protein
GMP	Granulocyte-macrophage progenitor
HSC	Hematopoietic stem cell
IL-1β	Interleukin 1 beta
IκBα	nuclear factor of kappa light polypeptide gene enhancer in B-cells inhibitor, alpha
IKK	IκB kinase
KI	Knock-in
KO	Knock-out
LPS	Lipopolysaccharide
MDM2	murine double minute 2
N.C.R.	Nuclear-to-cytosolic ratio
NF-κB	Nuclear factor kappa-light-chain-enhancer of activated B cells
ODEs	Ordinary differential equations
PRR	Pattern recognition receptor
RHD	Rel homology domain
ROI	Region of Interest
RT	Room Temperature
smFISH	Single-molecule fluorescence *in situ* hybridization
SSB	Single-strand break
TF	Transcription Factor
TLR	Toll like receptor
TNF-α	Tumor necrosis factor alpha
WT	Wild-type

LIST OF FIGURES AND TABLES

1. INTRODUCTION

1.1. The importance of temporal dynamics of transcription factors.

A plethora of diverse stimuli and stresses destabilizes cells homeostasis, which in turn react by activating *ad hoc* transcriptional programs, for which specific proteins called transcription factors (TFs) are in charge. Emerging evidence highlights that some TFs involved in different physiological processes exhibit a complex temporal evolution, including rhythmic fluctuations in their abundance or activity over time. Interestingly, hence, many TFs cannot be represented as mere switches, but display elaborate dynamics and crosstalks that have crucial effects at the transcriptional level. Such different dynamics arise from systems called "feedback loops", in which the molecular network reacts to perturbation either by reinforcing the input signal (positive feedback) or by countering it in the opposite direction (negative feedback) (Mengel et al. 2010). Such systems involve proteins regulating the activity of specific genes, that in turn regulate (thus inhibiting or activating) the function or the concentration of another protein (see **Box 1**).

For example, in the context of somitogenesis, different TFs are characterized by an oscillatory behaviour. Notch is a TF implicated in a complex transcriptional network regulating morphogenesis, by integrating different temporal signals. Notch oscillations have been found to be crucial in the physiological mesoderm segmentation process, especially their asynchronicity with the oscillatory dynamics of another TF, Wnt (Sonnen et al. 2018) (Lloyd-Lewis et al. 2019). Notch signalling pathway involved other different TFs, like Hes7 (Maroto et al. 2012). By directly binding to the Hes7 promoter, it induces self-repression, leading to oscillatory dynamics (Bessho et al. 2003). When Hes7 dynamics is perturbed, somites become completely fused (Takashima et al. 2011), while the acceleration of Hes7 oscillations accelerates somite generation (Harima et al. 2013). Moreover, the speed of biochemical reactions governing the segmentation clock in which Hes7 is involved has been found to be decisive in embryo development, with differences between mice and humans (Matsuda et al. 2020).

In the context of development, Hes1 is another important dynamic TF regulated by Notch: its oscillations are fundamental in proliferating neural progenitor stem cells, while Hes1 dynamics is blocked in differentiating neurons: this leads to an increase in the expression of pro-neural factors (Kageyama et al. 2015).

The circadian clock is another system in which regulatory genes are rhythmically activated, following the day/night period of 24 hours. Many TFs exhibiting oscillatory dynamics (like CLOCK, BMAL1, CRY, PER) are involved in transcriptional-translational feedback loops that are the core of the circadian clock (Lowrey & Takahashi, 2004) (Partch et al. 2014). The coupling between these TFs with several kinases and phosphatases (that regulate their stability and localization), are involved in the supervision of different processes, like metabolism, hormone secretion, and cell cycle (Richards & Gumz, 2013) (Droin et al. 2019).

YAP (Yes-associated protein 1) and its paralogue TAZ (transcriptional coactivator with PDZ-binding motif) provide an additional interesting example. These two TFs form a pivotal duo involved in the regulation of organ size control, tissue homeostasis, tumour suppression, and mechanotransduction (Moroishi et al. 2015). Several studies have unveiled the dynamic nature of YAP activity, characterized by oscillations in its nuclear/cytosolic localization. Upon diverse mechanical cues, like tension and compression, YAP dynamically shuttles between the cytoplasm (where is quiescent) and the nucleus (where it is activated), orchestrating transcriptional programs related to cell stemness and its response to the microenvironment (Panciera et al. 2017) (Ortega et al. 2021). YAP oscillatory dynamics resulted to be independent of substrate stiffness, but rather on the intensity of nuclear compression level (Koushki et al. 2023). Moreover, it has been found that YAP activity is related to both its nuclear level and shuttling dynamics. (Franklin et al. 2020) demonstrated how protracted retention of YAP in the nucleus perturbs the transcription of its targets. Both YAP levels and dynamics have been identified as key parameters in regulating the expression of the TFs Oct4 and Nanog, that are YAP downstream targets involved in pluripotency maintenance and mesoderm differentiation (Meyer et al. 2022).

Also in cancer biology, some TFs are characterized by oscillatory dynamics, which is decisive in tuning cell response to stresses. p53 and NF-κB are two key players regulating cancer gene expression (Gudkov et al. 2011) and they both display oscillations in their nuclear abundance (Lev Bar-Or et al. 2000) (Hoffmann et al. 2002)). These TFs are the two principal subjects of this PhD thesis, and their systems and dynamics will be discussed in the following paragraphs [2. for p53, 3. for NF-κB].

Therefore, to precisely respond to a myriad of stimuli, cells have embraced intricate transcriptional networks that delicately modulate their response in accordance with the inputs received. The different dynamics followed by these TFs allow a fine

elaboration of the stimulus, orchestrating the regulation of gene expression, crucial in optimizing the cell's adaptive capabilities.

Box 1 – Feedback loops in systems biology

Transcriptional networks are intricate systems that govern the expression of genes in response to various internal and external cues and rely on feedback loops. Feedback loops have been found in various organisms and among different TF-proteins systems (Shen-Orr et al. 2002) and can be modelled via differential equations, describing how single players involved in the feedback may evolve in time. Feedback loops in transcriptional networks can be classified into two main types: negative and positive feedback loops.

1) Negative feedback loops

Negative feedback loops are fundamental in maintaining system stability and overcoming system perturbation. In this kind of loops, the output of a process inhibits or reduces the initial stimulus. In transcriptional networks, negative feedback loops can involve a transcription factor X that in turn represses its own gene expression or function: this system is called negative autoregulation (a) (Alon 2007). f_x is a decreasing function of X and γ_x is the degradation rate of X. Many TFs in *E. coli* and eukaryotic repressors have been shown to undergo negative autoregulation (Rosenfeld et al. 2002) (Lee et al. 2002). In other negative feedback loops, the protein X activates the transcription of another target gene Y, which, once the concentration of Y reaches a certain threshold, can repress the transcription of X or inhibit its activity (b) (Alon, 2007). This kind of network (called a two-component negative feedback loop) can be modelled with two ordinary differential equations and produces damped oscillations of X and Y over time. This kind of system can incorporate a time delay, whose effect is the emergence of oscillations within the network (Novák & Tyson, 2008). An example of such a system is the p53-MDM2 feedback loop, in which p53 promotes the transcription of MDM2, that in turn represses p53 activation: this results in p53-MDM2 asynchronous oscillations (Lahav et al. 2004; Lev Bar-Or et al. 2000).

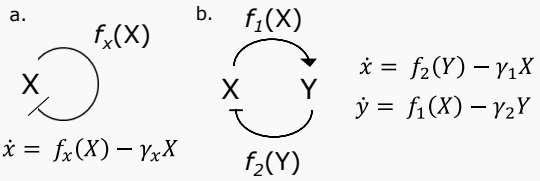

- $\dot{x}$ and $\dot{y}$ represent the time-derivative of X and Y levels, respectively.
- f_1 and f_2 are specific functions regulating the increase of Y due to X and the decrease of X due to Y, respectively.
- γ_1 and γ_2 are the degradation rates of X and Y, respectively.

2) Positive feedback loops

Positive feedback loops amplify the initial stimulus, leading to a rapid change in system behaviour. In biological networks, they play crucial roles in tuning the transcriptional regulatory system (Mitrophanov e Groisman 2008). A positive autoregulatory loop involves a TF X that activates its own transcription. As X accumulates, it leads to even more X production, resulting in a self-sustaining loop. Such systems enable slow response dynamics after the trigger and proportionally reach a steady state. MyoD is an example of a TF that undergoes positive autoregulation during embryonic stem cells differentiation into muscle cells (Osborn et al. 2011). Two-component positive feedback loops involve two proteins (X, Y) and can be double positive or double negative. This system can undergo different dynamics according to the gene activation state of X and Y. Positive feedback loops are often responsible for abrupt transitions in gene expression, driving cells from one state to another and are involved in cell differentiation and cell cycle regulation. An example of a two-component feedback loop is the GAL system, where Gal2p and Gal3p co-regulate gene expression in response to variations in galactose concentration (Venturelli et al. 2012).

1.2. p53 is a dynamic transcription factor.

p53 is crucial for regulating cellular response to various stresses. It forms a negative feedback loop with MDM2, which keeps p53 levels low in unstimulated cells. Activation of p53 leads to MDM2 transcription, inhibiting its own expression. This loop's activation or disruption results in dynamic p53 expression, essential for proper response to stressful stimuli. It has been shown that different p53 dynamics lead not only to different gene expression, but also to alternative cellular fates. Elucidating the interplay between p53 and MDM2 has not only improved our understanding of normal cellular processes, but has also shed light on such feedback loop dysregulation in different human cancers. In this section, we will discuss p53's role in tumour suppression, its dysregulation in cancer, the triggers of the p53-MDM2 loop, and the diverse p53 dynamic responses, with a focus on literature examples illustrating unique cellular reactions according to distinct p53 temporal evolution.

1.2.1. p53 is a key tumour suppressor.

Since its discovery and the first insights of its role as a tumour antigen in mice (Lane & Crawford, 1979) (DeLeo et al. 1979), p53 has been extensively studied over the last decades due to its pivotal role in tumour suppression and it is commonly called "the guardian of the genome" (Lane, 1992).

Cells are continuously subjected to a plethora of different genotoxic stresses, that can induce DNA damage: this breaks cell homeostasis and, if not correctly repaired, DNA damage persistence and spreading can cause genetic mutations and the activation of oncogenes (Basu, 2018). To face this scenario, damage-sensing kinases (like ATM) activate p53. The triggered transcriptional program depends on the stimulus and can induce distinct cellular outcomes. Depending on the nature and the severity of DNA damage, p53 activates cell cycle arrest genes, like *CDKN1A* and *GADD45a*, that allow repair processes and damage resolution, so that the cell can survive (Riley et al. 2008) (Tamura et al. 2012). In case of irreversible damage, instead, to avoid the spread of genetic errors to daughter cells, transcriptional programs leading to apoptosis (via the expression of genes like *PUMA* and *BAX*) or senescence (via the expression of genes like *CDKN1A* and *PAI-1*) are triggered by p53 (Toshiyuki & Reed, 1995) (Nakano & Vousden, 2001) (Kortlever et al. 2006).

Given its anti-tumoural role, different cancer types display a modulation or repression of p53 activity, blocking the activation of pro-apoptotic programs and allowing

proliferation. Mutations in the p53 gene (*TP53*) are commonly found in more than 50% of human cancers, thus perturbing the activation of p53 transcriptional programs (Levine & Oren, 2009). In fact, high levels of mutp53 proteins and its stabilization were found to be crucial in oncogenic pathways, involving components of the Hsp90 chaperone machinery, a stress-induced system that promotes cancer cell survival (Mantovani et al. 2019). In the latter half of tumours, which includes different examples of breast, lung, liver cancers and haematological tumours, the p53 wild-type (WT) form is retained. However, its signalling pathway, and then its transcriptional activity, is dysregulated, for example, via the overexpression of the murine double minute 2 (MDM2) protein, the negative regulator of p53 (Oliner et al. 2016) (Hou et al. 2019). The upregulation of MDM2 in these kinds of tumours has been found to be related to *Mdm2* gene amplification, increased transcriptional-translational levels, mRNA stability and perturbed post-translational modifications (Riley & Lozano 2012) (Li & Lozano, 2013) and actually decreases the effectiveness of conventional therapies (Hou et al. 2019).

Since MDM2 is usually a key player in p53 inhibition in cancers retaining WT p53, in the last decades various attempts have been made to target MDM2-p53 interactions and restore p53 activity in the perspective of a therapeutic treatment (Vassilev, 2007) (Shangary & Wang, 2008). Several molecules have been developed to bind the hydrophobic pocket of MDM2 (Kussie et al. 1996), thus preventing the binding with p53. The first classes of molecules with these properties are called Nutlins and were synthesized and tested in 2004: in a pioneer work it has been demonstrated how cells treated with these compounds display an accumulation of WT p53 and, consequently, its pathway activation (leading to an increase in MDM2 and p21 proteins level) (Vassilev et al. 2004). Over the years, different new molecules interfering with p53-MDM2 interactions have been designed and proposed: among all, nine were authorized for clinical trials, frequently in conjunction with other therapeutics (Haronikova et al. 2021) (Zhu et al. 2022). However, resistance to therapy was found to be the main obstacle arising from trials and therapies based on MDM2 inhibition (Shen et al. 2008) (Aziz et al. 2011). Even short treatments alone lead to the emergence of non-responsive cell populations, characterized by new mutations in the *TP53* gene (Michaelis et al. 2011) (Skalniak et al. 2018). New clinical trials and research are currently ongoing: tuning doses and timings of p53-MDM2 inhibitors and their couplings with other tumour-specific drugs represent a future opportunity for these small molecules in cancer treatments.

To sum up, we described the pivotal role of p53 in tumour suppression and the modulation of its activity (or dysregulation) in different cancer types. As we shall see, the negative feedback loop in which p53 is involved with MDM2 is strictly related to p53 transcriptional activity and, consequently, to cell fate under stressful conditions. We will deepen into p53 activation and regulation in the following paragraphs.

1.2.2. The p53-MDM2 feedback loop and its triggers.

Given its capability to induce the expression of genes involved in cell key life/death decision activating senescence/apoptosis programs, in physiological conditions, p53 is kept at low levels by its negative regulator, MDM2. Following diverse stimuli, mostly related to cell-intrinsic danger signals, p53-MDM2 interaction is broken, so that p53 starts accumulating inside the nucleus where transcribes different genes. Importantly, one of the key target genes activated by p53 is *Mdm2* itself. The increased expression of MDM2, in turn, promotes p53 degradation and attenuates its transcriptional activity, allowing cells to recover from the stress and return to homeostasis **(Figure 1.1)**. The activation of p53-MDM2 feedback loop involves a signalling cascade that is initiated by various stress signals. Each of these stimuli activates specific upstream molecular players and mediators that interfere and finally perturb p53-MDM2 interactions, thus modulating the downstream signalling cascade.

Hypoxia is a trigger of the p53-MDM2 feedback loop via the hypoxia-inducible factor 1-alpha (HIF-1α) mediator. Under hypoxic conditions, HIF-1α accumulates and directly interacts with p53, leading to post-translational modifications that stabilize and activate p53 (An et al. 1998) (Roe et al. 2006).

In addition, nutrient deprivation can trigger p53 pathway via the AMP-activated protein kinase (AMPK) or the serine/threonine kinase (AKT), key sensors of energy homeostasis (Humpton & Vousden, 2016). After inducing glucose starvation, AMPK can operate by phosphorylating and stabilizing p53, hence initiating the feedback loop (Jones et al. 2005). Concurrently with nutrients deprivation, AKT levels drop, inducing the phosphorylation and the nuclear translocation of MDM2 (Mayo & Donner, 2001) (Feng et al. 2004), thus allowing p53 stabilization and its downstream pathway activation.

Oncogene activation can also trigger the p53-MDM2 feedback loop without p53 modifications (Moll & Petrenko, 2003). Oncogenes such as Ras induce the production of p14ARF protein that in turn can inhibit the E3 ligase function of MDM2 and

sequester it into the nucleolus, thereby inducing p53 activation (Tao & Levine, 1999). Similarly, the hyper-activation of the oncogene Myc has been found to increase the transcriptional and translational rate of some ribosomal proteins that in turn can directly bind MDM2 and inhibit its ligase functions (Hu et al. 2012).

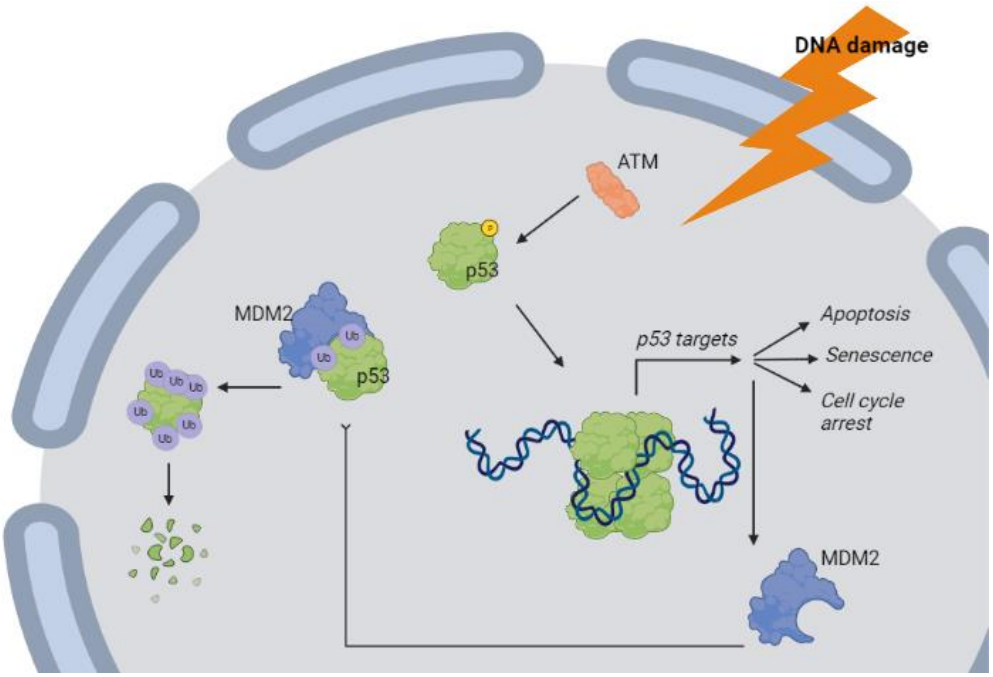

Figure 1.1. p53-MDM2 feedback loop. *In normal conditions, p53 is inhibited by its negative regulator, MDM2. After DNA damage, ATM phosphorylates p53, thus preventing its proteasomal degradation mediated by MDM2. p53 then accumulates in the nucleus, where it transcribes, among different genes involved in cell cycle arrest or apoptosis, MDM2 itself. Image created using BioRender.com.*

Finally, the most common "trigger" of the p53-MDM2 feedback loop is DNA damage. In eukaryotic cells, the "DNA damage response" (DDR) signalling pathway is regulated and coordinated by different sensors and effectors (Zhou & Elledge, 2000). The first and predominant DDR kinases are ATM (ataxia-telangiectasia mutated) and ATR (ATM- and Rad3-Related) (Canman et al. 1998). While the activation of ATM is primarily triggered by DNA double-strand breaks (DSBs), ATR is responsive to a wide range of DNA damage, including single-strand breaks (SSBs) and various DNA lesions interfering with DNA replication. When DSBs occur, DNA repair and signalling proteins accumulate at the foci of DNA damage, that act as sensors for ATM recruitment and activation (Mirzoeva & Petrini, 2001) (Lavin & Kozlov, 2007). ATM, in turn, phosphorylates both MDM2 (Maya et al. 2001) and p53 at Ser15 residue (Canman et al. 1998), thus promoting p53 nuclear accumulation (Cheng & Chen, 2010). It has been shown that ATM-mediated phosphorylation of p53 can also employ other

mediators like the checkpoint kinase Chk2 (Marechal & Zou, 2013). All these pathways have as output the phosphorylation and stabilization of p53: the weakening of its binding with MDM2 prevents its degradation and triggers its activation.

1.2.3 Different triggers, different p53 dynamics, different cellular outcomes.

p53 gets activated by all the mentioned stimuli, but different p53 dynamics arise according to the stimulus's nature and its strength.

DSBs, caused by γ-irradiation, for example, induced sustained p53 oscillations, with the first peak at 3 hours after the trigger, with a period of around 6 hours, that can persist in rising and falling over days (Lev Bar-Or et al. 2000) (Lahav et al. 2004). It has been also demonstrated that both strength and period of p53 oscillations are independent of the dose of γ-irradiation delivered to cells, but both the number of oscillations per cell and the number of cells displaying p53 oscillations increases with increasing dose of irradiation in a digital fashion (Geva-Zatorsky et al. 2006). As MDM2 expression is under the control of p53 itself, MDM2 levels oscillate as well, with a delay of 1 hour compared to p53 (Monk, 2003) (Geva-Zatorsky et al. 2010).

Conversely, UV light lays the cell exposed to SSBs, thus inducing a DNA damage response mediated by ATR. This, in turn, triggers a sustained p53 nuclear accumulation, since the synthesis rate of MDM2 by p53 is lower than MDM2 protein degradation with these settings (Lu et al. 2005). As demonstrated by Lahav's research group, a short burst of UV light induces irregular p53 pulses, weaker than those observed after γ-irradiation. Moreover, the higher the UV light dose, the higher the response and the duration of p53 pulse, without any periodicity nor oscillation (Batchelor et al. 2011). This different dynamical behaviour was explained with a secondary feedback loop that involves p53 and Wip1: after damage induction by UV, p53 activates the expression of Wip1 (wild type p53-induced phosphatase), which in turn dephosphorylates p53, leading to a decrease in its stability (Batchelor et al. 2011).

In the last decade, several studies highlighted how p53 dynamics can vary between cell lines, tissues and even species (Stewart-Ornstein et al. 2017) and how this behaviour can be correlated to different cell fate decisions. In a study conducted by (Stewart-Ornstein et al. 2017), p53 dynamics was studied across 12 different cell lines commonly used in cancer research, including MCF-7, A549 and U2OS. After DNA damage induction, while some cells display sustained p53 oscillations, other lines do

not have oscillations or show dose-independent p53 dynamics. The reason for such differences was found in the ATM kinase activity and in the variability of proteins involved in the DNA repair mechanism. The same research group extended the size-scale of p53 dynamics observation from single cells to tissues in a later study, starting from some previous evidence reporting that different tissues display different p53-target genes activation after DNA damage (Fei et al. 2002). The authors demonstrated how, despite similar p53 levels, different tissues display different p53 dynamics after ionizing radiation, correlating with tissue radiation sensitivity: while radioresistant tissues (like the gut) show p53 oscillations and transient activation of its target genes, radiosensitive tissues (like the thymus or the spleen) display a sustained accumulation of p53 (Stewart-Ornstein et al. 2021). In another study, (Yang et al. 2018) demonstrated how p53 dynamics diverge between cell lines according to their sensitivity or resistance to different doses of etoposide, a drug that induces DSBs. At higher etoposide doses, resistant cells display a high first peak of p53 activation, followed by some smaller oscillations, while a sustained accumulation of p53 is detected in sensitive cells. These differences in p53 dynamics lead to different cellular outcomes, with etoposide-resistant (oscillating) cells surviving more. Different p53 dose responses and cellular outcomes were also noticed among Nutlin and 5-fluorouracile treatments between different cell lines (Xie et al. 2022).

Given the wide range of transcriptional programs activated by p53 that can lead to opposite fates (apoptosis vs cell cycle arrest/survival), as depicted in **Figure 1.2**, several attempts have been made to answer this question: is it only the dynamics of p53, its effect on the expression of target genes, or both that modulate and determine cell fate under stressful conditions?

Initially, an "affinity model" was proposed, sustaining that high levels of p53 induce the expression of genes with "low affinity" promoters, involved in apoptosis (*BAX*); instead, low levels of p53 trigger genes with "high affinity" promoters, implicated in cell cycle arrest (*CDKN1A*) (Weinberg et al. 2005) (Murray-Zmijewski et al. 2008) **(Figure 1.3a)**. Subsequent studies, however, revealed that both pro-arrest and pro-apoptotic genes were activated in presence of low- and high-p53 levels: this suggested a threshold mechanism by which p53 mediates the concentration of apoptotic molecules, thus inferring cell fate decision (Kracikova et al. 2013). Therefore, attempts were made to artificially perturb p53 dynamics by blocking p53-MDM2 interactions: by using the small molecule Nutlin-3, (Purvis et al. 2012) turned p53 oscillations induced by γ-irradiation into a sustained nuclear accumulation. These different p53 dynamics have as an outcome the activation of different sets of p53

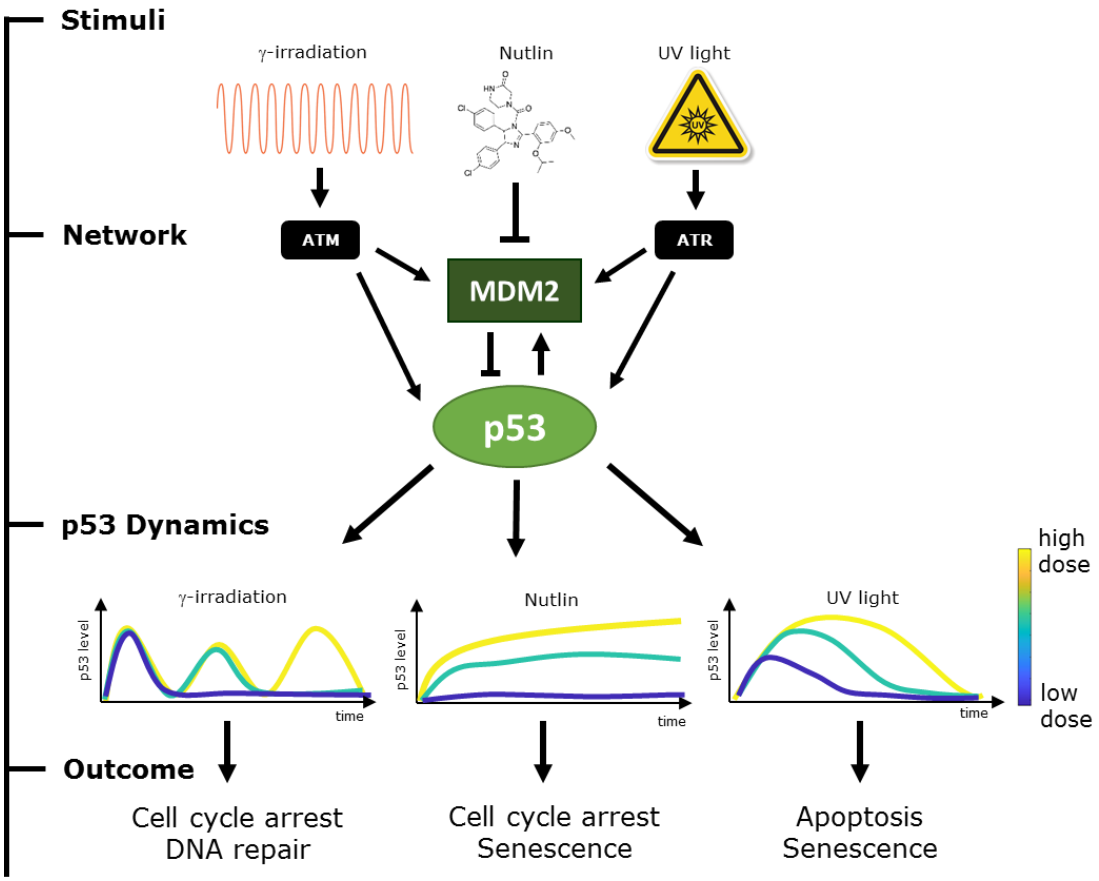

Figure 1.2. How different stimuli can trigger different p53 dynamics and cellular outcomes. *DNA double strand breaks caused by γ-irradiation trigger p53 signalling pathway via ATM: p53 levels undergo oscillations and the expression of genes related to DNA repair mechanism or cell cycle arrest is induced. Nutlin is a drug that block p53-MDM2 interactions, leading to a sustained p53 dynamic. This kind of dynamics induces p53-dependent cell cycle arrest or apoptosis. UV radiation causes single strand breaks and triggers p53 signalling pathway through the mediation of ATR. This causes a single p53 pulse, whose strength and duration depends on the intensity of the damage, and triggers transcriptional programs related to apoptosis and senescence. This figure was made by adapting Figure 3 from Luo Q. et al. Genes, 2017,8,66 and Figure 1 from Friedel L. & Loewer A. The FEBS Journal, 2021*.

target genes: oscillatory dynamics induced the expression of genes related to cell cycle arrest and DNA damage repair (*CDKN1A*; *GADD45A*), while sustained dynamics activated genes involved in apoptosis and senescence (*BAX; PML*). Moreover, at low levels of DNA damage, p53 sustained dynamics raised the fraction of senescence phenotype, while p53 pulses allowed cells to divide and proliferate. From this evidence, several studies then made efforts to understand the molecular mechanisms regulating p53 dynamics - genes expressions - cellular outcomes. By computing different features of p53 dynamics from single-cell profiles, (Paek et al. 2016) demonstrated how apoptotic and surviving cells can reach similar p53 levels after

cisplatin treatment, but p53 accumulation rate is the key parameter in apoptosis induction. In fact, they found that apoptotic cells accumulated p53 earlier and faster than surviving cells and p53 should reach a critical threshold level to trigger effective apoptosis. Moreover, this apoptotic threshold increases after treatment with Cysplatin **(Figure 1.3b)**.

How p53 dynamics is then involved in regulating the expression of such different genes? It has been shown that the promoters of p53 target genes have different thresholds for their activation: *MDM2* promoter has a lower threshold and it is more frequently activated by p53 oscillations; on the contrary, *CDKN1A* promoter shows an activation rate strongly modulated by p53 pulses amplitudes (Harton et al. 2019). Such a mechanism can also explain why p53 oscillations spontaneously induced by transient DNA damage are sufficient to trigger *MDM2* but avoid the activation of *CDKN1A* (Loewer et al. 2010).

Several attempts to understand how p53 dynamics regulates cellular outcomes have also been made by considering p53 "downstream genes dynamics", thus looking at the temporal evolution of mRNAs and proteins levels of p53 targets (Hafner et al. 2019) (Hafner et al. 2020). After DNA damage induction, different types of mRNAs dynamics of p53 target genes have been found: their temporal evolution (oscillations, plateau, and accumulation) was found related to mRNA half-life, rather than p53 binding affinity and transcription level (Porter et al. 2016) (Hafner et al. 2017). A subsequent study by (Jiménez et al. 2022) quantified the temporal evolution of different sets of genes following different p53 dynamics (oscillatory vs sustained). Not only do downstream mRNA/protein dynamics depend on p53 dynamics itself, but also their temporal dynamics revealed a degree of heterogeneity among different genes, suggesting exclusive gene-specific transcription and translation mechanisms (like feedback forward loops, positive/negative regulation or activation threshold).

A new perspective on how different p53 dynamics (oscillations vs sustained) affect cellular outcome recently came out, proposing a theoretical model that includes the biophysical properties of p53 oscillations and foci involved in DNA damage repair mechanism (Heltberg et al. 2022). DSBs cause DNA damage foci, characterized by hallmarks like the presence of phospho-H2AX (Mah et al. 2010), that physically resemble liquid droplets containing the molecules in charge of DNA repair (Mirza-Aghazadeh-Attari et al. 2019) (Miné-Hattab et al. 2022). It was recently found that p53 is directly recruited at damage foci in a short time after damage induction and concurs with the engagement of other molecules involved in the DNA damage repair

mechanism (Wang et al. 2022). However, the presence of multiple liquid droplets triggers a phenomenon called "Ostwald ripening", by which droplets with higher dimension progressively attract molecules from the dispersed phase, growing at the expense of smaller droplets (Houk et al. 2009). Heltberg et al. proposed a biophysical model in which oscillations are the optimal way to redistribute p53 molecules and avoid the Ostwald ripening: if this phenomenon occurs, only bigger damage foci will be repaired because all repair molecules will fall in those droplets. With oscillation, p53 can be distributed homogenously in a higher number of damage foci, increasing repair efficiency **(Figure 1.3c)**. If p53 oscillations are perturbed, for example by small molecules like Nutlin, DNA damage foci are worse repaired. Although there is a need for wider results in study confirmation, the proposed model represents a first attempt to provide a biophysical explanation of how p53 dynamics can regulate cellular response to insult.

p53 dynamics have turned up to be a pivotal feature in tuning gene expression and cell fate, but different tissues and cancers exhibit different p53 dynamics (Stewart-Ornstein et al. 2021) (Xie et al. 2022). This heterogeneity in p53 response has been hypothesized to be related to different proliferative conditions, important in modulating cell's receptiveness to DNA damage and regulation of repair mechanism (Stewart-Ornstein et al. 2021). With this in mind, the choice of appropriate or new anti-cancer drugs should take into account also the transcriptional programs and global effects that a perturbed p53 dynamics can produce (Luo et al. 2017) (P. Wang et al. 2023). Some attempts have been already made: it has been demonstrated how, after DNA damage induction, the treatment with a chemotherapeutic drug called rucaparib (Papa et al. 2016), directly alters p53 dynamics and the expression of several genes, thus promoting cell proliferation (Hanson & Batchelor, 2020). Moreover, since p53 dynamics is a crucial feature in tuning gene expression and cell fate, it is worth considering not only perturbations by different external factors (Jentsch et al. 2020), but also that p53/MDM2 feedback loop can be entangled with other regulatory networks (N. Yang et al. 2020) (Xie et al. 2022). Indeed, various studies proposed that the regulation of different responses to stresses by p53 also involves NF-κB, another TF involved in immune and inflammatory response (Carrà et al. 2020). The next chapter will describe NF-κB, its pathway, and its functions.

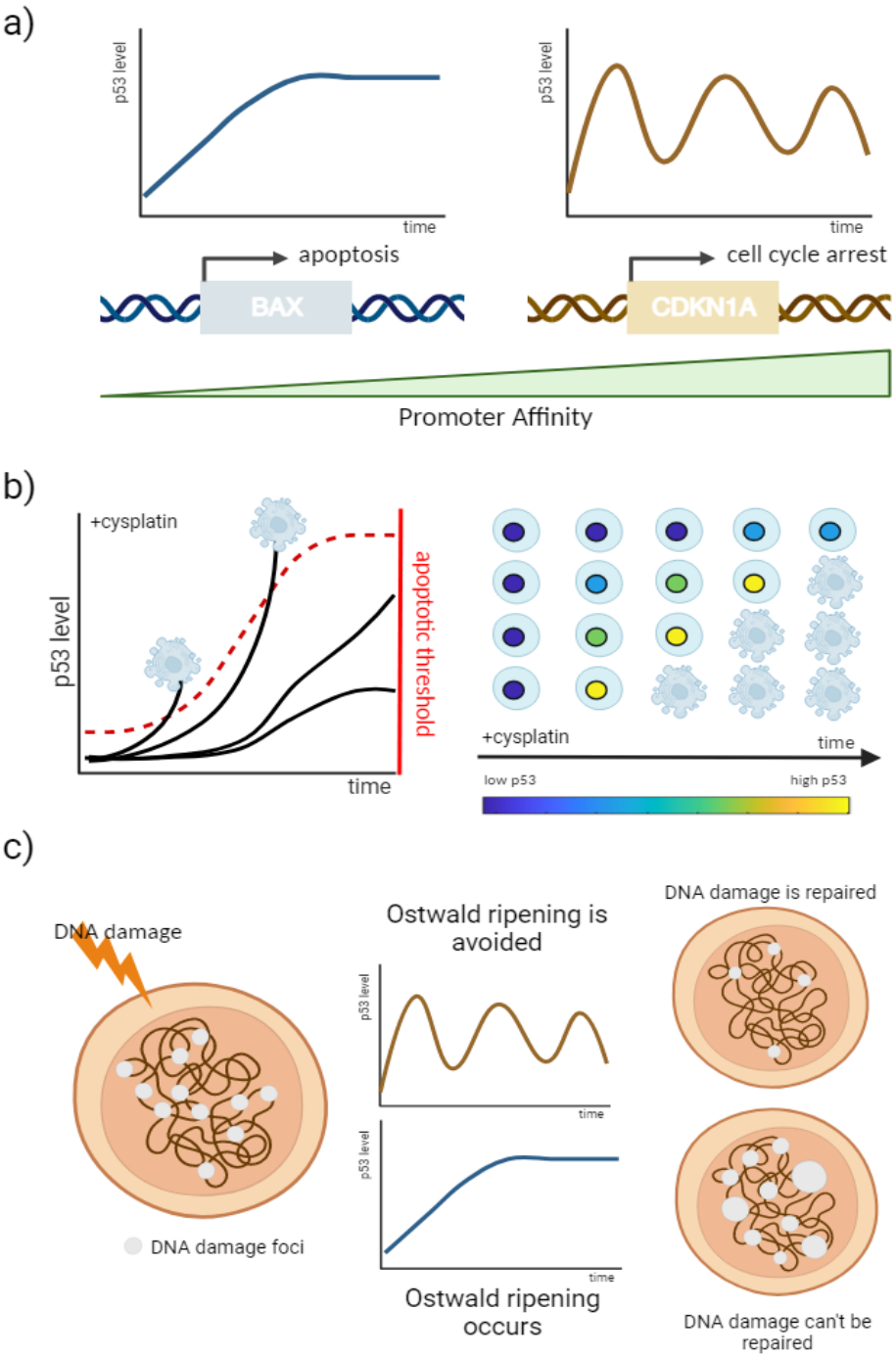

Figure 1.3. Different models proposed to explain why different p53 dynamics induce different transcriptional programs and cellular outcomes. (a) *In the "affinity model", while a sustained dynamics induce high p53 levels and trigger genes with low affinity promoters, oscillations (so lower p53 levels) induce the expression of "high affinity" genes.* ***(b)*** *Different dynamics induce different cell fates. Only cells that show a more rapid accumulation of p53 undergo apoptosis since they early bypass an "apoptotic threshold", which increase over time after the treatment.* ***(c)*** *p53 oscillations can be the best strategy to resolve DNA damage, by avoiding the Ostwald ripening phenomenon. In case of sustained p53 dynamics, Ostwald ripening occurs and only foci with big size will be repaired due to a higher attraction of repair molecules, included p53. Image created using BioRender.com.*

1.3. NF-κB: a dynamic transcription factor as well.

NF-κB is a transcription factor that orchestrates the cellular response to a variety of stresses and it is mainly involved in immune and inflammatory responses. NF-κB is kept inactivated and sequestered by different inhibitors (including IκBα) in the cytoplasm: upon stimuli, the inhibitors are degraded, and NF-κB translocates inside the nucleus where it transcribes, among all, also genes related to its negative regulators (like *NFKBIA*, encoding for IκBα), thus forming a negative feedback loop. This kind of system induces oscillations, so that NF-κB transcriptional activity is tightly controlled, strongly modulating gene expression and cell response to many stimuli in different contexts. In this section, we will elucidate the significance of NF-κB in inflammation and cancer. Next, we will delineate the activation mechanisms of the NF-κB-IκBα feedback loop and the dynamic responses exhibited by NF-κB. To underscore the significance of NF-κB dynamics, we will present studies from the literature that detail how diverse transcriptional regulation and cellular responses are related to specific temporal evolutions of NF-κB.

1.3.1 NF-κB is a master regulator of inflammatory and immune responses.

The Nuclear Factor of κB (NF-κB) was firstly found in activated B cells as a DNA-binding protein (Sen & Baltimore, 1986). NF-κB is actually a family of dimeric transcription factors composed of various combinations of subunits, primarily including p50, p52, p65 (RelA), RelB, and c-Rel (Hayden & Ghosh 2008). These subunits assemble in different combinations to form NF-κB dimers that can be either activators or repressors of gene transcription (Park & Hong, 2016). However, only p65/RelA, RelB and c-Rel can recruit the transcriptional machinery, since they carry a transactivation domain (Lee et al. 2014). Since the predominant heterodimer found in most of cells is RelA-p50 (Oeckinghaus & Ghosh, 2009) and RelA/p65 is the only protein with a transcription activation domain in this dimer, in the next paragraphs "NF-κB" will refer to dimers including p65, unless otherwise stated.

Over the years, NF-κB multifaceted role in regulating hundreds of genes involved in different processes and cell types has been thoroughly investigated (Karin & Greten, 2005) (Taniguchi & Karin, 2018). NF-κB is particularly important in the context of inflammation, a process that involves immune cells and is adopted to protect tissues from infections and injuries. In such a scenario, NF-κB mediates the expression of pro-inflammatory genes, the transcriptional induction of cytokines, chemokines and

the recruitment of innate immune cells, like macrophages (Lawrence, 2009) (T. Liu et al. 2017). These cells in turn secrete different inflammatory molecules and can differentiate into two possible phenotypes, called classically activated (M1) and alternatively activated macrophages (M2) (Wang et al. 2014). M1 macrophages secrete pro-inflammatory cytokines like IL-1, IL-6, IL-12, and TNF-α, as well as chemokines implicated in diverse inflammatory pathways and also induce the differentiation of some kind of inflammatory T cells, key orchestrator of the inflammatory response (Martinez, 2008) (N. Wang et al. 2014). M2 macrophages, instead, release anti-inflammatory cytokines such as IL-10 and IL-13, thus subsiding inflammation and facilitating the process of wound healing (Mosser, 2003). Several chemokines (like MCP-1 and various CCLs) and adhesion molecules (like E-selectin and ICAM-1), all regulated by NF-κB, mediate the recruitment of immune cells to the site of inflammation and promote the expression of proteins for antigen presentation (Tilstra et al. 2011).

In addition, it has been found that NF-κB is strongly implicated in the apoptotic process, where it becomes active during or just prior to cell death (Magné et al. 2006). Interestingly, it can activate both anti- and pro-apoptotic genes. To avoid the induction of cell death, NF-κB promotes the transcription of genes coding for anti-apoptotic proteins, like IAP-1, c-IAP-2, that interfere with caspases activity (Stehlik et al. 1998) (Erl et al. 1999); c-FLIP, that can inhibit caspase-8 functions (Fiore et al. 2018); Bcl-xl and Bfl-1/A1, that prevent cytochrome-c release and subsequent caspase-9 activation (Khoshnan et al. 2000). Conversely, in other cases, NF-κB can promote the transcription of genes like *PI3K* (Mortezaee et al. 2019), *Bax* (Shou et al. 2002) and the Fas Ligand gene (*FasL*), whose upregulation promote the expression of transmembrane receptors involved in cell death processes (Hsu et al. 1999) (Serasanambati & Chilakapati, 2016).

Since NF-κB has the capability to tune cellular fate, its misregulation is commonly found in cancer: NF-κB constitutive activation is a key hallmark of different kinds of tumours (Prasad et al. 2010). Genetic alterations such as cancer-related chromosomal translocations, deletions, and mutations can interfere with NF-κB pathway and its regulators, thus resulting in a sustained activation of NF-κB. Additionally, the persistent presence of pro-inflammatory cytokines secreted by the tumour microenvironment promotes the activation of NF-κB upstream signalling molecules and then its chronic activation (Karin et al. 2002) (Ben-Neriah & Karin, 2011). All these factors, in turn, promote cancer-cell proliferation, impede apoptosis, and allow the expression of angiogenic and angiostatic molecules, like VEGF, IL-1,

IL-8 and IL-6, enhancing tumour's possibilities to escape apoptotic programs (B.R. Lane et al. 2002) (Serasanambati & Chilakapati, 2016). NF-κB activation can also have pro- or anti-tumourigenic effects, according to the context. Colitis-associated colon cancer cells are characterized by a high expression of genes related to anti-apoptotic pathways and growth factors secretion (Greten et al. 2004). On the contrary, in squamous cell carcinoma, NF-κB inactivation through the overexpression of IκBα can increase epidermal growth, probably via an oncogene-induced senescence mechanism (Dajee et al. 2003) (Ben-Neriah & Karin, 2011).

Taken together, we have that NF-κB signalling pathway has been found to be central in immune responses, regulation of inflammatory processes and cancer. As we shall see, the negative feedback loop in which NF–κB is involved is at the basis of its transcriptional activity and hence might influence its role in cancer. We will describe NF-κB regulation in the following paragraphs.

1.3.2 NF-κB signalling pathway and feedback loop.

In the absence of NF-κB-activating stimuli, a set of proteins called IκBs (Inhibitor of κB) are in charge of keeping NF-κB sequestered in the cytoplasm (Oeckinghaus & Ghosh, 2009). NF-κB signalling pathway can then be activated by different signals, mediated by specific receptors. Among them, toll-like receptors (TLR) ligands are pattern recognition receptors (PRRs) that detect molecules typical of bacteria, viruses and pathogens (Kawai e Akira 2010) as lipopolysaccharide (LPS), a structural molecule present on the outer envelope of all gram-negative bacteria (Bhattacharyya et al. 2010). NF-κB pathway is also activated by antigen receptors present on T-cells and B-cells (Barnes et al. 2015), as well as by different growth factors (Müller et al. 2002). It has been also found that ATM can activate NF-κB in a DNA damage scenario (Wu et al. 2006). Finally, cytokines such as those belonging to Tumour Necrosis Factors and Interleukins can also activate NF-κB. Interestingly, many members of these cytokine families are also transcriptional targets of NF-κB (Tilstra et al. 2011), leading to a positive feedback loop.

The NF-κB pathway is triggered by the binding of cytokines (like TNF-α) to their transmembrane receptors, that in turn activate the IκB kinase (IKK) (Liu et al. 2012). Once activated, IKK phosphorylates IκBα, the main negative regulator of NF-κB, at two serine residues; IκBα is therefore poly-ubiquitinated and degraded by the proteasome, freeing NF-κB, which in turn can translocate inside the nucleus (Tak & Firestein, 2001). Once NF-κB translocates inside the nucleus, it activates up to 500

genes, including IκBα itself. This forms a negative feedback loop: newly synthetized IκBα in turn forms a complex with NF-κB, inhibiting its activity and relocating it into the cytoplasm **(Figure 1.4)**. While IκBα is the stronger inhibitor of NF-κB, other IκBs isoforms, like IκBβ and IκBε, are also degraded analogously upon stimuli and can be transcribed by NF-κB and hence are involved in the feedback loop (Hoffmann et al. 2002). For the record, this pathway (including p65/RelA-carrying dimers) is called the "NF-κB canonical pathway"; another pathway exists, the "non-canonical" one, that has in NF–κB inducing kinase (NIK) and p52/RelB subunit its core players (Solan et al. 2002) (Gilmore, 2006) (Sun 2017). Whereas the canonical pathway is mainly implicated in the control of genes involved in inflammation and innate immunity, the non-canonical pathway seems to be crucial in regulating gene expression during lymphoid organogenesis (Strickland & Ghosh, 2006) (Tilstra et al. 2011). Another transcriptional target of NF-κB, that creates an additional negative feedback loop, is the zinc finger protein A20 (ubiquitin-editing enzyme TNFAIP3) that inhibits the signalling upstream of IKK, thus ending IκBs degradation processes (Hutti et al. 2007) (Werner et al. 2008).

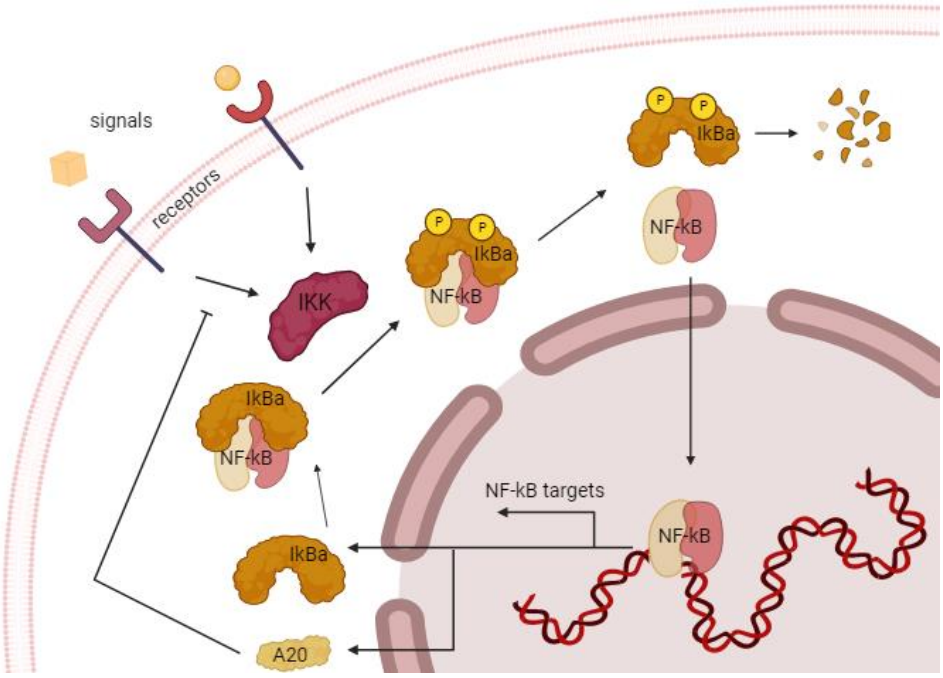

Figure 1.4. NF-κB-IκBα feedback loop. *In absence of stimuli, NF-κB is sequestered in the cytoplasm by its negative regulator, IκBα. After a triggering stimulus (cytokines, chemokines, LPS…), IKK phosphorylates IκBα, freeing NF-κB that can translocate inside the nucleus. Here, NF-κB activates different transcriptional programs involved in inflammatory and immune responses. Among all genes involved in immune and inflammatory response, NF-κB transcribes IκBα itself. Image created using BioRender.com.*

These feedback loops ensure both stability and flexibility to NF-κB system. Moreover, in a tumour environment where inflammatory stimuli are continuously renewed, such feedbacks give rise to oscillations in NF-κB localization, between the cytoplasm and the nucleus, where it exerts its transcriptional functions (Colombo et al. 2018).

1.3.3 NF-κB dynamics can tune gene expression.

NF-κB oscillations were firstly detected via classical biochemical assays at the bulk population level on TNF-α treated cells (Hoffmann et al. 2002). Some years later, the group by M.R. White was able to follow NF-κB dynamics in single-cells after TNF-α treatment via fluorescence microscopy. This tool enabled to directly quantify features of NF-κB oscillations, revealing clues correlating dynamics and gene expression modulation (Nelson et al. 2004). Additionally, the use of microfluidic devices helped a more precise tuning of NF-κB triggering inputs, by modulating the amplitude, frequency and signal duration (Colombo et al. 2018). Interestingly, several studies highlighted that the dynamics of NF-κB are cell-specific and change according to the triggering stimulus (Bartfeld et al. 2010), opening new questions on the role of these dynamics in the regulation of gene expression.

It has been then demonstrated how continuous stimulation with TNF-α triggers multiple NF-κB nuclear-to-cytosol translocations and out-of-phase oscillations in IκBα levels (Nelson et al. 2004). Moreover, while continuous perfusion with TNF-α induces sustained NF-κB oscillations with a period of one hour and a half in 3T3 cells, "sawtooth-like" TNF-α pulses synchronize NF-κB oscillations and also transcriptional output, reducing heterogeneity in cell-to-cell responses (Kellogg & Tay, 2015). Squared pulses of TNF-α, that synchronize NF-κB oscillations, led to different target mRNA expression dynamics (oscillating, sustained increased and intermediate dynamics). Hence, genome-wide analysis revealed different dynamic patterns of gene expression, each of which was enriched for genes with similar biological functions (Zambrano et al. 2016). At the downstream level, different populations of responding genes can be detected according to NF-κB oscillations: early, intermediate and late genes, transcribed in one hour, at 1.5 hour and after 3 hours after TNF-α stimulation, respectively (Sung et al. 2009). The modulation of TNF-α pulses, inducing different types of NF-κB dynamics, affects downstream gene expression depending on whether the target gene belongs to one of the three classes (Ashall et al. 2009).

Since NF-κB-mediated transcriptional programs are critical in different cellular process, this question could arise: is NF-κB nuclear abundance or its temporal dynamics responsible for transcriptional regulation? Actually, (Lee et al. 2014) demonstrated how the fold-change of nuclear NF-κB, rather than its nuclear levels, is the key feature involved in transcriptional regulation. Moreover, they found that different genes have different patterns of transcription, related to their sensitivity to NF-κB fold change. From this evidence, the authors hypothesized that NF-κB-mediated dynamic transcription is regulated as a type 1 feedforward loop motif. This kind of system is sensitive to fold changes and is tuned by different competitors, that are other molecules specific for each gene (they proposed three of them: p50, p52 and BCL3).

Furthermore, the artificial perturbation of NF-κB dynamics was proved to strongly affect gene expression. (Sung et al. 2009) co-treated cells with TNF-α and Leptomycin, which keeps NF-κB sequestered in the nucleus, but unable to interact with chromatin, due to its binding with IκBα. This treatment induced a general decrease of the transcription of intermediate and late genes (like *VCAM*, *LIF* and *IL-15*). Conversely, co-treatment with TNF-α and Cycloheximide, which blocks inhibitor translation and hence keeps NF-κB in the nucleus, while not interfering with its chromatin interactions, enhances the transcription of early and intermediate genes. These findings suggest that NF-κB oscillations might function as a fine-tuning of the expression of early and late genes, allowing NF-κB to monitor the chromatin landscape evolution and genes accessibility over time. In a subsequent study, (Cheng et al. 2021) triggered NF-κB sustained dynamics in macrophages by abolishing oscillations via IκBα knock-out (KO): this induced a change of their epigenetic state, whose immune response-related gene expression was upregulated. These results led the authors to hypothesize that NF-κB dynamics can tune the transcriptional activation of inflammatory genes in macrophages by changing the epigenetic state and chromatin accessibility, with non-oscillatory NF-κB engaging latent enhancers.

Different NF-κB dynamics can also lead to different cell fates. In a work by (Lee et al. 2016) it has been demonstrated that a short pulse of TNF-α is unable to trigger anti-apoptotic programs, thus enabling the caspase pathway and causing a higher level of cell death. Conversely, a longer exposure to TNF-α (with pulses lasting from 5 to 60 minutes) leads to a sustained NF-κB transcriptional activity, leaning towards pro-survival and mitigating caspase pathway. This evidence was found in Hela cells, but different cell types display different cell fate regulation. In a work by (Yamashita e Passegué 2019), it has been demonstrated that, while TNF-α has pro-death effects

in granulocyte-macrophage progenitors (GMPs), it plays a critical role in survival and regeneration of hematopoietic stem cells (HSCs).

All this evidence confirms even more how relevant is NF-κB dynamics in regulating gene expression and cell fate (**Figure 1.5**). However, several studies highlighted how these dynamics are not only cell type-specific, but also different at single cell level, revealing a high degree of heterogeneity in NF-κB dynamical response and in its target genes activation (Lee et al. 2014) (Zambrano et al. 2020). It has been hypothesized that such heterogeneity arises from single cells susceptibility to triggering stimuli and depends on the stochastic nature of transcription itself (Lee & Covert, 2010) (Zambrano et al. 2014) (Tunnacliffe & Chubb, 2020). Even within a homogeneous cell population, NF-κB dynamics can be heterogeneous at the single-cell level (Kizilirmak et al. 2022). The fraction of TNF-α-responding cells increases with the dose (Tay et al. 2010) and a prolonged and mild stimulation results in the activation of a smaller number of cells compared to a brief and strong pulse (Kellogg et al. 2015). These studies suggest that an activation threshold is present and is single-cell specific (Zhang et al. 2017). In addition, the feedback loop system in which NF-κB is embedded and other molecular players involved (like E2F) can be identified as a source of heterogeneity (Paszek et al. 2010) (Ankers et al. 2016) (Kizilirmak et al. 2022).

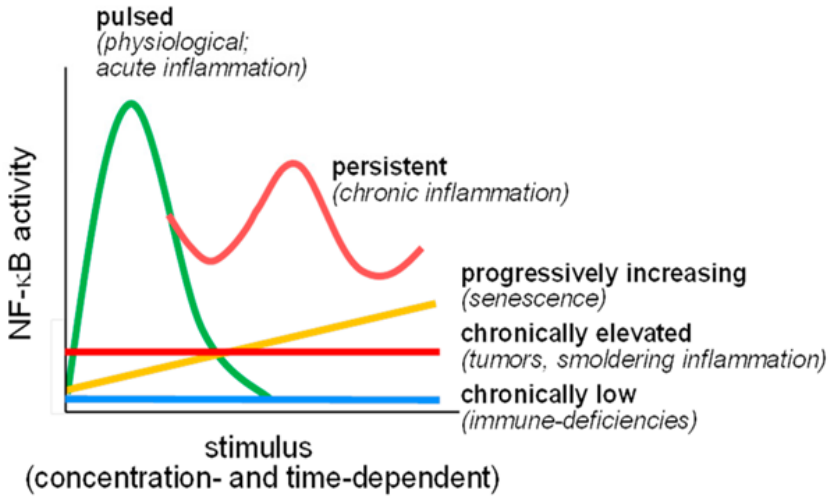

Figure 1.5. Different NF-κB dynamics can arise from concentration- and time-dependent triggers and induce different cellular outcomes. *Such different kinetics characterize inflammatory processes and different kinds of pathologies. Figure is taken from Bacher et al. by permission from Cells, Regulation of Transcription Factor NF-κB in its Natural Habitat: the Nucleus by S. Bacher et al. 2021, 10(4), 753.*

NF-κB regulates different cellular processes, including differentiation, development, and inflammation, with implications for cancer progression and chemoresistance (Bacher et al. 2021). Understanding its dynamics is vital for comprehending its functions in cancer. Integrating pathways related to inflammation and non-inflammation in dynamic tumour contexts is essential (Kizilirmak et al. 2022) (Kaur et al. 2023). Different studies suggest that p53, known primarily for its role in DNA repair and cell cycle regulation, is directly involved in NF-κB signalling regulation in various physiological contexts. Exploring the interplay between NF-κB and p53 could not only shed new light on how these pathways influence each other and tune cellular homeostasis, but also on how cancer cells respond to therapies in inflammatory contexts: the next chapter will describe the evidence present in the literature on p53 and NF-κB crosstalk.

1.4. The crosstalk between p53 and NF–κB.

In the intricate landscape of cancer, tumour progression and its response to therapy are tightly regulated by both p53 and NF–κB. Their transcriptional activity profoundly influences disease progression and therapeutic outcomes. It is now established by scientific literature that a reciprocal influence between p53 and NF–κB influences different kinds of cellular processes. If we imagine a tumoral context, where cancer cells are subjected to therapy and inflammation is an active process in the tumour microenvironment, we can assume that both p53 and NF–κB pathways are simultaneously activated. The crosstalk between them forms an intricate regulatory network that orchestrates cellular responses to stress and inflammation, thus influencing the effect of therapies aimed at inducing cancer cells death. Exploring the multifaceted interplay between p53 and NF–κB in the context of cancer could provide crucial insights into the underlying mechanisms of tumorigenesis. Moreover, understanding the nuanced interactions between p53 and NF–κB could offer new potential avenues for developing anti-cancer therapies that privilege the pro-apoptotic pathway of p53 over the pro-survival one of NF-κB. In this section, we will describe the shreds of evidence of p53/NF-κB crosstalk, both at the functional and molecular level. There will be particular emphasis on what is still missing in this research field, thus motivating the core topic of this PhD thesis.

1.4.1. Functional crosstalk between p53 and NF–κB.

Both p53 and NF–κB signalling pathways are related to how a cell integrates different kinds of stresses and elaborates a proper response. This is particularly important in cancer, where cell response can be quite different according to the transcriptional program induced by these TFs. p53 and NF–κB exerts completely opposite functions in response to intrinsic and extrinsic sources of stress and for this reason, they have usually been described as mutual antagonists. Indeed, upon genotoxic stress, p53 elicits different transcriptional programs, that can result in temporary cell arrest, senescence or induce apoptosis (Murray-Zmijewski et al. 2008b). On the contrary, NF–κB enhances inflammation, promoting cell proliferation and resistance to chemotherapy-induced apoptosis (Ak & Levine, 2010). These contrasting outcomes of p53 and NF-κB pathways rely on the specific set of target genes. While p53 includes among its target genes those that regulate the cell cycle, apoptosis and growth-inhibiting factors, NF-κB, instead, triggers the transcription of genes promoting

cellular growth, preventing apoptosis, and releasing cytokines and chemokines involved in immune response (Gudkov et al. 2011).

Given the implication of both p53 and NF−κB in tumourigenesis and the importance they have in key cellular processes regulating cell fate, their functional antagonism could be a target of potential anti-cancer strategies (Schneider & Krämer, 2011). The simultaneous activation of p53 and the inhibition of NF−κB hold significant promise in developing a therapy aimed at balancing their effects. Eligible compounds should simultaneously activate the biological functions of p53 (not just stabilize its expression), and inhibit the NF−κB pro-survival transcriptional program (Dey et al. 2008) (Shankar et al. 2017) (Rasmi et al. 2020). Different compounds and small molecules that showed this dual mechanism are reported in **Figure 1.6**. Other compounds (not reported in **Figure 1.6**), that were found to both inactivate NF−κB and activate p53 are Curaxins (Gasparian et al. 2011) and curcumin (Allegra et al. 2018).

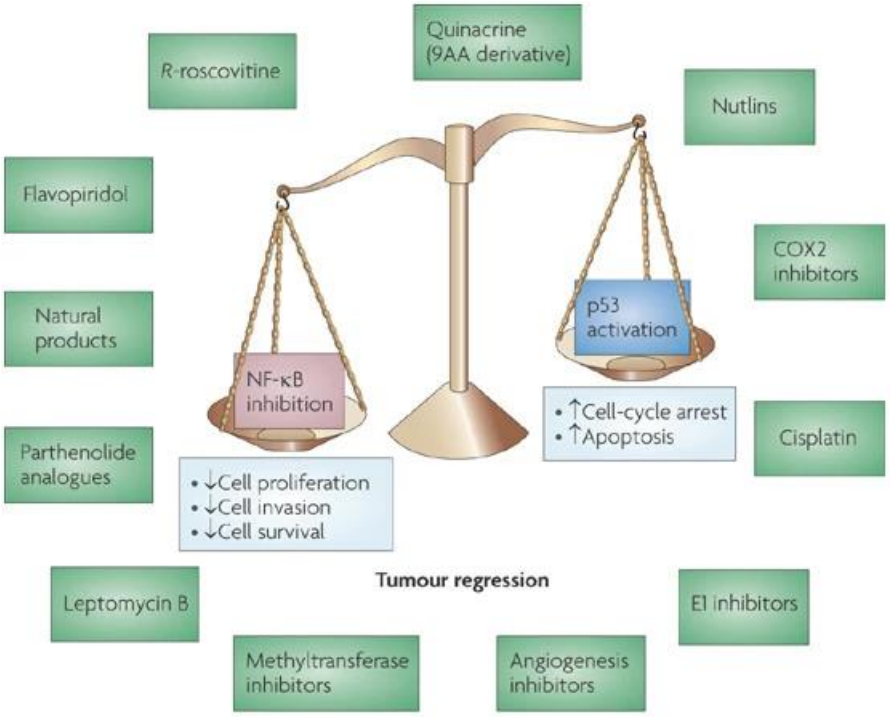

Figure 1.6. Examples of compounds that have been reported to both promote p53 functions and inhibit NF-κB activity. *A therapy targeting cancer cells should induce cell-cycle arrest or apoptosis (transcriptional programs mainly related to p53) and avoid proliferation and the enhancement of inflammation (effects related to NF-κB activation). Figure is taken from "Double-edged swords as cancer therapeutics: simultaneously targeting p53 and NF-κB pathways" by Anwesha Dey (2008).*

Nevertheless, categorizing p53/NF-κB crosstalk as a purely pro- or anti-survival process based on their functional antagonism is an oversimplification (Schneider & Krämer, 2011b); indeed, other studies revealed a sort of cooperation between these TFs. Ryan et al demonstrated that NF–κB is essential for p53-mediated cell death in osteosarcoma cells, since its impairment abrogates p53-induced apoptosis (Ryan et al. 2000). Positive regulation by NF-κB on p53 downstream functions were found by (O'Prey et al. 2010), that reported how p53-driven *Noxa* and *p53AIP1* (p53 target genes) expressions require the p65 subunit of NF-κB. Also in Neuroblastoma cells, p53 and NF–κB were found to cooperate in regulating apoptosis through the activation of MEK1 pathway (Armstrong et al. 2006). In the context of immune regulation, Lowe *et al.* demonstrated that p53 and NF–κB work synergically in human macrophages. The activation of both TFs enhanced the expression of inflammatory cytokines genes (*IL-6*, *IL-8* and *CXCL1*), suggesting an amplifying mechanism of macrophages in responding to tissue-damaging insults (Lowe et al. 2014). Inhibition of both p53 and NF–κB in IMR-90 fibroblasts resulted in both an increase of cell growth and an impairment of senescence-associated β-galactosidase (SA-β-gal) induction: this evidence suggested cooperation between p53 and NF–κB in promoting senescence (Chien et al. 2011).

Although several clues regarding its functionality, the study of p53/NF-κB crosstalk at the molecular level has revealed more complex regulatory mechanisms that cannot be reduced to mere antagonism. In the next paragraph, we will describe literature studies investigating how p53/NF-κB works at the molecular level.

1.4.2. Molecular crosstalk between p53 and NF-κB.

It is now widely known that p53/NF-κB crosstalk is involved in many different cellular processes **(Figure 1.7)** (Carrà et al. 2020). Different studies indicated that both a direct and indirect interplay between p53 and NF-κB is present at the molecular level. By "direct interplay", we mean a regulation that includes only p53 and NF-κB, while for "indirect interplay" we instead intend an interplay that involves other molecules.

The first studies investigating the direct interplay between p53 and NF–κB reported how both p53 and NF–κB (the RelA subunit, specifically) can compete for a restricted pool of p300 and CREB bind protein (CBP) complexes (Ravi et al. 1998) (Webster & Perkins, 1999). These molecules are required by both TFs for an efficient activation of their target genes and are involved in a wide array of cellular programs (Karamouzis et al. 2007). A direct interaction between p53 and NF-κB has also been

reported both in vitro and in vivo: such interplay involves TFs' respective dimerization and tetramerization regions and leads to the suppression of each other's transcriptional activity (Ikeda et al. 2000).

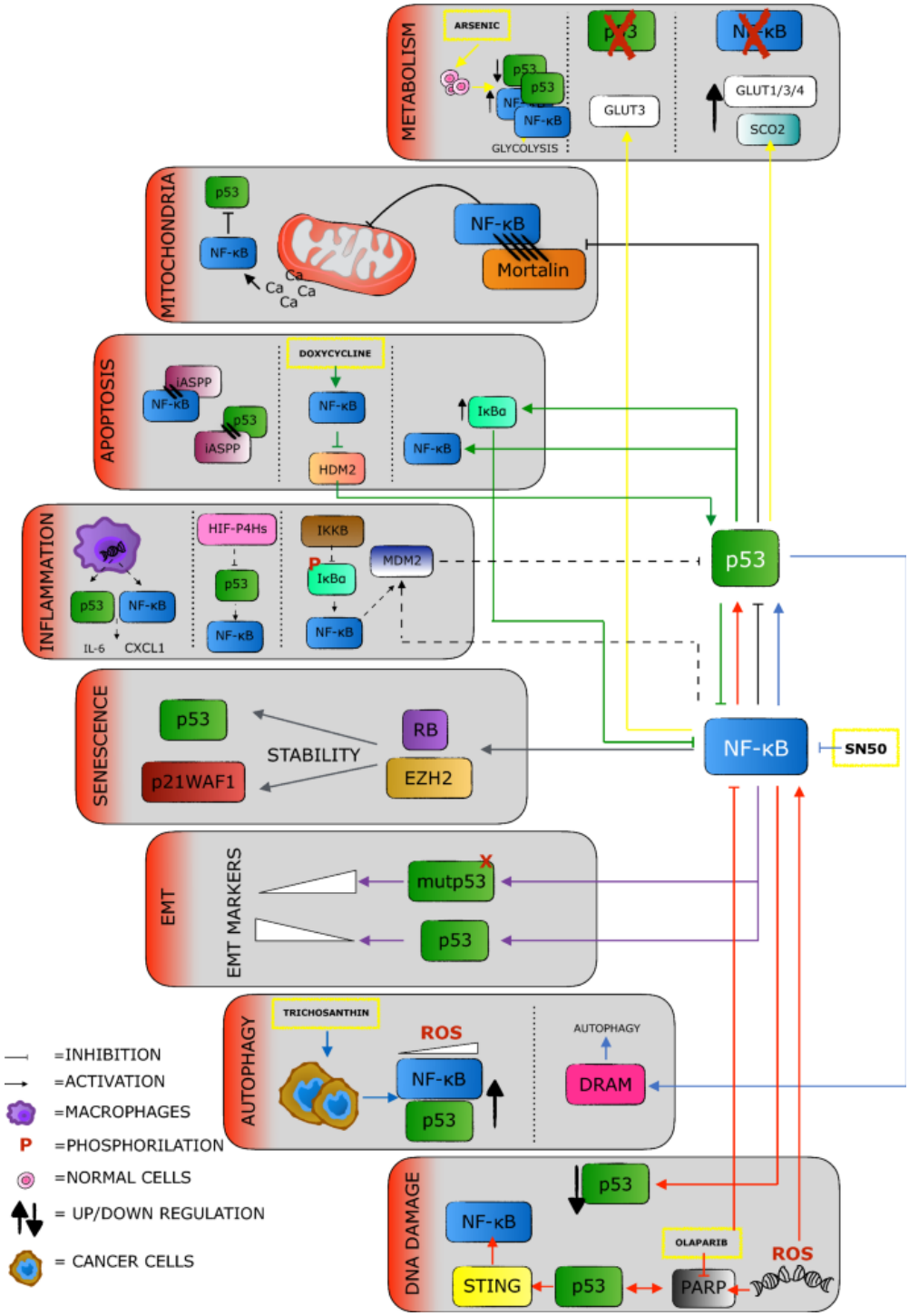

Figure 1.7. The crosstalk between p53 and NF-κB in different tumoural contexts and cellular processes. *Antagonistic or synergic behaviours are context-dependent. Figure is taken from "P53 vs NF-κB: the role of nuclear factor–κappa B in the regulation of p53 activity and vice versa" by Giovanna Carrà et al. (2020).*

These findings, however, were obtained by over-expressing p53 and NF-κB via transient transfections. The competition between p53 and NF−κB for p300/CBP binding is mediated by IKKα, which can directly phosphorylate CBP, switching its protein binding affinity from p53 to NF−κB: this contributes to the upregulation of NF−κB-mediated anti-apoptotic genes and the downregulation of p53-mediated pro-apoptotic genes (Huang et al. 2007). Another direct antagonistic interplay between p53 and NF-κB was reported by (Kawauchi et al. 2008), who investigated p53-mediated repression of NF-κB-mediated transcriptional activity. They demonstrated that upon its activation, p53 could enhance NF-κB binding to DNA, but reducing its transcriptional activity in mouse embryonic fibroblasts: the formation of a complex between p53, the p65 subunit of NF-κB and IKKα induces the phosphorylation of histone H3, thus suppressing NF-κB transcriptional activity. This study, however, was conducted with ectopically and probably over-expressed p53. In another study, the crosstalk between p53 and NF-κB was addressed in renal cell carcinoma at the molecular level, by using small molecule suppressing NF-κB activity (Gurova et al. 2005). By artificially decreasing NF-κB activity with a super-repressor of IκB, Gurova et al. showed how treatment with the small molecule 9AA (9-aminoacridine) enhances p53 response and decreases tumour growth. However, this approach employed a strong deregulation of NF-κB by using the super-repressor and triggered p53 in a non-canonical manner: p53 was phosphorylated at Ser392 residue, which is different from the residue that is typically phosphorylated by MDM2, Ser15 (Loughery et al. 2014).

Conversely, other studies reported a sort of direct positive interplay between p53 and NF-κB in regulating each other. (Wu e Lozano, 1994) highlighted that the p65 subunit of NF−κB might directly induce p53 expression, since the promoter sequence of p53 contains a binding site for NF−κB. This evidence was obtained in Hela cells under transient transfection settings. Other works revealed that the KO of p53 resulted in a repression of NF−κB transcriptional activity (Murphy et al. 2011) and in a loss of p65 occupancy, indicating that p53 is involved in maintaining NF−κB chromatin association (Cooks et al. 2013). In another work, the p52 subunit of NF-κB was found to be recruited at the promoters of p53 target genes (like *p21*, *DR5* and *PUMA*) (Schumm et al. 2006). The suppression of p52 compromised the expression of *p21* and *PUMA*, two key p53 target genes involved in the cell cycle.

Yet, beyond their individual role in influencing each other's expression and transcription of the other TF's target genes, other works have investigated indirect interactions between p53 and NF-κB at the molecular level: both MDM2 and IκBα,

key regulators of p53 and NF−κB, respectively, have been found to be involved in p53/NF−κB crosstalk.

One of the key players involved in p53 feedback loop, MDM2, can interact with NF−κB. Indeed, not only p53, but also NF−κB can transactivate the *MDM2* gene (Kashatus et al. 2006). In the context of antagonism with p53, the transcriptional upregulation of MDM2 by NF−κB, which could be mediated by IKK2 (a subunit of IKK) and Bcl3, attenuates p53 stability and promotes its degradation: this strategy was found in different kinds of cancer (Tergaonkar et al. 2002) (Kashatus et al. 2006) (Pavlakis & Stiewe, 2020). A p53-independent role of MDM2 in regulating NF−κB is also reported in the literature: (Mulay et al. 2012) demonstrated how MDM2 acts as a co-factor in the binding of NF−κB to the promoters of its target genes. Blocking MDM2 resulted in an attenuation of inflammatory response after kidney injury. It has been demonstrated that *MDM2* is a target gene of NF−κB itself and its upregulation by NF−κB is found in activated T-cells (Busuttil et al. 2010). Conversely, (Heyne et al. 2013) showed that MDM2 could bind a fraction of RelA/p65 molecules; this binding occurs at the N-terminal Rel homology domain (RHD) of RelA/p65 subunit of NF−κB and results in its ubiquitination and degradation. This evidence has been though found in H1299 lung adenocarcinoma cells (lacking p53), transfected to over-express a flag-tag version of both p65/RelA and MDM2, to study their interactions via co-precipitation assay. Interestingly, also NF−κB activation state can modulate MDM2: in rhabdomyosarcoma cells with unperturbed NF−κB pathway, MDM2 induces not only the inhibition of p53 activity, but also the activation of the NF-κB pathway; conversely, when dysregulated p65/RelA elicits constitutive NF-κB pathway activity, MDM2 was found to inhibit this pathway promoting tumour-suppression (Cheney et al. 2008).

If we instead consider the NF-κB feedback loop, it was discovered that the crosstalk with p53 can involve IκBα. It is reported that IκBα can directly interact with p53, negatively modulating its functions. In unstimulated cells, a portion of cytosolic p53 complexes with IκBα, but its dissociation (induced by the phosphorylation of p53 at Ser46 residue) can occur in response to apoptotic stress, hypoxia, DNA damage, and TGF-β1-mediated growth suppression (Chang, 2002) (Zhou et al. 2003). These interactions between IκBα and p53 may be explained by the fact that both p53 and p65 subunit of NF-κB have homologous structures in the Rel homology domain of p65 and the p53 core domain, as sustained by (Dreyfus et al. 2005) that performed alignment of p53 and p65 crystal structures. The same group demonstrated a specific interaction between IκBα and p53, which is partly mediated by the DNA binding

region of p53, and the amino terminus of IκBα. Notably, mutations in the IκBα structure strongly regulate the capability to bind, and then interfere, with NF–κB and p53. While the IκBα244C (mutant in the C-terminal domain) significantly increases the transcription levels of NF–κB and p53, causing an enhancement in p53-mediated cell death, IκBαM (dominant negative mutant) bounds both p53 and p65, inhibiting their transcriptional activities (Li, 2006). This last mutant form of IκBα is found in acute lymphoblastic leukaemia cells, where p53-induced apoptotic programs are impaired (M. Zhou et al. 2003). It has been also hypothesized that IκBα conformation can be perturbed by BCR-ABL (a kinase protein mainly involved in leukaemia), thus promoting IκBα-p53 interactions that impair p53 functions in myeloid leukaemia cells (Crivellaro et al. 2015) (Carrà et al. 2016). Conversely, p53 was found to reduce ubiquitin-proteasome related gene expression in ovarian cancer cells, thus preventing IκBα proteasomal degradation, inhibiting the NF-κB signalling pathway and promoting anti-inflammatory effects (Son et al. 2012).

In addition, IKK2, the kinase that phosphorylates IκBα, freeing NF–κB, was found to be involved in p53/NF–κB crosstalk. After DNA damage, IKK2 was found to phosphorylate p53 at Ser362 and Ser366, different residues than those involved in MDM2 binding (Xia et al. 2009). In this way, p53 levels are kept low promoting melanoma development and oncogene-induced melanocyte transformation (Yang et al. 2009) (Schneider & Krämer, 2011b). It was shown that the inhibition of IKK2 resulted in an increase in p53 levels, as well as a higher expression of p21 and the induction of cell cycle arrest and apoptosis (Yang et al. 2009). Notably, IKK2 inhibition was found to perturb p53 oscillations (triggered by DNA damage) by modulating both p53 and MDM2 degradation rates (Konrath et al. 2020). Moreover, the isoform IKKα is involved in the crosstalk between p53 and NF–κB since it can phosphorylate CBP protein modulating the competition between the two TFs for CBP binding (Huang et al. 2007) (Tergaonkar & Perkins, 2007).

From all the information reported, the crosstalk between p53 and NF–κB turns out to be very complicated, despite holding an undeniable significance in understanding cancer cells' responses to stress, chemotherapy and inflammation. This intricate interplay revealed a multifaceted phenomenon, orchestrated by different intermediary and subsidiary proteins: all the previously mentioned relationships between p53, NF–κB and their regulators are reported in the scheme in **Figure 1.8**. This scenario highlights the complexity inherent in p53/NF-κB interactions, which appear even contradictory; moreover, such different interplays and consequent outcomes are strictly related to the cellular context. In addition to mutual

antagonism/cooperation, other degrees of complexity may be considered as well. Mutations of p53, a common hallmark of cancer, were found to be implicated in enhancing NF-κB activity and inflammation (Weisz et al. 2007) (Cooks et al. 2013). Moreover, new different genes have been identified as targets of both p53 and NF-κB and could act as key nodes of their crosstalk. It has been found via genomic analysis that *CDKN1A*, *IL4I1*, *SERPINE1* and *RRAD* are genes co-regulated by p53 and NF-κB in cells treated with ionizing radiation. The degree of activation of such genes relies on p53/NF-κB balance and can result in different cellular outcomes (Szołtysek et al. 2018).

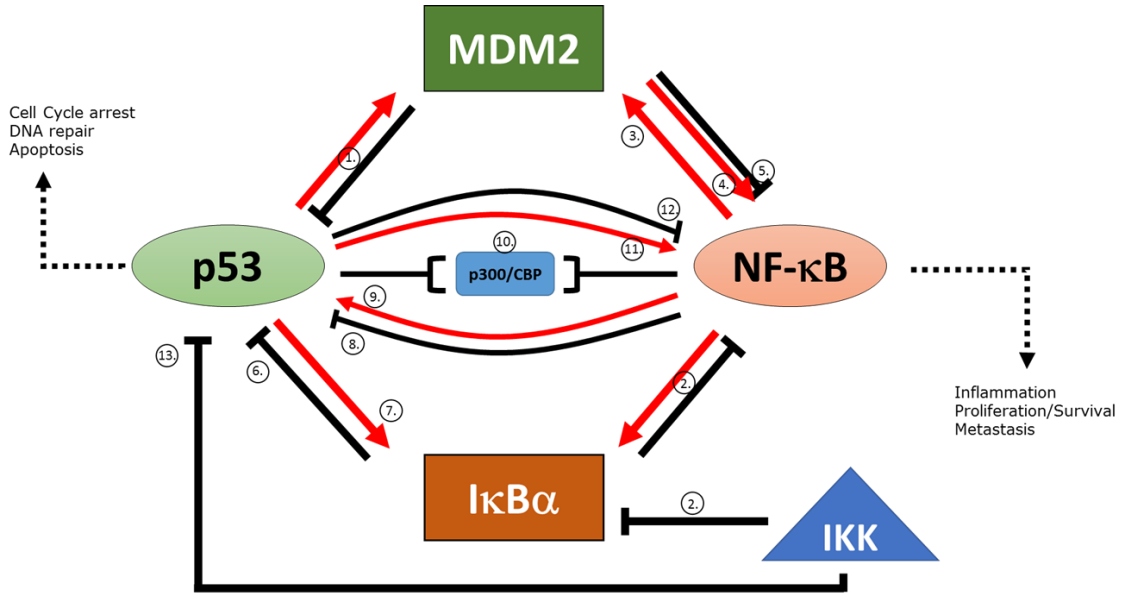

Figure 1.8. Scheme of the crosstalk between p53, NF-κB and other players involved in their feedback loops (MDM2, IκBα and IKK). *Red arrows indicates positive regulation, black arrows indicate negative regulation, dotted lines indicates the cellular processes induced by p53 and NF-κB. Single relationships between these molecules are reported with citations from the specific study describing it. References:* ***1.*** *Lahav G. et al. Nat. Genet. 2004.* ***2.*** *Hoffmann A. et al. Science, 2002.* ***3.*** *Lowe G. et al. J. of Bio. Chem. 2010.* ***4.*** *Thomasova D. et al. Neoplasia, 2012.* ***5.*** *Heyne K. et al. Cell Cycle, 2013.* ***6.*** *Carrà G. et al. Int. J. Mol. Sci, 2016.* ***7.*** *Shao J. et al. Oncogene, 2000. Son D. et al. Plos One, 2012.* ***8.*** *Gurova K. et al. Proceedings of the National Academy of Sciences, 2005.* ***9.*** *Wu & Lozano, Journal of Biological Chemistry, 1994.* ***10.*** *Ravi R. et al. Cancer Research, 1998.* ***11.*** *Bohuslav J. et al. J. of Biol. Chemistry, 2004; Cooks T. et al. Cancer Cell, 2013.* ***12***. *Gudkov & Komarova. Cold Spring Harbor Perspectives in Medicine, 2016.* ***13***. *Xia Y. et al. Proceedings of the National Academy of Sciences, 2009.*

However, previous studies investigated p53/NF-κB crosstalk, highlighting either their antagonism or cooperativity, by using transient transfections, over-expressing one TF (H. Wu & Lozano, 1994) (Ikeda et al. 2000) (Gurova et al. 2005). These approaches, although valid, can mask the effect of one TF on the other or modify the complex transcriptional network in which they are entangled, activating non-

canonical pathways, or leading to TFs non-physiological levels that can significantly alter the transcriptional outcomes.

Further, what is also lacking is a dynamic perspective on this interplay, that could help clarify the complexity of the interactions arising from the wide variety of experimental evidence described above. As described in the previous paragraphs, both p53 and NF-κB are involved in two feedback loops, resulting in different dynamical accumulation in the nucleus. Such different dynamics are crucial in regulating their functions since they strongly influence the expression of target genes and global cell fate. Previous studies investigating p53/NF-κB crosstalk were performed in a "static" manner, and the clues found may appear incomplete. To further decipher the regulatory nodes common to these two pathways, we must move beyond snapshots of their behaviours and delve into the real-time temporal dynamics, accounting also for cell heterogeneity. A comprehensive view of how p53 and NF-κB dynamically communicate, regulate, and influence each other's functions is a missing piece in the puzzle.

2. AIM OF THE WORK

Cells integrate stresses through the activation of different transcriptional programs. p53 and NF–κB are two core TFs involved in cell response to DNA damage and inflammation. They are typically described as antagonists in cancer: while p53 induces cell cycle arrest or tumour suppression, NF–κB promotes a chronic inflammatory status thus enhancing tumour development. They are often dysregulated in cancer: p53 is mutated or repressed, while NF–κB is upregulated and persistently activated. A reciprocal influence between them has emerged as a hallmark of different cellular processes in cancer cells. However, it is not totally understood how p53 and NF–κB crosstalk leads to reciprocal up/downregulation or tunes their target genes and cell fate.

p53 and NF–κB pathways are coupled at multiple regulatory nodes: the resulting gene expression and cellular outcomes (e.g., apoptosis vs. cell cycle arrest) could depend on such interplay. The mechanism behind such crosstalk requires further investigation, especially since targeting p53/NF-κB crosstalk is increasingly considered crucial to induce apoptosis in cancer cells. A possible limitation of previous studies is that they were performed in "static" conditions and do not provide a description of how the crosstalk might be regulated over time. Indeed, time is a fundamental dimension in this context: the activation of both p53 and NF–κB result in dynamic and pulsatile modulation of their nuclear levels. Moreover, different p53 and NF–κB dynamics can cause different gene expression profiles and cellular fates. Their dynamics – and their role in modulating cellular functions – have been so far studied separately, a condition that poorly represents a tumour scenario where multiple stimuli (e.g., therapy for p53 and inflammation for NF–κB) simultaneously impinge both TFs pathways. How the oscillatory dynamics of both TFs are integrated into their crosstalk, modulate gene expression and cell fate remains to be unravelled.

The general purpose of this PhD thesis is to investigate the crosstalk between p53 and NF-κB with a dynamic perspective and study how the interplay between their dynamics regulates cellular life/death decisions in response to stresses. To investigate this, we (a) applied live-cell fluorescence microscopy to assess whether p53 and NF–κB dynamic behaviours affect each other in breast cancer cells; (b) performed gene editing on p53/NF–κB to evaluate the contribution of one TF in regulating the other one's dynamics; (c) investigated whether p53/NF–κB coupled dynamics can modulate the expression of related genes and cellular outputs (like DNA damage repair and cell fate).

3. RESULTS

3.1. First evidence of p53/NF–κB crosstalk in MCF-7 cells.

In this first part, we illustrate the cellular model adopted in this work and its validation after gene editing to obtain both p53 and NF–κB fluorescently tagged, necessary to characterize TFs dynamics with live-cell microscopy. We then show how p53 dynamics result perturbed after a simultaneous activation of both p53 and NF–κB upon specific stimuli triggering sustained or oscillatory p53 dynamics.

3.1.1. Cellular model validation and first evidence of p53/NF-κB crosstalk.

To investigate the crosstalk between p53 and NF–κB we chose the breast cancer MCF-7 cell line. These cells carry both NF-κB and p53 functional pathways, as we assessed by RT-qPCR. At 1 hour after TNF–α treatment (10 ng/mL), *NFKBIA* expression increases **(Figure 3.1A)**, thus indicating an activation of NF–κB-mediated transcription. At 8 hours after Nutlin (10 μM) treatment (that induces a sustained accumulation of p53, by blocking its interaction with MDM2), *CDKN1A* expression is raised **(Figure 3.1B)**.

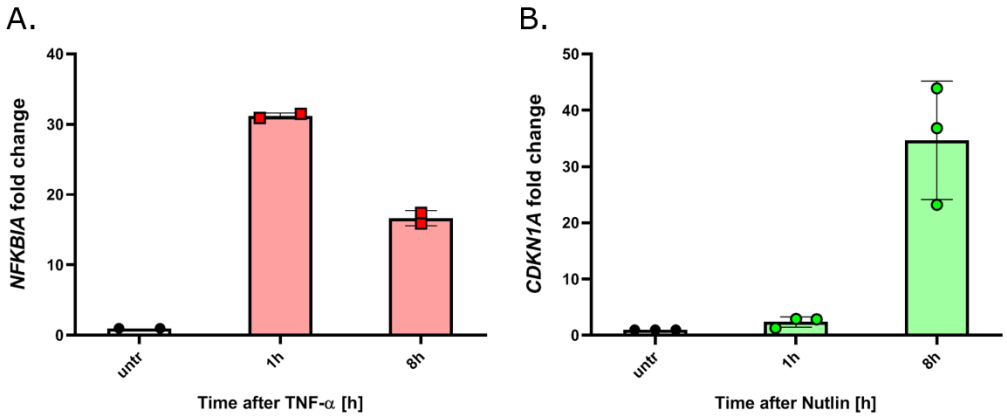

Figure 3.1. qPCR assessing the expression of p53 and NF-κB targets in MCF-7*. (A) NFKBIA expression in MCF-7 cells at 1 and 8 h after TNF-α. N° biological replicates = 2. (B) CDKN1A expression in MCF-7 cells at 1 and 8 h after Nutlin. N° biological replicates = 3.*

In order to study TFs dynamics via live-cell imaging, our lab developed an MCF-7 line in which p53-GFP was knocked-in (KI) via gene editing. Cells were collected at several time points after γ-irradiation and p53 dynamics was assessed via Western Blot (**Figure 3.2A**), giving an oscillatory dynamic of p53-GFP after DNA damage induction

(with a period of oscillations of around 5 hours after γ-irradiation), consistent with previous reports. This cell line was also validated via qPCR, thus comparing the expression of two p53 target genes (*CDKN1A* and *MDM2*) with the parental line: both genes are upregulated at 4 hours after γ-irradiation (10 Gy)(**Figure 3.2B**).

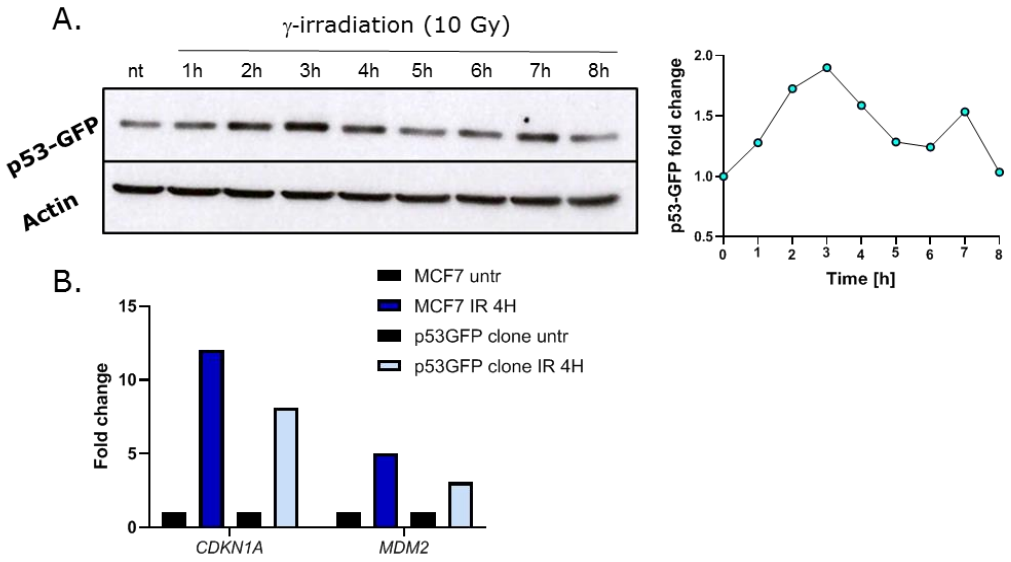

Figure 3.2. Validation of MCF-7 p53-GFP line. *(A) Western Blot assessing p53-GFP oscillations upon DNA damage induction via γ-irradiation. N° biological replicates = 1. (B) qPCR on CDKN1A and MDM2 expression upon DNA damage induction via γ-irradiation. N° biological replicates = 1.*

We wondered if triggering p53 pathway had some effects on NF-κB dynamics and vice versa. For this reason, we firstly evaluated both p53 nuclear levels and NF–κB nuclear/cytosolic localization upon stimuli triggering one or both TFs using specific stimuli (Nutlin, TNF-α and Nutlin+TNF-α, respectively) via immunofluorescence assay.

As a first result, NF-κB dynamics did not seem to be affected by p53 activation. Treatment by Nutlin alone did not result in NF-κB translocation in the nucleus, as expected (**Figure 3.3A**). Additionally, NF-κB nuclear-to-cytosolic localization, computed with the nuclear-to-cytosolic ratio (N.C.R.), over time did not seem to be majorly perturbed upon co-stimulation: both TNF-α and Nutlin+TNF- α treatments trigger NF-κB translocation within 1 hour after the stimulus (N.C.R. => 1) and then it is mostly cytosolic up to 8 hours (N.C.R. < 1). We note that NF-κB N.C.R. at 30 mins and 1 hour is slightly lower for the Nutlin+TNF-α, but we do not expect this difference to be related to p53 activation, since at these early time-points, Nutlin has not yet led to a significant p53 accumulation.

We next observed that, while TNF–α treatment does not activate p53 at all, p53 progressively accumulates inside the nucleus upon Nutlin treatment, as expected.

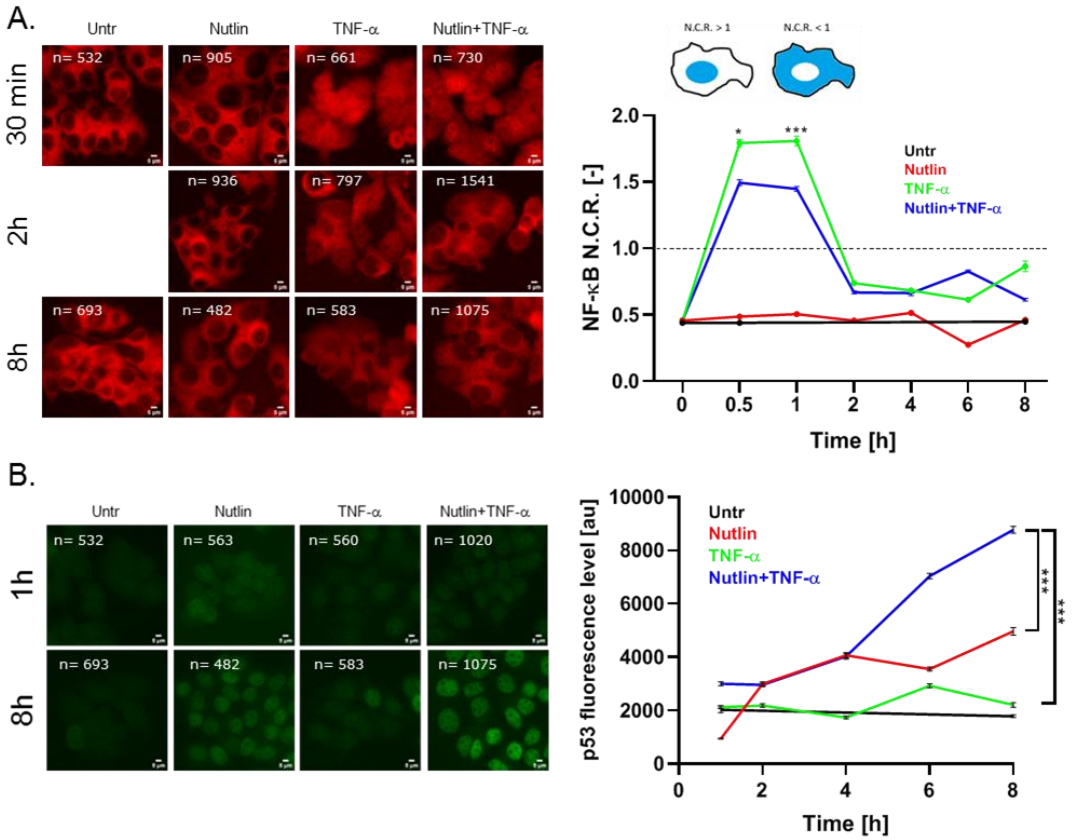

Figure 3.3. Time-course on p53-GFP and NF-κB upon Nutlin and TNF-α treatments. *(A) Immunofluorescence up to 8 hours on NF-κB reveals that NF-κB dynamics is not perturbed by simultaneous p53 activation by Nutlin. (B) Immunofluorescence up to 8 hours on p53 reveals that its nuclear accumulation is higher if cells are co-treated with Nutlin and TNF-α. Representative images; n stands for the number of analysed cells. Scale bar = 5 μm. Data plotted: mean ± S.E.M. N° biological replicates = 1. Statistical test: Kruskal-Wallis (*p< 0.05, **p< 0.01, ***p< 0.005).*

Interestingly, by activating both pathways with Nutlin and TNF-α, p53 nuclear abundance increases to higher levels than with Nutlin treatment alone over time (**Figure 3.3B**). To confirm this observation, we quantified p53 protein levels via Western Blot by treating cells with Nutlin and Nutlin+TNF-α. We were able to assess the enhancement in p53 accumulation, also with this technique, by Nutlin upon a coupled activation of NF-κB by TNF-α (**Figure 3.4**). We next wondered if this enhancement in p53 levels upon TNF-α is transcriptionally functional.

We then performed single-molecule fluorescence *in situ* hybridization (smFISH), a technique that enables to measure the number of copies of a selected mRNA with single-cell sensitivity by employing multiple fluorescently labelled oligonucleotides to target the mRNA of interest (Imbert et al. 2021). With this technique, we quantified

the expression of *CDKN1A*, a major target gene of p53, upon Nutlin and TNF-α at 1 and 8 hours after treatments. We obtained that the greater levels of nuclear p53 observed upon Nutlin+TNF-α treatment also induce a stronger expression of *CDKN1A* gene expression (**Figure 3.5**), suggesting that the higher amount of accumulated p53 is functional and enables the transcription of its targets.

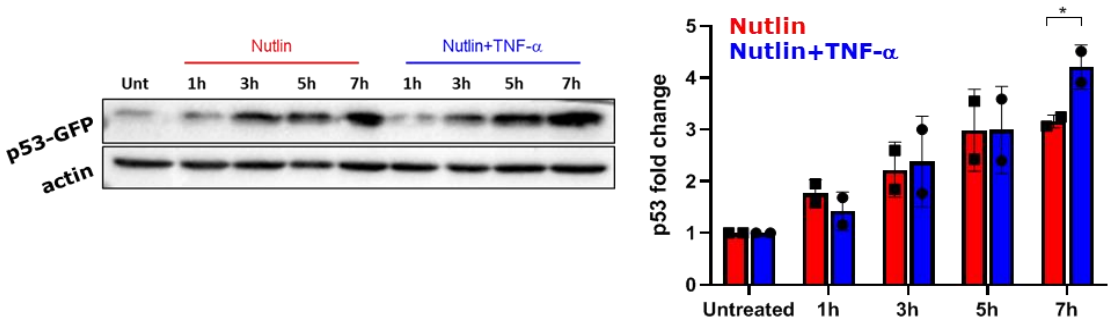

Figure 3.4. Western Blot to evaluate p53 response to Nutlin and Nutlin+TNF-α. *We compared the effects on p53 accumulation by Nutlin and Nutlin+TNF-α and the double treatment induces a stronger accumulation of p53, a trend similar to that obtained from immunofluorescence assay. N° biological replicates = 2. Statistical test: unpaired T-test, one-tailed p-value (*p< 0.05, **p< 0.01, ***p< 0.005).*

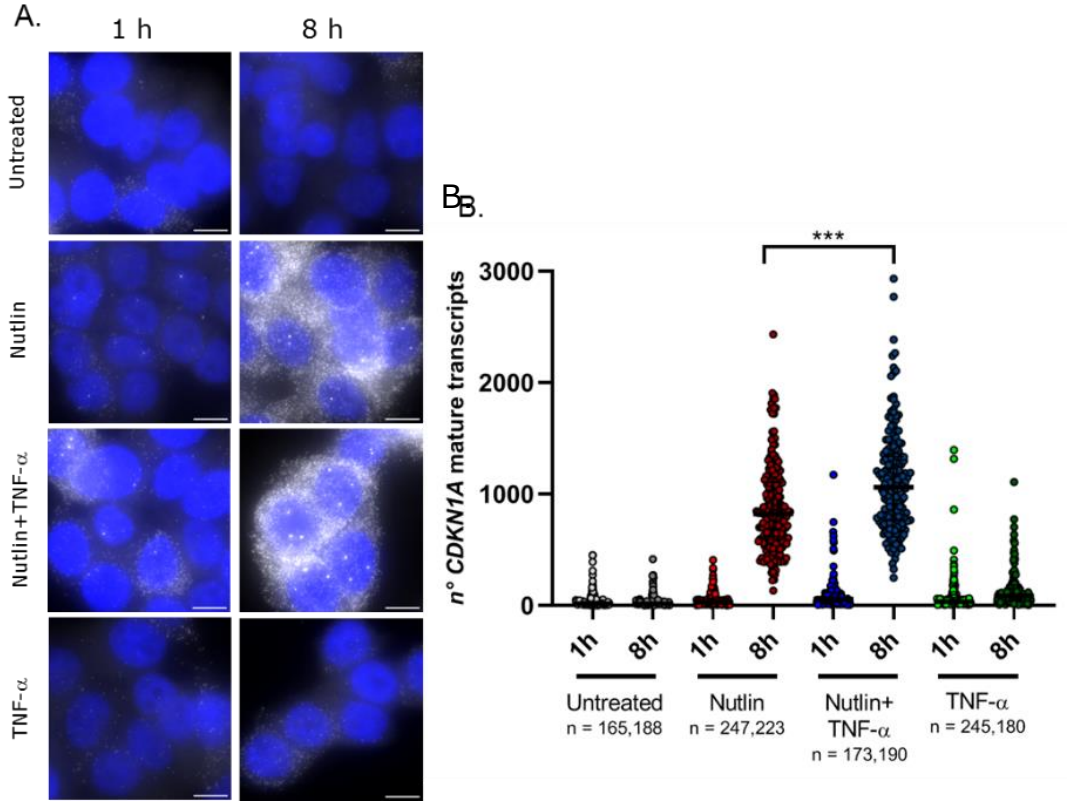

Figure 3.5. smFISH on CDKN1a upon simultaneous activation of p53 and NF-κB. *(A) Exemplary smFISH acquisitions (blue = Hoechst, white = CDKN1A probe). Scale bar = 5 μm. (B) Quantification of mature mRNAs levels. The double treatment results in a greater activation of CDKN1A gene, indicating that the enhancement in p53 levels with this coupled activation with NF-κB is functional at the transcriptional level. N° of analysed cells are reported for each condition. N° biological replicates = 1. Black bar = median, with interquartile range. Statistical test: Kruskal-Wallis (*p< 0.05, **p< 0.01, ***p< 0.005).*

3.1.2. Live cell imaging reveals an enhanced p53 accumulation upon Nutlin when NF-κB is simultaneously activated.

To further investigate previous findings in fixed MCF-7 cells (p53-GFP line), we moved to confocal microscopy. To follow coupled p53 and NF-κB dynamics in living cells, we performed a lentiviral infection (see details in Materials and Methods, **paragraph 5.3**) on this cell line so they express the p65/RelA subunit of NF−κB fused with the fluorescent tag mScarlet, under the control of the endogenous p65 promoter. We chose this combination of fluorescent molecules since they have separated spectra (GFP: $\lambda_{exctiation}$ = 475 nm, $\lambda_{emission}$ = 509 nm; mScarlet: $\lambda_{exctiation}$ = 569 nm, $\lambda_{emission}$ = 594 nm), so we did not expect bleedthrough in the fluorescence emission of the two fluorophores. After the infection, mScarlet-positive cells were sorted and NF−κB activation was validated via confocal imaging. The setup for live-cell imaging includes an incubator that ensures a standard environment for cells (5% CO_2 at 37°C) and enables time-lapse acquisitions. We validated fluorescently tagged TFs dynamics upon previous cited treatments. The treatment with Nutlin induces a progressive accumulation (sustained dynamics) of nuclear p53 (**Figure 3.6A**), while γ-irradiation (10 Gy) generates p53 oscillations, with two major peaks detectable at around 3 and 8 hours after irradiation (**Figure 3.6B**). The addition of TNF-α leads to partial NF−κB translocation to the nucleus within 30 minutes after the stimulus. After 1 hour, NF−κB is already back into the cytosol and no further translocations are observed at later

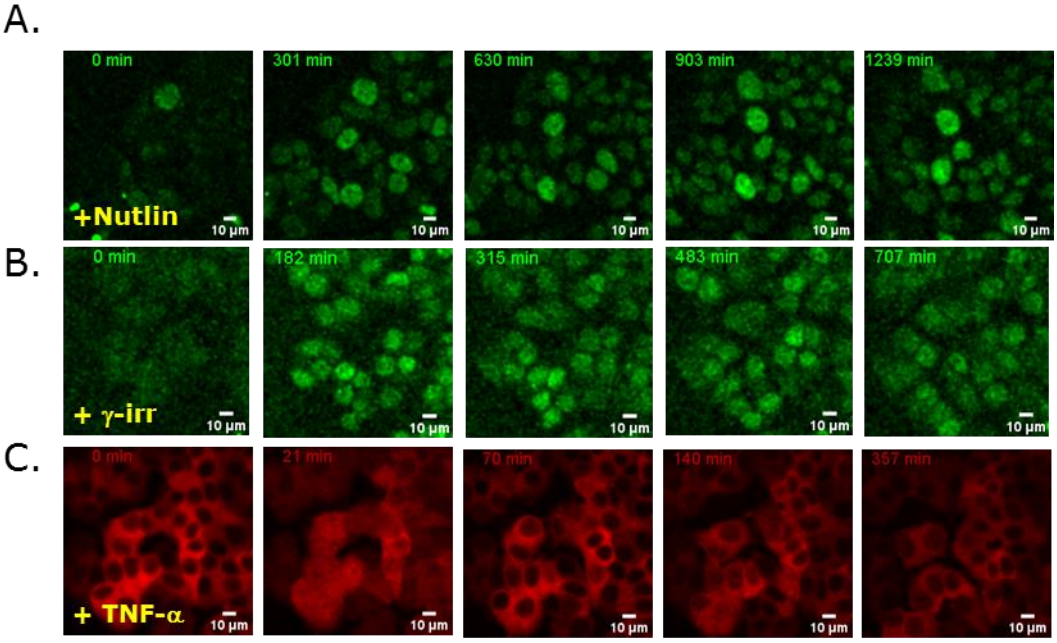

Figure 3.6. Validation of MCF-7 double-tagged line with live-cell confocal imaging. *(A) p53-GFP sustained dynamics upon Nutlin and (B) oscillations upon γ-irradiation are perceptible. (C). NF-κB-mScarlet translocation is visible at around 30 minutes upon TNF-α treatment. Scale bar: 10 μm.*

times (**Figure 3.6C**). Hence, this model allows following both p53 and NF-κB dynamics using live-cell imaging and such dynamics follow physiological trends.

To analyse single-cell dynamics of both p53 and NF-κB, we generated a semi-automatic pipeline written in ImageJ Macro language and MATLAB (see details in Materials and Methods, **paragraph 5.9**). Briefly, movies acquired at confocal microscope are separated according to stimuli and fields of view. Usually, to determine the mean cytosolic NF–κB intensity, a ring with a radius slightly larger than the nucleus is generated around each nucleus, and the average intensity within this region is calculated (Kizilirmak et al. 2021). However, MCF-7 cells tend to grow very close to each other and this worsens the correct quantification of the nuclear-to-cytosolic ratio (N.C.R.) for NF-κB. We then used a Machine learning trained network called Cellpose (Stringer et al. 2021) for automatic and precise segmentation of both cell nuclei and entire cell boundaries in each frame. A stack with the time-course of single-cell masks is then generated. Next, single nuclei masks are associated with the respective cytoplasm masks and both the nuclear intensity of p53 and the nuclear to cytosolic fluorescent intensity ratio of NF–κB are calculated. Then, each cell is tracked between frames via an algorithm called the Hungarian linker method (Jaqaman et al. 2008) (Careccia et al. 2019). Single-cell profiles are then extracted and grouped in matrices, from which different features of TFs dynamics, can be computed (**Figure 3.7**), like the area-under-the-curve (AUC, that quantifies the total protein level accumulation), timings and intensities of peaks of oscillation.

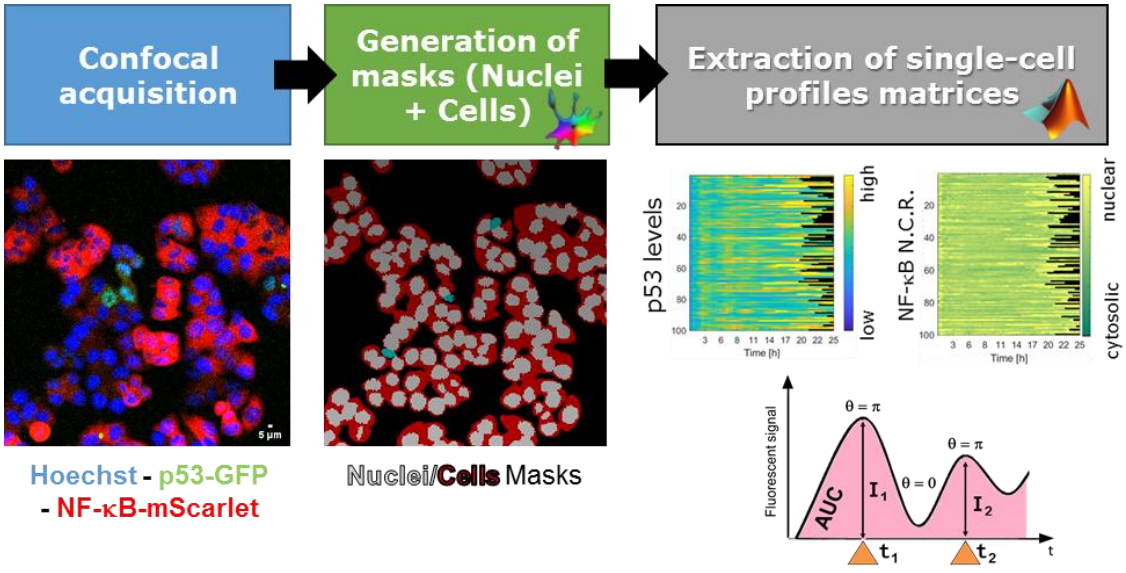

Figure 3.7. Pipeline for time-courses analysis. *Time-lapses at confocal microscope are processed via custom-written routines, extracting single-cell profiles of both p53 and NF-κB and quantifying features of their dynamics.*

We then triggered p53 sustained dynamics with Nutlin and NF-κB translocation with TNF-α and we followed cells after these single and coupled treatments. With our pipeline, we were able to extract single-cell profiles, as shown in **Figure 3.8A** for NF-κB and **Figure 3.9A** for p53. From this matrix representation, where dynamics differences can be visually displayed, a first strong peak of NF–κB nuclear localization is detectable at the beginning of the time-course. After this first synchronous peak among the cell population, a clear NF–κB translocation is no longer detectable, except in isolated cases and for brief moments. This leads to the observation that in MCF-7 cells NF-κB does not show persistent oscillations after a first trigger, as instead happens in other cell lines (Kellogg & Tay, 2015). However, this kind of behaviour has also been observed for other cell lines, like HeLa cells (Lee et al. 2016) (Zambrano et al. 2020). As we previously saw from experiments in fixed cells, NF-κB dynamics triggered by TNF-α is not perturbed if p53 is activated by Nutlin at the same time (**Figure 3.8B-C**). No differences are detectable from average profiles and, despite a small but significant difference of maximum NF-κB translocation level after Nutlin+TNF-α, its timing is around 30 minutes after the stimulus with TNF-α, so

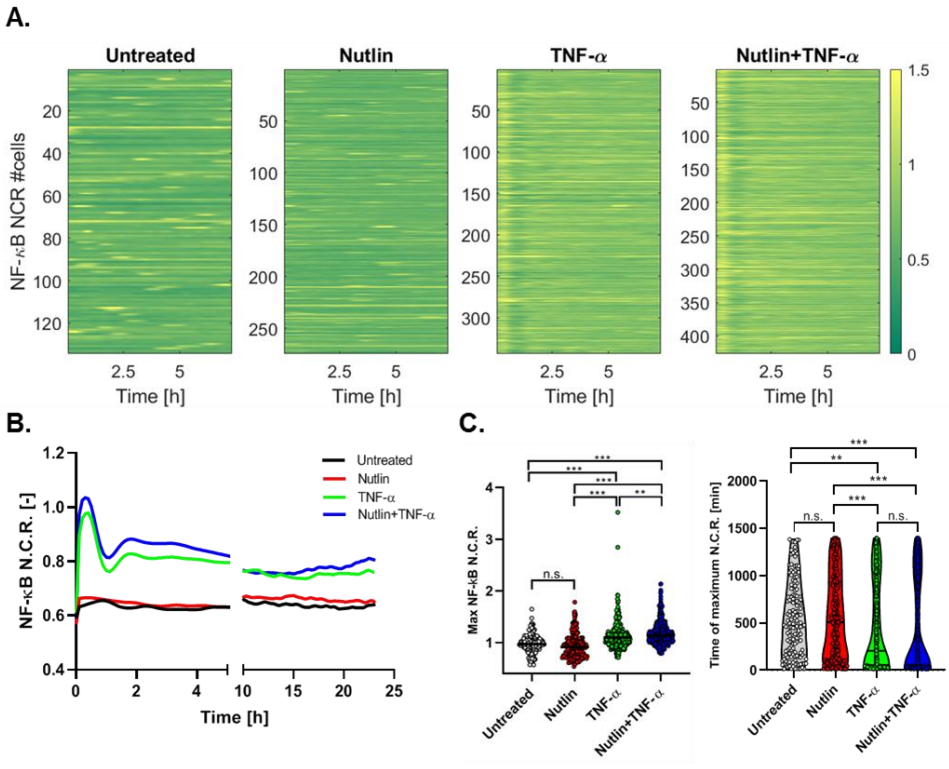

Figure 3.8. Quantification of NF-κB dynamics features. *(A) After TNF-α treatment, NF-κB translocates in around 30 minutes and then returns in the cytoplasm. NF-κB N.C.R. profiles are plotted up to 7 hours to enhance early NF-κB translocation. (B) Average profiles on NF-κB N.C.R. (C) Quantification of maximum NF-κB translocation level (left) and respective timing (right). Black bar = median, with interquartile range. Statistical test: Kruskal-Wallis (*p< 0.05, **p< 0.01, ***p< 0.005).*

before p53 activation by Nutlin. Interestingly, p53 sustained dynamics induced by Nutlin is instead enhanced by the addition of TNF-α. As shown in single-cell matrices, p53 levels accumulated more if cells were treated with both Nutlin and TNF–α than with Nutlin alone (**Figure 3.9A**). Exemplary profiles of how p53 sustained dynamics behave in single cells and the average profiles of cell population are reported in **Figure 3.9B** and **Figure 3.9C**, respectively. These results are also confirmed via the area-under-the-curve quantification, assessing a greater accumulation of p53 upon Nutlin+TNF-α treatment than Nutlin alone (**Figure 3.10**). We therefore wondered what happens if we trigger a different kind of p53 dynamics and activate NF-κB at the same time.

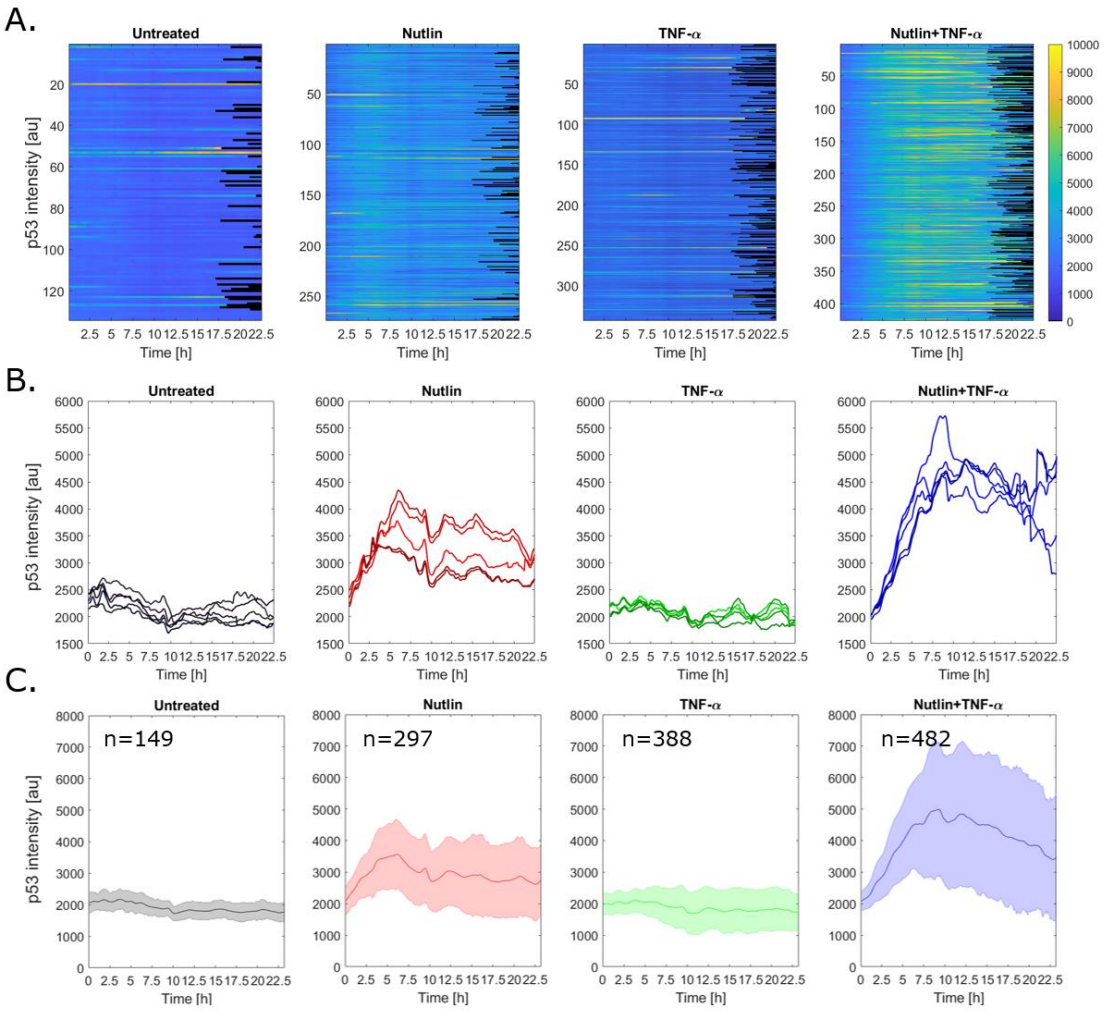

Figure 3.9. Single-cell p53 profiles upon Nutlin. *(A) We triggered p53 sustained dynamics by adding Nutlin to our cells. Simultaneous activation of NF-κB with TNF-α enhanced p53 response to Nutlin. Single-cell matrices of p53 profiles. (B) n° single-cell p53 profiles = 5. (C) Median of p53 profiles; coloured area: interquartile range, n = number of analysed cells.*

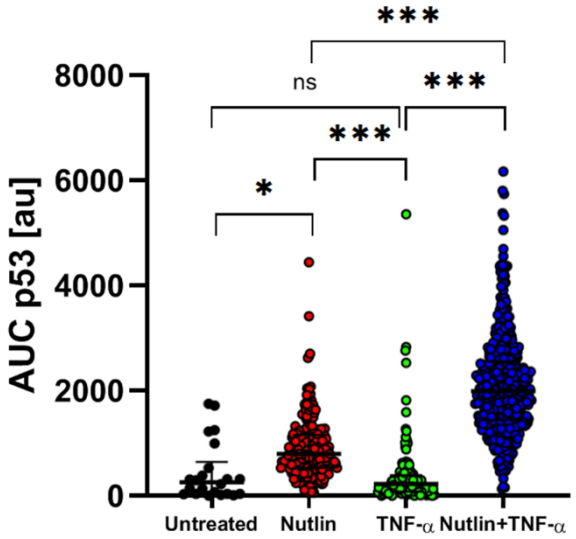

Figure 3.10. Quantification of p53 accumulation upon Nutlin and TNF-α. *We quantified the area-under-the-curve from single p53 profiles. Nutlin+TNF-α treatment induces a higher accumulation of p53 than Nutlin treatment alone. Black bar = median, with interquartile range. Statistical test: Kruskal-Wallis (*p< 0.05, **p< 0.01, ***p< 0.005).*

3.1.3. p53 oscillations are perturbed by TNF-α stimulation.

We next exposed our cells to γ-irradiation (10 Gy), a stimulus that induces DNA damage and triggers p53 oscillations (Lev Bar-Or et al. 2000). We also activated the NF–κB pathway by adding TNF-α. Upon γ-irradiation alone, p53 levels oscillate and two peaks of oscillations are clearly visible from the single-cell matrix (at around 3 and 7 hours after the stimulus) **(Figure 3.11A)**. Upon activation of both TFs with γ-irradiation and TNF–α, p53 dynamics is perturbed. The second peak of oscillation is much more recognizable and p53 levels reach a higher intensity than with γ-irradiation alone. From exemplary profiles from single cells and the population median profile of p53, it seems that NF–κB activation via TNF-α perturbs p53 oscillations, turning this kind of dynamics into a more sustained accumulation over time (**Figure 3.11B-C**). We quantified the parameters of these dynamics. First, p53 oscillations result to be accelerated if we also activate NF–κB with TNF-α: in this case, the second peak of oscillation occurs earlier, reducing the inter-peak time interval (**Figure 3.12A-B**).

Moreover, a greater amount of p53 accumulates in nuclei after the co-activation with NF–κB and the second peak of oscillation reaches higher levels (**Figure 3.12C-D**). Therefore, while γ-irradiation alone brings a damped p53 oscillation, the addition of

TNF-α induces more rapid p53 oscillations that turn into a monotonic increase in this time span.

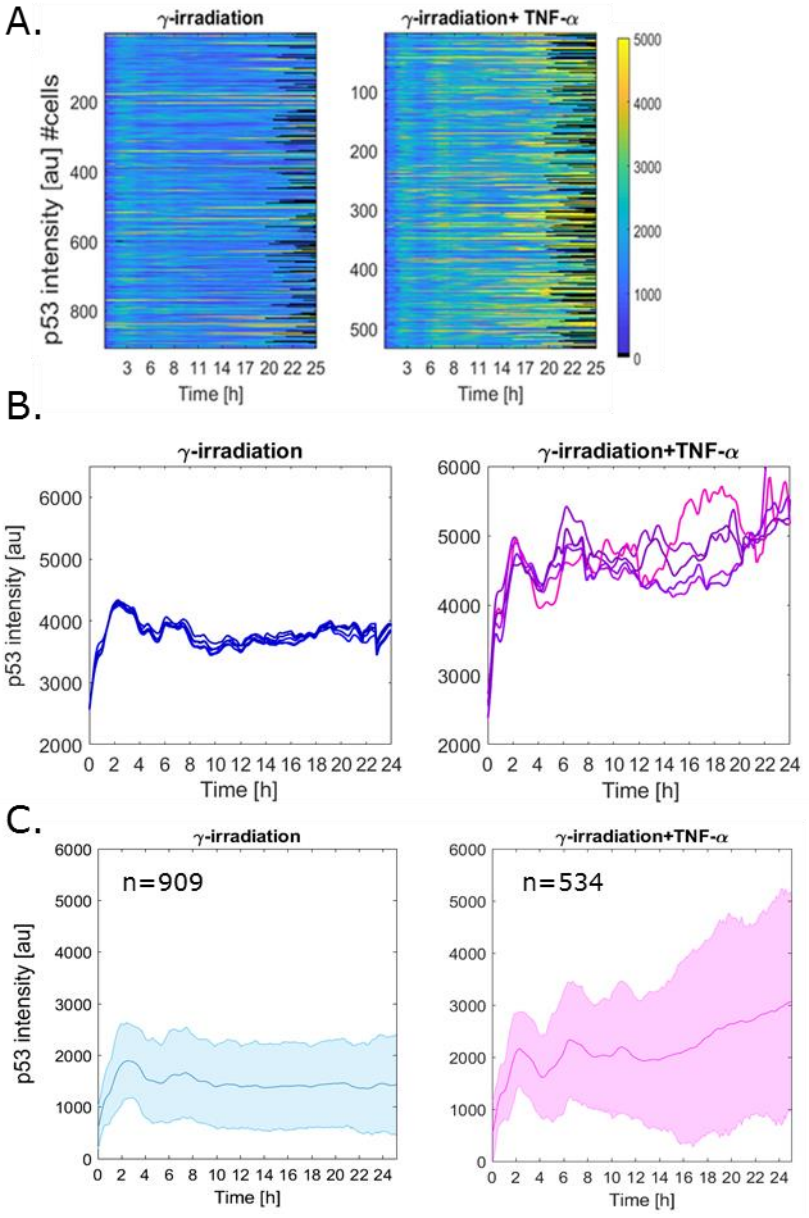

Figure 3.11. Single-cell p53 profiles upon DNA damage induction. *(A) We triggered p53 oscillatory dynamics with γ-irradiation. A coupled treatment with TNF-α, that triggers NF-κB activation, perturbs p53 oscillations. Single-cell matrices of p53 profiles. (B) n° single-cell p53 profiles = 5. (C) Median of p53 profiles; coloured area: interquartile range, n = number of analysed cells.*

Overall, these results suggest a possible crosstalk between p53 and NF–κB in MCF-7 cells that has a more drastic effect on p53 dynamics: when we activate both TFs, p53 dynamics (sustained and oscillatory) result perturbed by TNF-α. However, TNF-α can

trigger other different pathways than NF–κB that may have effects on the regulation of p53 activity (Milne et al. 1994) (Sabio & Davis, 2014). Furthermore, the system used for live-cell imaging had both the endogenous (untagged) version of NF-κB, so the fluorescently tagged version might not mirror the dynamics of the endogenous one. Hence, we next decided to generate more suitable cellular models to address these issues and to perform live cell imaging experiments to understand if these perturbations of p53 dynamics that we observed by adding TNF–α do indeed depend on NF–κB.

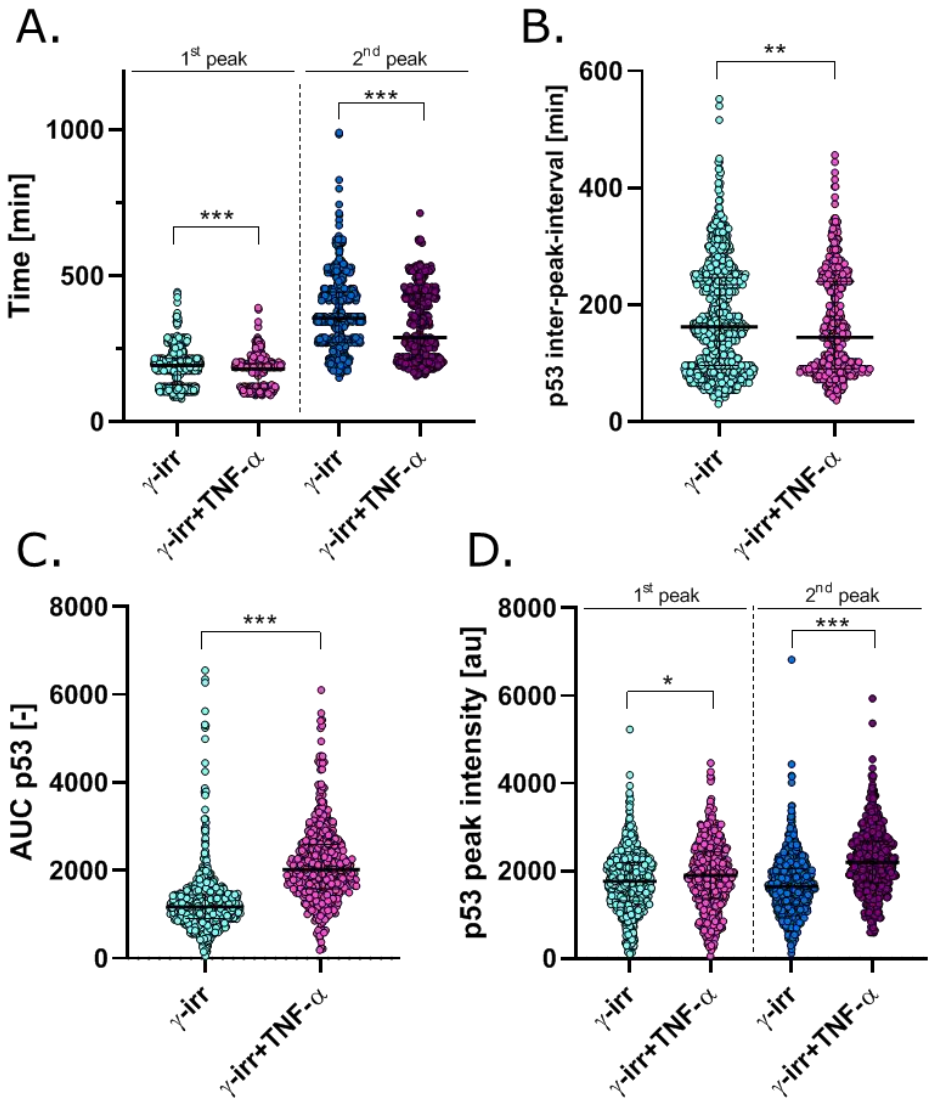

Figure 3.12. Quantification of p53 oscillations features upon γ-irradiation and TNF-α. *From single-cell p53 profiles we quantified (A) timings of oscillations peaks (statistical test: Kruskal-Wallis), (B) inter-peak-intervals (statistical test: unpaired t-test), (C) area-under-the-curve (statistical test: unpaired t-test) and (D) p53 intensity at the first two oscillation peaks (statistical test: Kruskal-Wallis). Significance: *p< 0.05, **p< 0.01, ***p< 0.005.*

3.2. NF–κB activation drives p53 dynamics perturbations.

In this section, we investigate whether NF-κB plays a role in the perturbation of p53 sustained and oscillatory dynamics we previously observed. We generated and characterized new MCF-7 cell lines: starting with the cell line carrying endogenous p53 labelled with GFP, we generated a first model where NF-κB was knocked-out and a second one where we re-introduced p65-mScarlet under the control of the endogenous p65 promoter, so all protein copies of both TFs were fluorescently tagged. We next studied p53 dynamics upon γ-irradiation/Nutlin and TNF-α comparing these cells. We also triggered NF-κB activation with another inflammatory cytokine (IL-1β), to assess whether an enhancement in p53 sustained dynamics upon Nutlin is still inducible, as we saw after coupled treatment with TNF-α.

3.2.1. Generation and validation of double tagged and NF-κB KO cell lines.

Following the preliminary results described above, we focused on developing the cellular material necessary for studying p53 dynamics in presence/absence of NF–κB. Briefly, we performed a knock-out (KO) by CRISPR-Cas9, to completely remove the p65/RelA monomer of the NF-κB protein, on the MCF-7 p53-GFP clone we previously generated. After the transfection with specific CRISPR-Cas9 vectors (see details in Material and Methods, **paragraph 5.3**), cells underwent antibiotic selection. We then obtained a pool of cells from which single-cell clones were isolated, expanded and screened. The first clone we obtained carries p53-GFP (without the endogenous protein) and is p65 KO (as confirmed by Western Blot in **Figure 3.13**), which will be called NFkB$^-$. From this new population, we repeated the lentiviral infection with the p65-mScarlet construct and we repeated clonal isolation and screening. In this way,

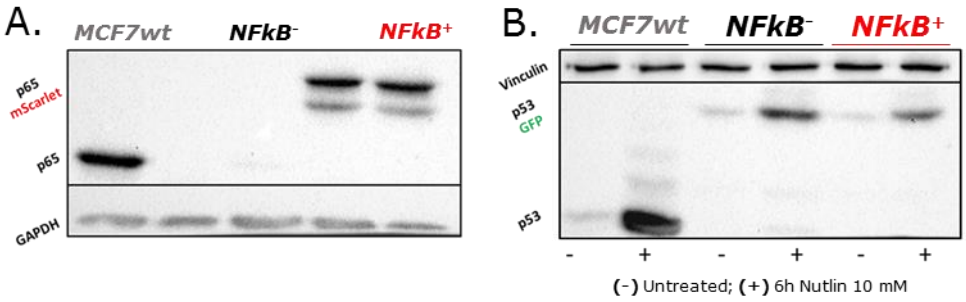

Figure 3.13. Validation of NFkB$^+$ and NFkB$^-$ cell lines via Western Blot. *We generated and validated two new cell lines. NFkB$^-$ cells carry p53-GFP and is KO for NF-κB. NFkB$^+$ cells carry both p53-GFP and p65-mScarlet, without the endogenous proteins. (A) α-p65 gel. (B) α-p53 gels. p53 levels were blotted both in normal conditions (-) and after a 6h-treatment with Nutlin 10 mM (+).*

we obtained a new clonal population, that will be called NFkB$^+$, in which both the endogenous p53 and p65 proteins were completely replaced with a fluorescently tagged version, p53-GFP and p65-mScarlet (**Figure 3.13**). Notably, expression levels of both p53-GFP and p65-mScarlet were found to be comparable to those of the untagged proteins in the parental population. Finally, we performed an RT-qPCR experiment to evaluate the expression of two NF-κB and p53 target genes (*NFKBIA* and *CDKN1A*, respectively) in NFkB$^+$ cells. While *CDKN1A* activation is maintained between the two clonal lines, meaning that p53 works in both clonal populations, *NFKBIA* expression is strongly reduced in NFkB$^-$ cells, in which we performed NF-κB KO (**Figure 3.14**).

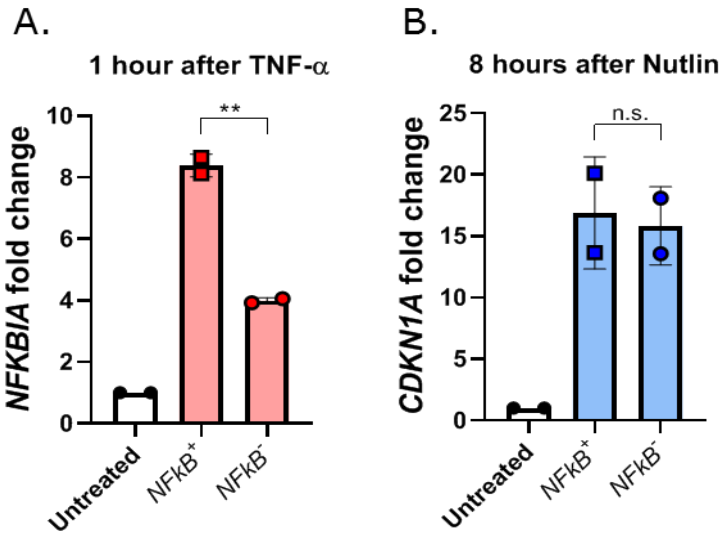

Figure 3.14. Validation of NFkB$^+$ and NFkB$^-$ cell lines via qPCR. *(A) NFKBIA expression quantification upon 1 hour of TNF-α. (B) CDKN1A expression quantification upon 8 hours of Nutlin. N° biological replicates = 2. Statistical test: unpaired t-test (*p< 0.05, **p< 0.01, ***p< 0.005).*

We then repeated live-cell imaging experiments, thus comparing NFkB$^+$ and NFkB$^-$ cells, triggering different p53 dynamics. With this control, we were able to investigate the role of NF-κB activation with TNF-α in p53 dynamics perturbation.

3.2.2. NF-κB enhances p53 sustained dynamics upon inflammatory stimuli.

To assess whether p53 dynamics perturbation upon a co-treatment with Nutlin and TNF-α depends on NF-κB, we performed live-cell confocal imaging of NFkB$^+$ and NFkB$^-$ cell lines at the same time. We then applied our analysis pipeline and we extracted single-cell p53 profiles. NFkB$^+$ cells displayed similar behaviour to the MCF-7 p53-GFP cells: Nutlin treatment activated sustained p53 dynamics, TNF-α did not activate p53 at all, and a simultaneous treatment of Nulin+TNF-α enhanced p53 nuclear

accumulation. This is visible from representative (**Figure 3.15A**) and median p53 profiles (**Figure 3.15B**). Interestingly, this enhancement in p53 response to Nutlin upon TNF-α is missing in NFkB$^-$ cells: both Nutlin and Nutlin+TNF-α treatments induce a similar accumulation of p53, as reported in **Figure 3.16.**

We then compared the area-under-the-curve computed from single-cell profiles between NFkB$^+$ and NFkB$^-$ cells (**Figure 3.17**). Also from this quantification, NFkB$^+$ cells accumulated more p53 after Nutlin+TNF-α treatment than with Nutlin alone.

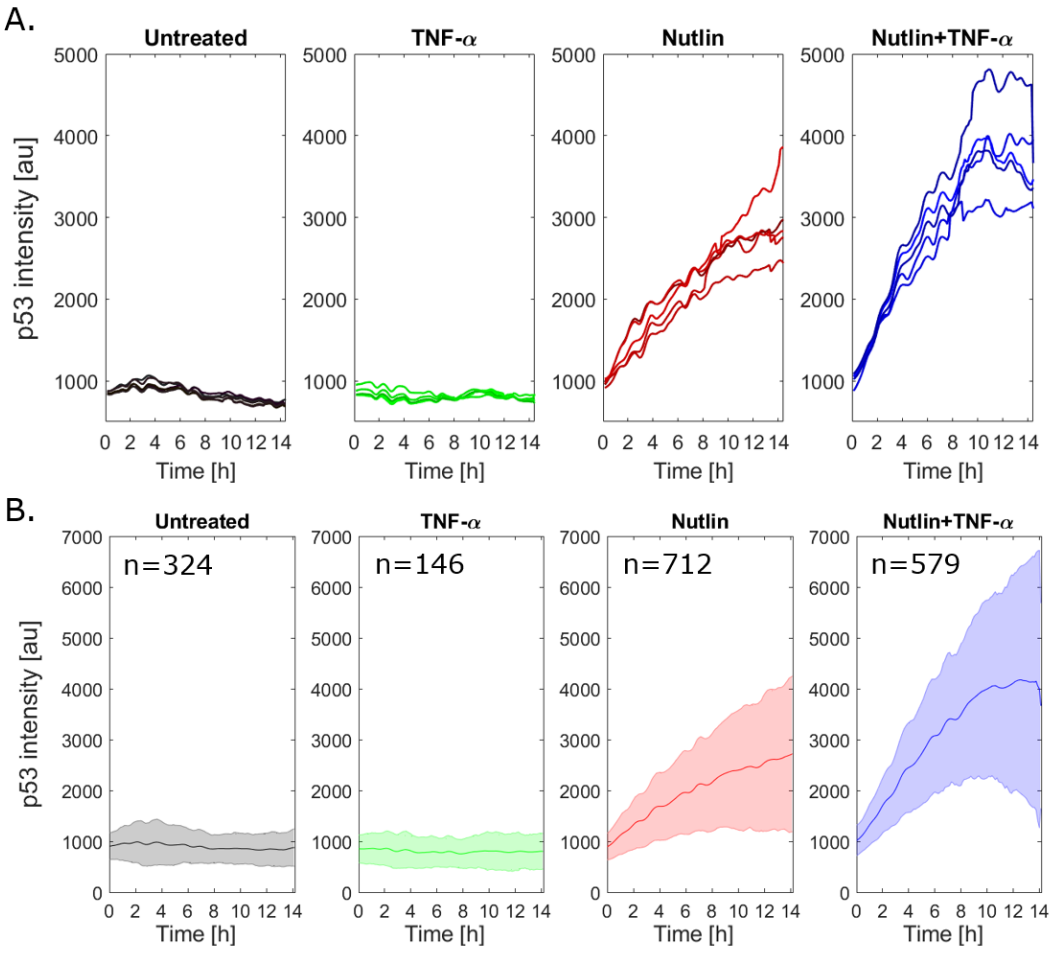

Figure 3.15. p53 sustained dynamics upon Nutlin and TNF-α in NFkB$^+$ cells. *(A) We triggered p53 sustained dynamics by adding Nutlin to NFkB$^+$ cells. A coupled activation with NF-κB enhanced p53 response to Nutlin, as saw from previous experiments. n° single-cell p53 profiles = 5. (B) Median of p53 profiles; coloured area: interquartile range, n = number of analysed cells.*

Instead, NFkB$^-$ cells do not display a significant difference in p53 nuclear accumulation between single and double treatment. These comparisons overall indicate that the enhancement of p53 response to Nutlin upon a simultaneous treatment with TNF-α depends on NF–κB.

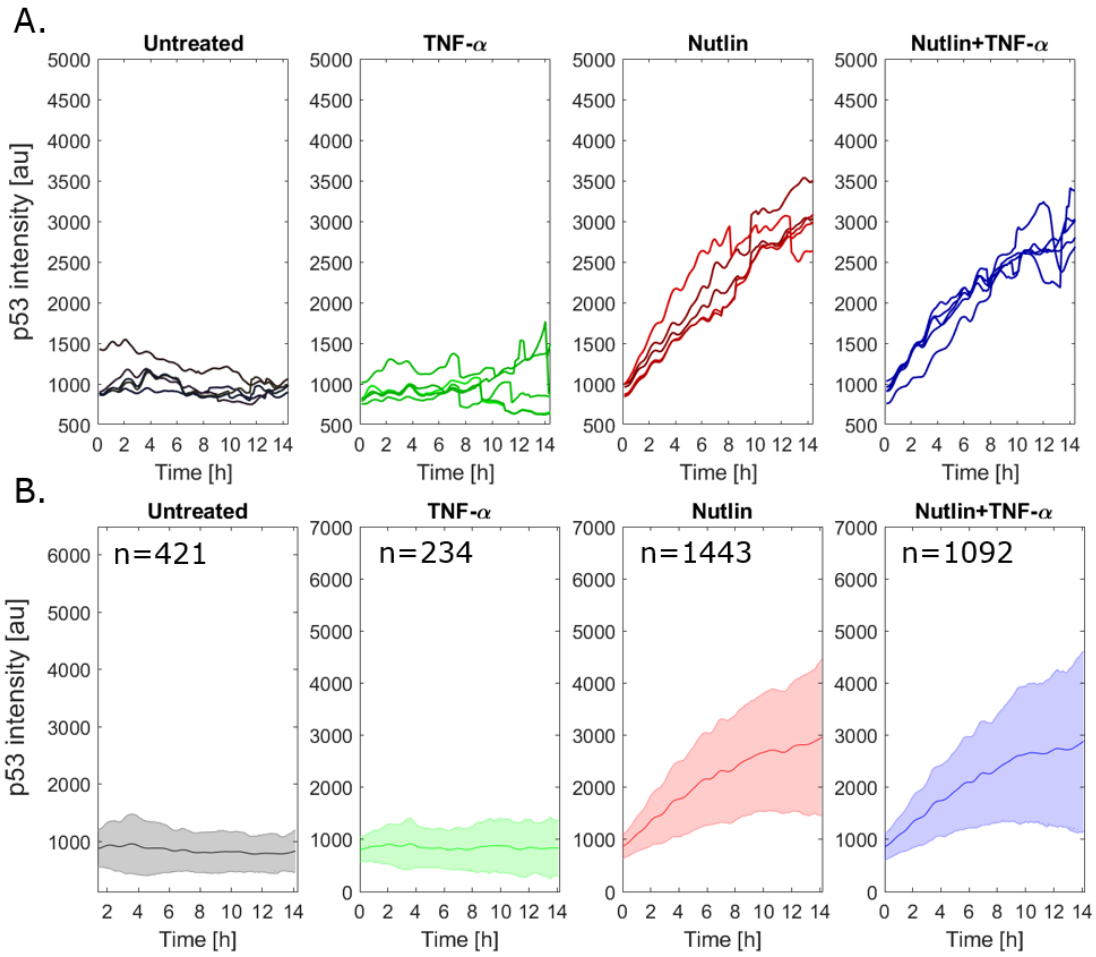

Figure 3.16. p53 sustained dynamics upon Nutlin and TNF-α in NFkB⁻ cells. *(A) We triggered p53 sustained dynamics by adding Nutlin to NFkB⁻ cells. Without NF-κB, p53 sustained dynamics upon Nutlin is not enhanced by TNF-α treatment. n° single-cell p53 profiles = 5. (B) Median of p53 profiles; coloured area: interquartile range, n = number of analysed cells.*

We next wondered whether another stimulus triggering the NF-κB pathway could induce similar changes in the Nutlin-induced p53 sustained dynamics we observed upon co-stimulation with TNF-α. We chose IL-1β (200 ng/mL), a pro-inflammatory cytokine that activates NF-κB signalling pathway, since it induces the phosphorylation, and subsequent degradation, of IκBα (Leibowitz & Yan, 2016) (Diep et al. 2022). We firstly validated the MCF-7 response by comparing NF-κB nuclear translocation dynamics between IL-1β and TNF-α (**Figure 3.18A-B**). TNF–α induced a quick and narrow peak of NF-κB translocation inside the nucleus around 30 minutes after the treatment and the presence of nuclear NF-κB (N.C.R. => 1) after this first peak can be seen in different cells. IL-1β, instead, triggered a delayed and broader peak of NF-κB translocation. Moreover, while TNF–α effects were quite homogeneous in the cell population, IL–1β did not act in all cells and NF-κB maximum N.C.R., was lower than TNF–α (**Figure 3.18C,** left).

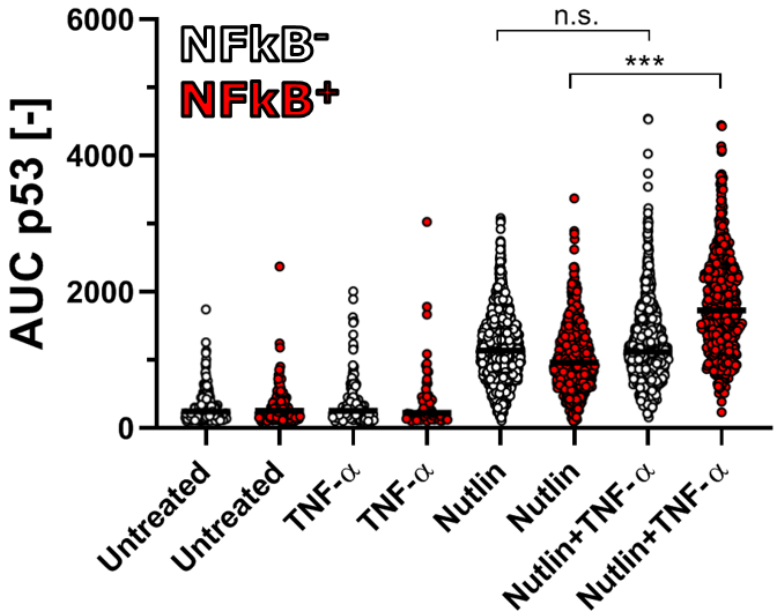

Figure 3.17. Comparison of p53 accumulation level between NFkB⁺ and NFkB⁻ cells. *We quantified the area-under-the-curve from single p53 profiles. Nutlin+TNF-α treatment induces a higher accumulation of p53 than Nutlin treatment alone only in NFkB⁺ cells (red dots). NFkB⁻ cells do not display differences in p53 accumulation (white dots). Black bar = median, with interquartile range. Statistical test: Kruskal-Wallis (*p< 0.05, **p< 0.01, ***p< 0.005).*

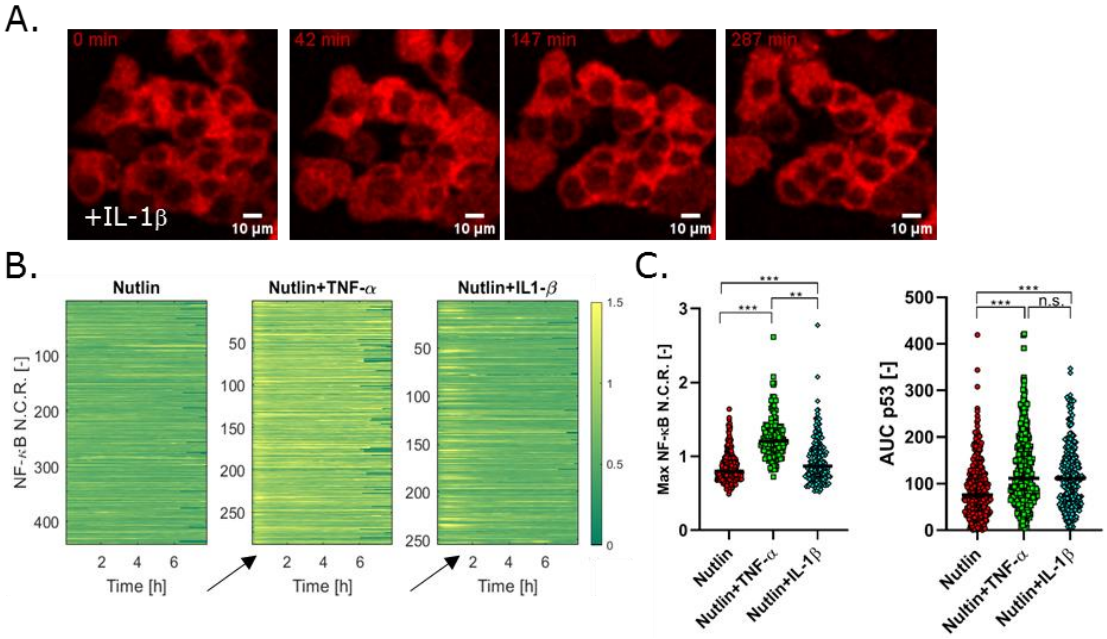

Figure 3.18. TNF-α and IL-1β trigger different NF-κB dynamics, but still enhance p53 response to Nutlin. *(A) Time-course of NF-κB translocation upon IL-1β treatment. Scale bar = 10 μm. (B) Single-cell NF-κB N.C.R. profiles are plotted up to 8 hours to enhance the difference in early NF-κB translocation between TNF-α and IL-1β (arrows highlight the peak of nuclear translocation). N° cells = 442 (Nutlin); 288 (Nutlin+TNF-α); 255 (Nutlin+IL-1β). (C) Quantification of NF-κB maximum translocation level (left) and enhancement in p53 response (right). Black bar = median, with interquartile range. Statistical test: Kruskal-Wallis (*p< 0.05, **p< 0.01, ***p< 0.005).*

Both IL-1β and TNF-α enhanced p53 sustained accumulation upon Nutlin (**Figure 3.18C,** right).

We then repeated the live-cell imaging experiments comparing p53 sustained response to Nutlin and Nutlin+IL-1β treatments. What we actually observed was similar trends to those obtained with TNF–α: IL-1β does not elicit p53 activation, Nutlin induced a sustained accumulation of p53 inside the nucleus and a double stimulation (Nutlin+IL-1β) enhances p53 levels, as reported from representative and median profiles in NFkB^{+} cells (**Figure 3.19**). In NFkB^{-} cells no enhancement is visible upon Nutlin+IL-1β treatment (**Figure 3.20**), and the accumulation of p53 is similar between the two treatments. These observations were quantified by calculating the area-under-the-curve (**Figure 3.21**). We can then conclude that p53 sustained accumulation upon Nutlin can be enhanced upon a stimulus that activates also NF-κB and this enhancement depends directly on the presence of NF-κB. We next wondered the effect on p53 oscillations if NF-κB is removed from the system.

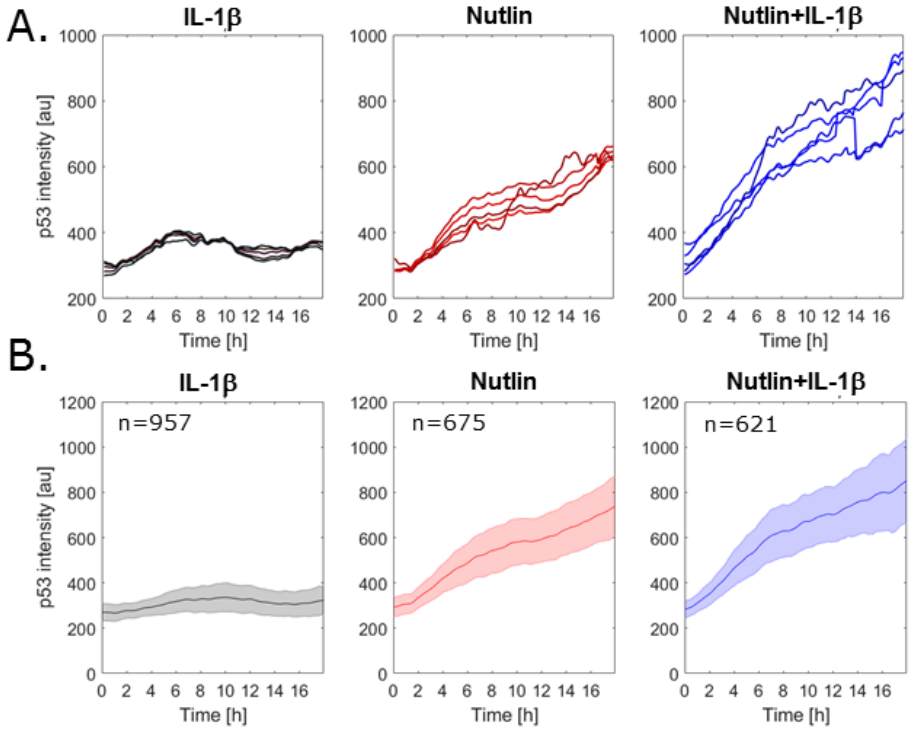

Figure 3.19. p53 sustained dynamics upon Nutlin and IL-1β in NFkB^{+} cells. *(A) We triggered p53 sustained dynamics by adding Nutlin to NFkB^{-} cells. A coupled activation with NF-κB through IL-1β enhanced p53 response to Nutlin, as saw from previous experiments. n° single-cell p53 profiles = 5. (B) Median of p53 profiles; coloured area: interquartile range, n = number of analysed cells.*

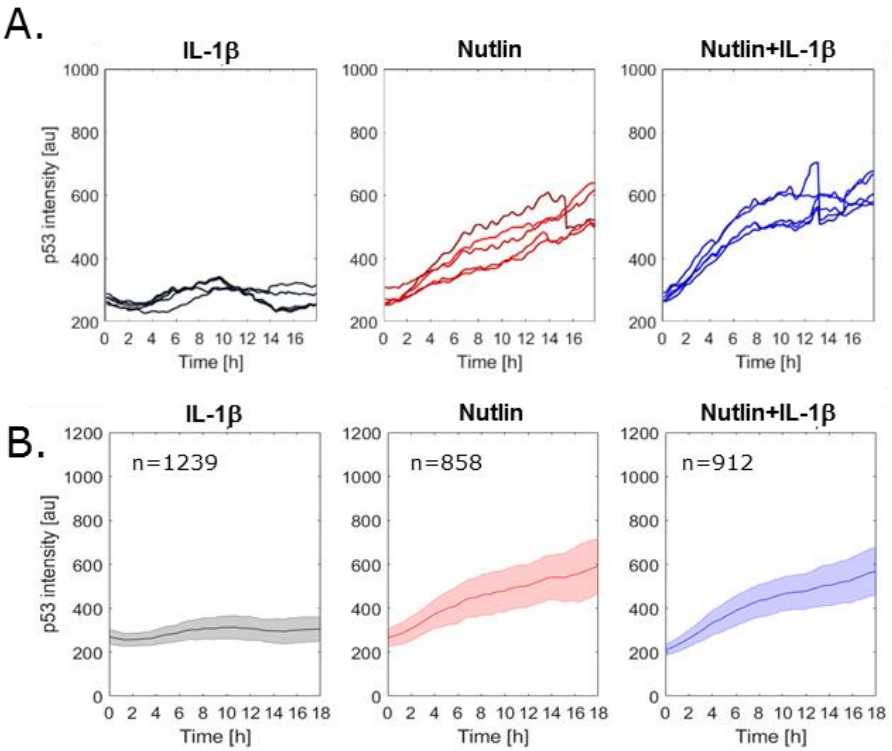

Figure 3.20. p53 sustained dynamics upon Nutlin and IL-1β in NFkB⁻ cells. *(A) We triggered p53 sustained dynamics by adding Nutlin to NFkB⁻ cells. Without NF-κB activation, p53 sustained dynamics upon Nutlin is not enhanced by IL-1β co-treatment. n° single-cell p53 profiles = 5. (B) Median of p53 profiles; coloured area: interquartile range, n = number of analysed cells.*

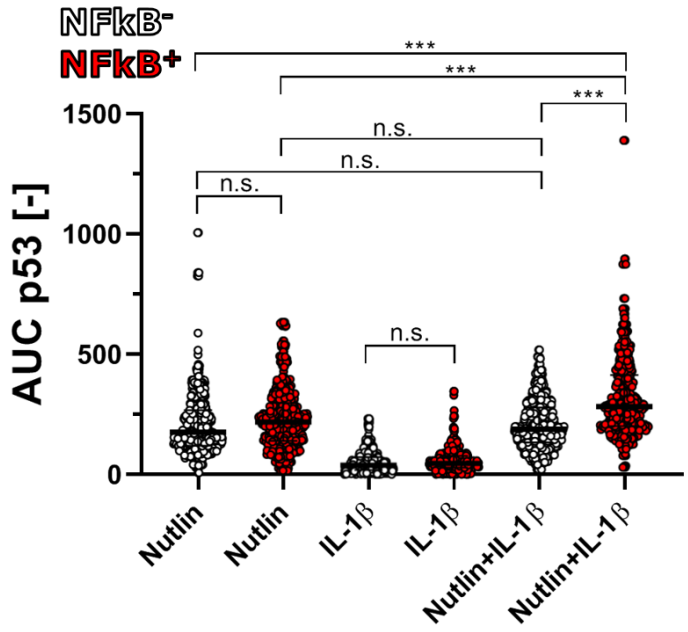

Figure 3.21. Comparison of p53 accumulation level between NFkB⁺ and NFkB⁻ cells (IL-1β experiment). *We quantified the area-under-the-curve from single p53 profiles. Nutlin+IL-1β treatment induces a higher accumulation of p53 than Nutlin treatment alone only in NFkB⁺ cells (red dots). NFkB⁻ cells do not display any p53 dynamics perturbation (white dots). Black bar = median, with interquartile range. Statistical test: Kruskal-Wallis (*p< 0.05, **p< 0.01, ***p< 0.005).*

3.2.3. NF-κB perturbs p53 oscillatory dynamics upon TNF-α.

We then compared p53 response between NFkB$^+$ and NFkB$^-$ upon a coupled stimulation with γ-irradiation (10 Gy) and TNF-α (10 ng/mL). NFkB$^+$ cells display similar behaviour to the starting population from which we generated this clone: while γ-irradiation alone triggers damped p53 oscillations, the coupled activation of NF-κB with TNF-α perturbs such oscillations, that become closer to a sustained dynamics (**Figure 3.22**).

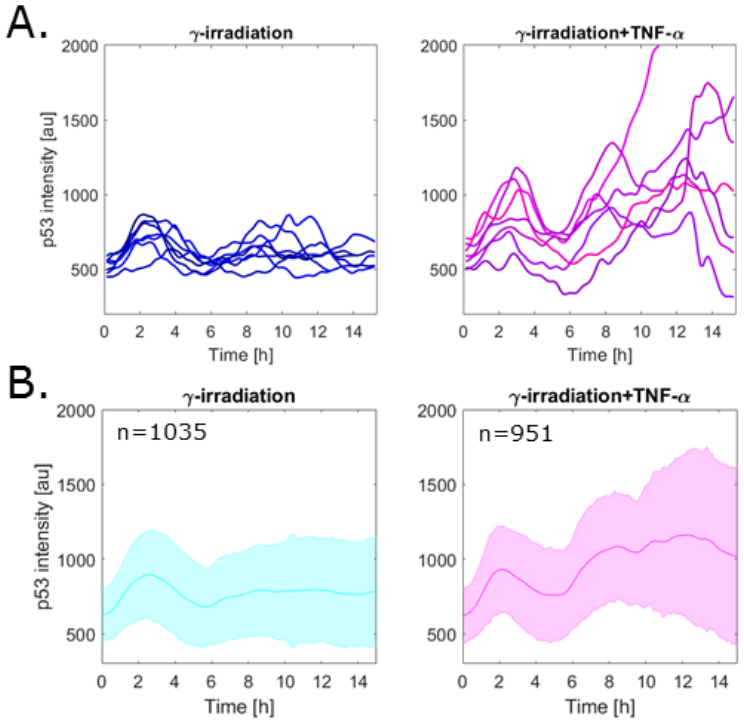

Figure 3.22. p53 oscillatory dynamics upon γ-irradiation and TNF-α in NFkB$^+$ cells. *(A) We triggered p53 oscillations by exposing NFkB$^+$ cells to γ-irradiation (10 Gy). Co-activation with NF-κB enhanced p53 oscillations after DNA damage, as seen from previous experiments. n° single-cell p53 profiles = 5. (B) Median of p53 profiles; coloured area: interquartile range, n = number of analysed cells.*

Under the same conditions, NFkB$^-$ cells responses to γ-irradiation and γ-irradiation+TNF-α have similar trends. Contrary to what happens in NFkB$^+$ cells, where NF-κB is activated upon TNF-α treatment, oscillations are not perturbed in NFkB$^-$ cells (**Figure 3.23**). In **Figure 3.24** we quantified the total amount of p53 nuclear accumulation via the area-under-the-curve computation from single-cell p53 profiles. Despite a significant difference between single and double treatments in NFkB$^-$ cells, higher levels of p53 are reached in NFkB$^+$ cells upon the double treatment with γ-irradiation and TNF-α.

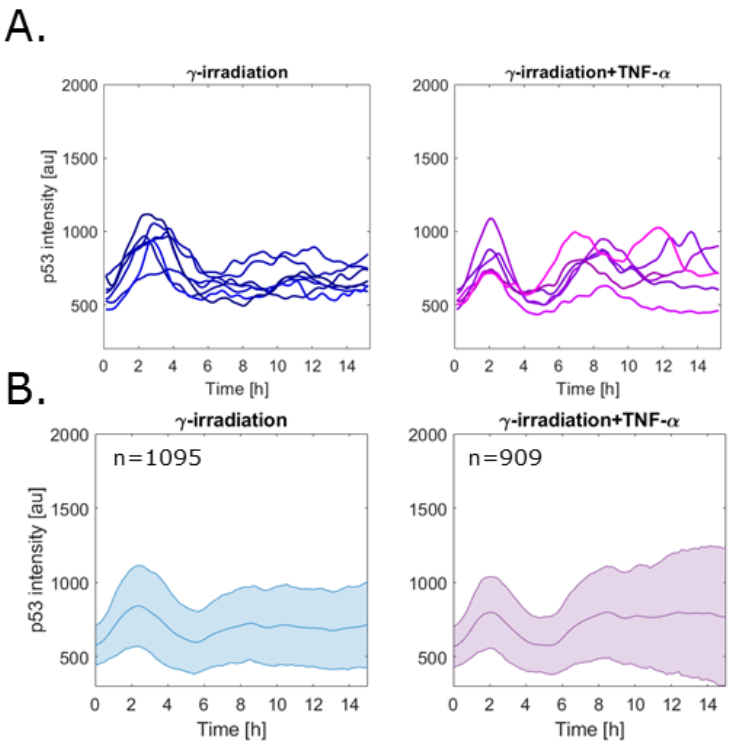

Figure 3.23. p53 oscillatory dynamics upon γ-irradiation and TNF-α in NFkB⁻ cells. *(A) We triggered p53 oscillations by exposing NFkB⁻ cells to γ-irradiation (10 Gy). Without NF-κB, p53 oscillations are not perturbed by TNF-α treatment. n° single-cell p53 profiles = 5. (B) Median of p53 profiles; coloured area: interquartile range, n = number of analysed cells.*

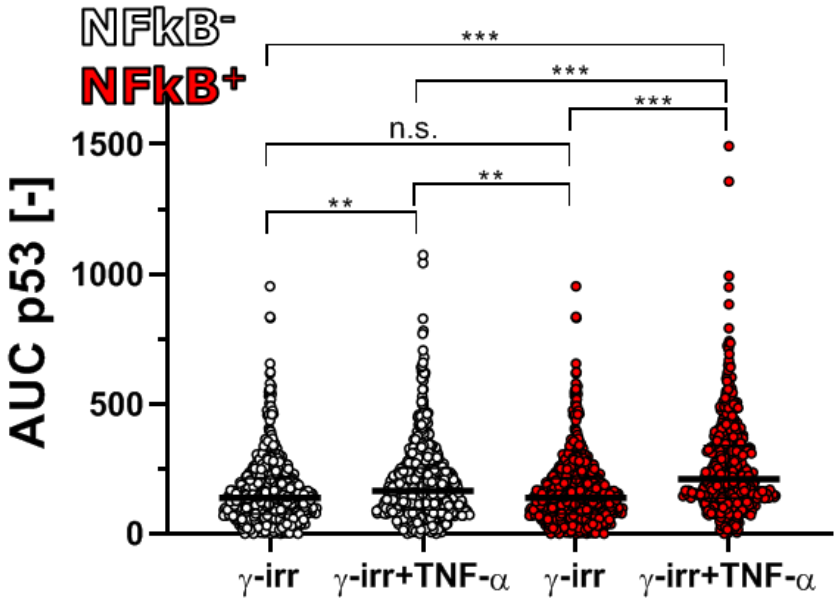

Figure 3.24. Comparison of p53 accumulation level between NFkB⁺ and NFkB⁻ cells after DNA damage + TNF-α. *We quantified the area-under-the-curve from single p53 profiles. γ-irradiation+TNF-α treatment induces a higher accumulation of p53 than γ-irradiation treatment alone in NFkB⁺ cells. NFkB⁻ cells display slightly higher p53 levels with the double treatment, but still lower than those computed in NFkB⁺ cells. Black bar = median, with interquartile range. Results from representative experiment, n° biological replicates = 2. Statistical test: Kruskal-Wallis (*p< 0.05, **p< 0.01, ***p< 0.005).*

When we computed parameters characterizing oscillations, we found that oscillations are more perturbed in NFkB$^+$ cells. p53 oscillations are accelerated upon γ-irradiation and TNF-α treatment in NFkB$^+$ cells, since both the first and second peak of oscillations occur earlier than γ-irradiation alone and timings computed in NFkB$^-$ cells (**Figure 3.25A**). We then looked at the intensity of 1st and 2nd peaks of p53 oscillatory dynamics. We obtained that, while small differences (despite significant) are detectable in the intensities of 1st peaks, 2nd peaks of oscillation are higher in NFkB$^+$ cells (**Figure 3.25B**). This corroborates our previous results, suggesting that upon a coupled activation with TNF-α, p53 oscillations progressively turn into a sustained accumulation.

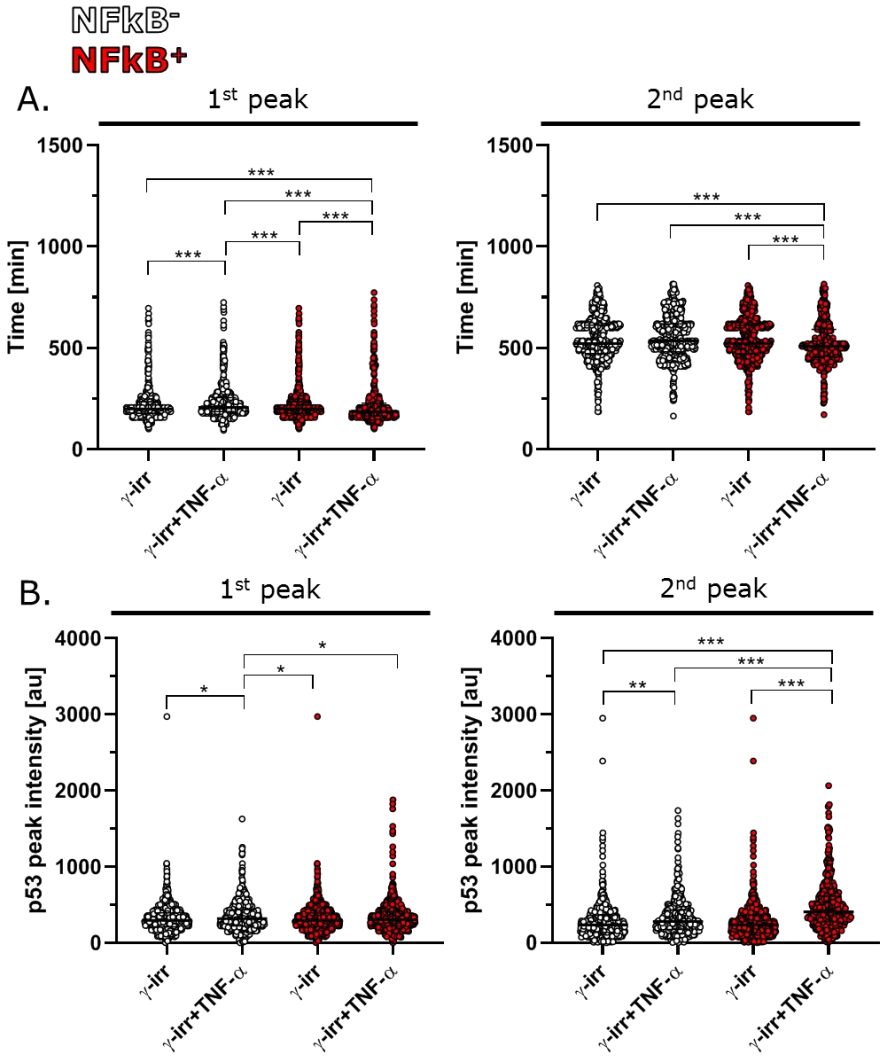

Figure 3.25. Comparison of p53 oscillations features between NFkB$^+$ and NFkB$^-$ cells after DNA damage + TNF-α. *From single-cell p53 profiles we quantified timings of oscillations peaks (A) and p53 intensity at the first two oscillation peaks (B), between NFkB$^-$ (black/grey) and NFkB$^+$ (red) cells. Results from representative experiment, n° biological replicates = 2. Statistical test: Kruskal-Wallis (*p< 0.05, **p< 0.01, ***p< 0.005, n.s. are not shown).*

3.3. Investigating the molecular mechanism of NF-κB-mediated perturbation of p53 dynamics.

Our previous results suggest that a crosstalk involving p53 and NF−κB dynamics is actually present in MCF-7 cells. When we trigger NF−κB and p53 signalling pathways at the same time, p53 sustained and oscillatory dynamics are perturbed in a way that globally increases the accumulation of p53. These results were somehow in contrast with most of the studies in the literature that highlight the molecular antagonism between p53 and NF−κB (Gudkov et al. 2011). Different studies reported how NF−κB can inhibit p53 activity by up-regulating MDM2 (Heyne et al. 2013) or via its target genes, which can interfere with p53-related pro-apoptotic processes (Perkins, 2007) (Gudkov et al. 2011) (**Figure 1.6**). However, previous studies did not include information or considerations regarding p53 and NF−κB dynamics in the context of their crosstalk. Therefore, our current results, although diverging from some previous studies, introduce a new variable into the system: the temporal evolution of p53 and NF−κB, pivotal in regulating their transcriptional program and cellular outcome after stresses (Purvis et al. 2012) (Bacher et al. 2021). We next decided to investigate the molecular mechanism behind these observations.

3.3.1. NF-κB and p53 activation and target gene expression correlate at single-cell level.

To provide some first insight in the molecular mechanism governing p53/NF-κB crosstalk, we decided to assess whether the NF-κB-derived perturbation of p53 dynamics is cell-intrinsic. We divided the cell population treated with stimuli triggering both p53 (Nutlin/γ-irradiation) and NF−κB (TNF-α/IL-1β) according to a threshold: the mean value in the population of NF−κB nuclear response over the time-course (through the AUC) and we used only profiles spanning for at least 12 hours. We chose this specific time-point due to the pronounced disparity in p53 responses we observed from fixed and live experiments upon treatments activating only p53 (Nutlin/γ-irradiation) and simultaneous treatments activating both p53 and NF-κB (Nutlin/γ-irradiation + TNF-α/IL-1β). In cells treated with both Nutlin and TNF−α, those cells that displayed a higher NF-κB nuclear response displayed a higher accumulation of p53 over time (**Figure 3.26A**). A similar result upon TNF-α is detectable upon γ-irradiation treatment, where a higher NF-κB nuclear response correlates with a stronger p53 accumulation over time in the same cells (**Figure**

3.26B). Interestingly, we obtained a similar trend after the double treatment with IL-1β (**Figure 3.26C**).

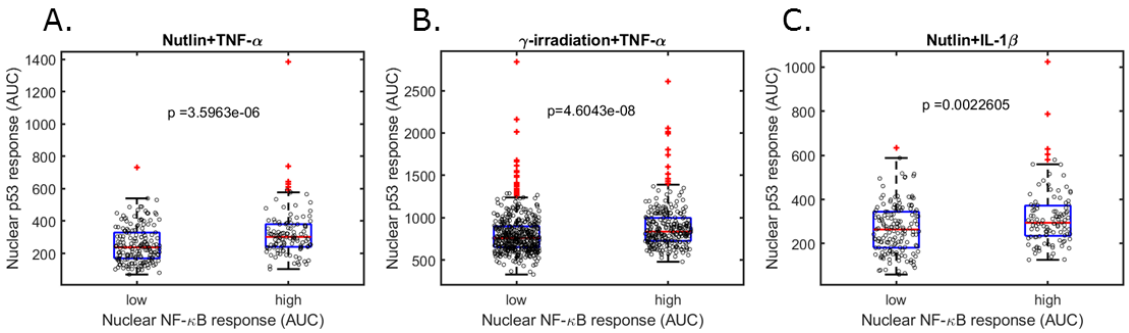

Figure 3.26. Comparison between p53 and NF-κB responses at single-cell level upon TNF-α/IL-1β. *Cells responses were split in two populations according to NF-κB response (low/high) and plotted against respective p53 response (AUC). (A). NFkB⁺ cells upon Nutlin+TNF-α treatment. (B) NFkB⁺ cells upon γ-irradiation+TNF-α treatment. (C) NFkB⁺ cells upon Nutlin+IL-1β treatment. Statistical test: Wilcoxon Rank Sum Test (p-values are reported in each figure).*

We next wondered whether this positive correlation between NF-κB and p53 responses to simultaneous stimuli occur also at the transcriptional level. To this aim, we then performed a smFISH on two p53 and NF-κB target genes, *CDKN1A* and *NFKBIA*, respectively, at the same time. We chose Nutlin and TNF-α as treatments and 8 hours as a time-point, since we previously saw an enhancement in *CDKN1A* expression upon a boosted p53 accumulation with these stimuli (**Figure 3.6**). In **Figure 3.27A**, we report example images of smFISH and quantification of mature mRNA is reported alongside them. Cells display a high level of *CDKN1A* and *NFKBIA* after Nutlin and TNF-α treatments, respectively, at 8 hours after the treatment. With Nutlin, no correlation between *NFKBIA* and *CDKN1A* is visible. Upon only TNF-α, we reported low levels of *CDKN1A* expression, that nevertheless weakly correlate with *NFKBIA* levels.

Interestingly, upon the double treatment with Nutlin and TNF-α, we have a stronger positive correlation between the expression levels of *NFKBIA* and *CDKN1A*, as reported in **Figure 3.27B**, lower-right panel. This result is in line with single-cell analysis previously reported for this type of treatment: those cells in which we detect a greater activation of NF-κB (and consequent greater expression of its target gene *NFKBIA*) display a higher nuclear accumulation of p53 (and consequent greater expression of its target gene *CDKN1A*).

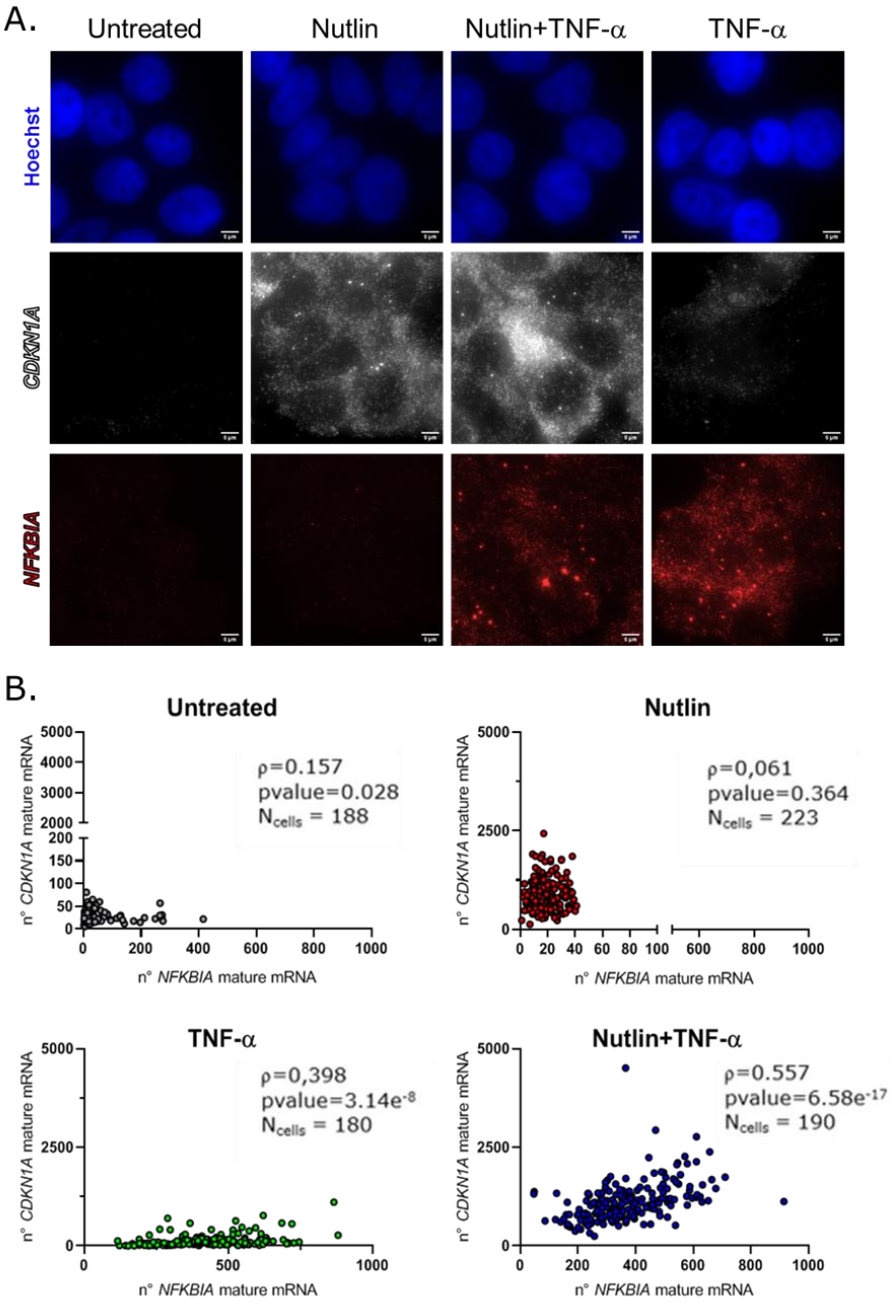

Figure 3.27. smFISH comparing CDKN1A and NFKBIA upon Nutlin+TNF-α treatment. *(A) Exemplary smFISH acquisitions (blue = Hoechst, white = CDKN1A probe, red = NFKBIA probe). Scale bar = 5 μm. (B) Quantification and correlation between NFKBIA and CDKN1A mature mRNAs levels. N° biological replicates = 1. N° of analysed cells are reported; Spearman's Correlation Coefficients (ρ) are reported with relative p-values in each condition.*

3.3.2. NF-κB activation enhances p53 transcription.

Given this evidence, we next asked: how does NF-κB activation enhance p53 levels, thus perturbing its dynamics? The hypothesis we made is that NF-κB can promote the transcription of p53 itself in the conditions we tested. Indeed, previous studies suggest that *TP53*, the gene of p53 protein, can be a transcriptional target of NF-κB since the promoter sequence of *TP53* contains a binding site for NF–κB (H. Wu & Lozano, 1994) (Pahl, 1999) (Schumm et al. 2006); *TP53* is also reported as a target gene of NF-κB in online databases (https://bioinfo.lifl.fr/NF-KB/). This could explain the increase in p53 protein levels observed from live-cell imaging upon γ-irradiation/Nutlin and TNF-α treatment (higher than Nutlin treatment alone) and the differences in p53 dynamics enhancement we observed when comparing $NFkB^+$ and $NFkB^-$ cells.

We next investigated the possibility that, after a simultaneous treatment activating both TFs, p53 response to Nutlin is enhanced by NF-κB due to an increase in NF-κB-mediated p53 transcription. We then performed a smFISH looking directly at *TP53* gene expression level after Nutlin+TNF-α treatment and we chose 1 and 8 hours as time-points. Results are reported in **Figure 3.28**. We obtained a slight but significant increase in the amount of mature *TP53* mRNAs at 8 hours after the treatment with Nutlin. This result can be explained by a positive autoregulation of the *TP53* gene, which is reported to be a target of p53 itself (Fischer, 2017) (Ghosh et al. 2022). Interestingly, we found a higher amount of *TP53* mature mRNAs after both TNF-α and Nutlin+TNF-α treatments. With TNF-α, despite an increase in the expression of the *TP53* gene, we did not observe an increase in p53 levels via live-cell imaging or immunofluorescence, potentially because MDM2 activity is not blocked. The simultaneous activation of both TFs via Nutlin and TNF-α induces the stronger expression of *TP53*, which can be explained with a sort of superposition of Nutlin and TNF-α effects.

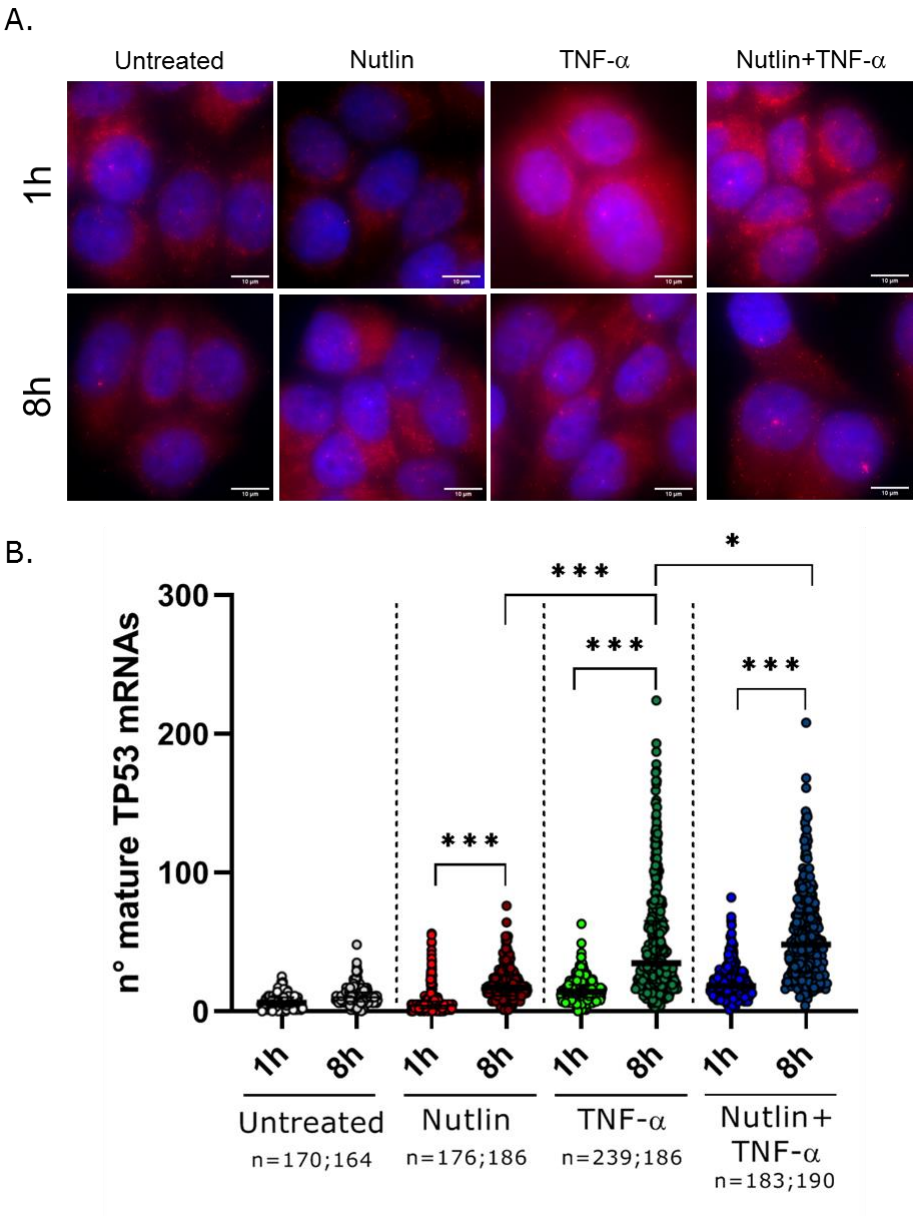

Figure 3.28. smFISH on TP53 gene expression upon Nutlin and TNF-α. *(A) Exemplary smFISH acquisitions (blue = Hoechst, red = TP53 probe). Scale bar = 10 μm. (B) Quantification of TP53 mature mRNAs levels. N° of analysed cells are reported for each condition. Data are merged from n° of biological replicates = 2. Statistical test: Kruskal-Wallis (*p< 0.05, **p< 0.01, ***p< 0.005).*

3.3.3. Mathematical simulations suggest that increased p53 transcription upon TNF-α causes perturbed dynamics.

To gain further insights into the crosstalk of p53 and NF-κB, we decided to use a mathematical model of the p53-MDM2 feedback loop. In the last decades, this kind of tool has emerged as an indispensable tool in the biologist's toolkit, since it offers a systematic and quantitative approach to dissecting transcriptional networks. The

negative feedback loop of the p53-MDM2 system has actually been extensively studied and different mathematical models have been proposed. Each model is built around differential equations that describe the temporal evolution of each player composing the system. Simpler models account only for p53 and MDM2 protein concentrations (Lev Bar-Or et al. 2000), while more complex models employ different "intermediaries", like other proteins involved in the loop and delays accounting for ongoing molecular processes (transcription, translation, mRNAs degradation) (Ahmed & Verriest, 2017) (Eliaš & Macnamara, 2021).

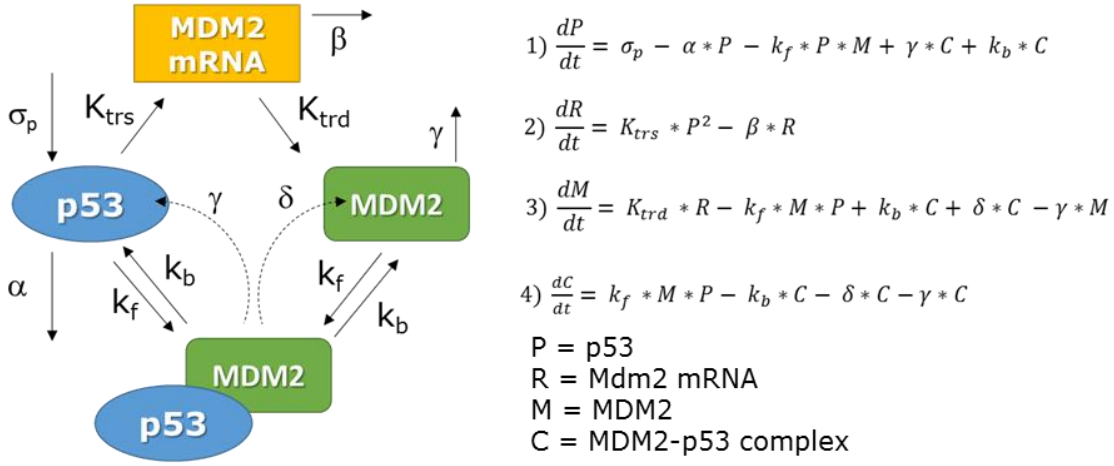

Figure 3.29. p53-MDM2 feedback loop model. *The model relies on four ordinary differential equations describing the temporal evolution of four concentrations: p53, MDM2, MDM2 mRNA and the complex between p53 and MDM2.*

In particular, we wanted to use mathematical modelling to understand to what extent the simple enhancement in *TP53* transcription, which we hypothesized is related to NF-κB activation, is able by itself to produce the perturbation of p53 response to DNA damage and to Nutlin we experimentally observed. We chose the model proposed by (Hunziker et al. 2010), whose structure and governing ordinary differential equations (ODEs) are reported in **Figure 3.29**, due to its relative simplicity and for being mathematically intuitive. A description of the parameters proposed in the original paper is reported in Materials and Methods **paragraph 5.10**. Contrary to other models that require time delays to generate oscillations (Geva-Zatorsky et al. 2006) (Purvis & Lahav, 2013), thus using delayed differential equations instead of ODEs, this model employs nonlinearities caused by the p53 oligomerization and by the p53-MDM2 interaction to trigger an oscillatory behaviour (Hunziker et al. 2010) upon different perturbations. To simulate DNA damage induction, the paper proposed to drastically change three parameters, specifically: increased MDM2 degradation (↑γ),

decreased MDM2-mediated ubiquitination of p53 ($\downarrow\delta$) and decreased binding between p53 and MDM2 ($\downarrow k_f$). To simulate Nutlin treatment, instead, (Hunziker et al. 2010) changed only one parameter ($\downarrow k_f$), arguing that Nutlin decreases the binding between p53 and MDM2 (Zajkowicz et al. 2013).

However, the model has some limitations and needed further refinement. First, their model was not able to reproduce the damped oscillatory behaviour of p53 that we observe experimentally upon DNA damage. As shown in Figure 2A in (Hunziker et al. 2010), their simulated p53 oscillations displayed a high first peak at 1 hour after trigger, then a 4 hours plateau below the basal level, followed by oscillations with a period of approximately 4 hours. To overcome this, we performed simulations with randomized parameters around the original values (Hunziker et al. 2010) and searched for p53 dynamics profiles similar to our experimental observations. With our method, we obtained parameter values (provided in Materials and Methods, **paragraph 5.10**) leading to a p53 dynamic profile that is similar to those observed in our MCF-7 cells from confocal imaging upon DNA damage induction (**Figure 3.30A**). The profile displays damped oscillations, with a first peak of oscillation at around 2.5-3 hours after the stimulus (time=0 in the simulation) and a second lower peak.

With this model, we then performed simulations to assess the effect of enhanced *TP53* transcription upon TNF-α treatment, as obtained from the smFISH experiment on *TP53* (**Figure 3.28**). Assuming constant translation and degradation rates of the mRNA, it should lead to an increase in p53 synthesis rate (σ_p). We then proposed a model of linear increase of σ_p, $\sigma_p(t)$, mirroring the mRNA accumulation observed experimentally (detail in Materials and Methods, **paragraph 5.10**), for different values of the fold change increase of $\sigma_p(t)$ between t=0h and t=24 h compatible with our experimental observation through smFISH. Doing so, we actually obtained a perturbation in p53 oscillatory dynamics, which is similar to that observed in live-cell imaging upon a simultaneous treatment with γ-irradiation and TNF-α. (**Figure 3.30B**). In particular, the simulations show how: (1) the first peak remains almost unchanged; (2) the second peak of oscillations was enhanced and anticipated; (3) oscillations progressively become a sustained accumulation. Hence, the results from mathematical modelling suggest that the NF-κB-dependent perturbation of p53 oscillations can be caused solely by an enhanced transcription of *TP53*.

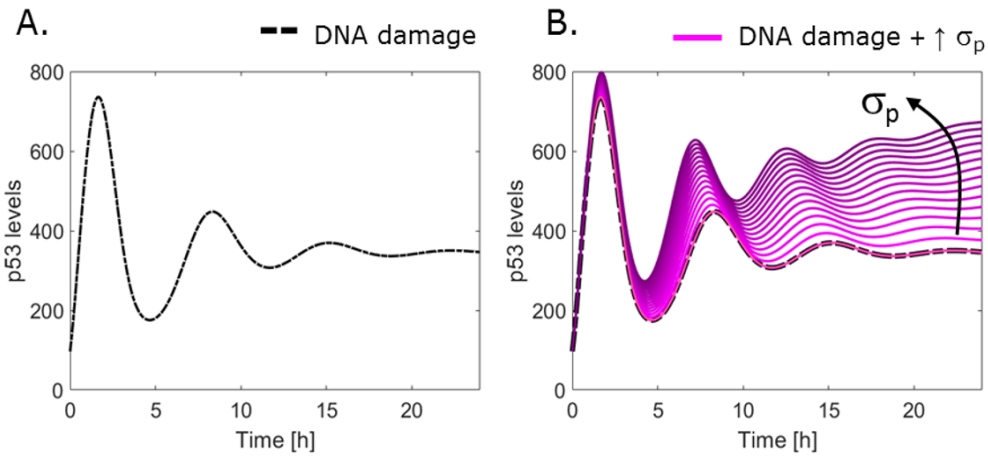

Figure 3.30. Mathematical simulations of p53-MDM2 feedback loop upon DNA damage and enhanced p53 synthesis rate. *(A) A profile of p53 oscillatory dynamics similar to those observed via live-cell microscopy, obtained through parameters randomization around the original model values. (B) Progressive increase of σ_p (to mirror NF-κB mediated enhance TP53 transcription) for increasing fold changes transformed p53 oscillations into a sustained accumulation, similarly to the behaviour we observed in MCF-7 after double treatment of γ-irradiation+TNF-α.*

We then decided to assess if for our model the effect of the co-treatment upon Nutlin could again be explained through an increasing p53 synthesis. However, the model needed further refinement since the perturbation proposed to simulate Nutlin in (Hunziker et al. 2010)(drastically reducing the binding constant k_f of p53 and MDM2) did not reproduce the progressive accumulation of p53 that we observed in our experiments (Figure 2A in (Hunziker et al. 2010)). So, we decided to model Nutlin pharmacokinetics with a Hill function, along the lines of others (Purvis et al. 2012), so it would affect gradually k_f, which will become time-dependent ($k_f(t)$, see Materials and Methods, **paragraph 5.10**). For appropriate kinetic values, we obtained profiles showing a progressive accumulation of p53, similar to live-cell imaging experiments (**Figure 3.31A**). With this model, we again assessed the effect of increasing the synthesis rate as observed for the co-treatment, analogously to what we did for gamma irradiation. This caused again an increase in the quantity of p53, which progressively accumulated (**Figure 3.31B**) indicating that a moderate increase in synthesis rate led to accumulations of p53 compatible with the ones observed experimentally.

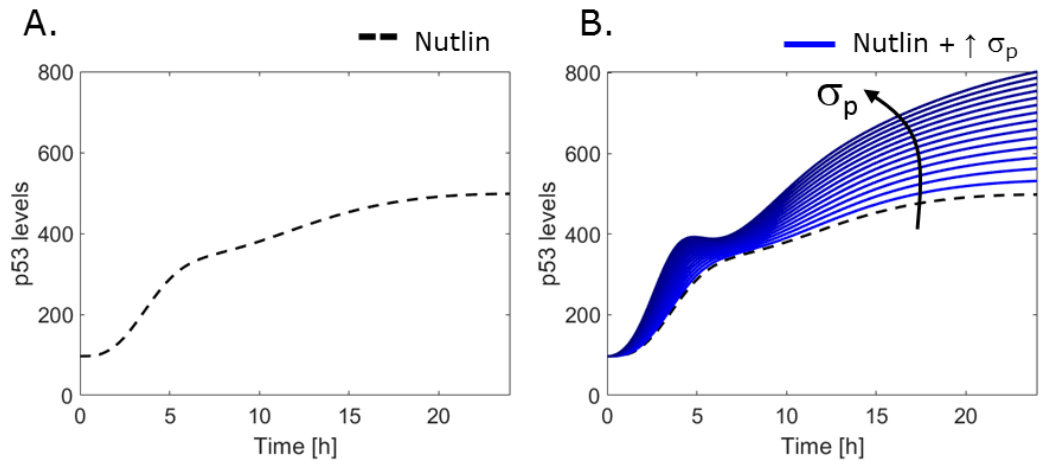

Figure 3.31. Mathematical simulations of p53-MDM2 feedback loop upon Nutlin and enhanced p53 synthesis rate. *(A) By properly simulating pharmacokinetics of Nutlin, a profile of sustained accumulation was obtained. (B) Progressive increase of σ_p enhanced p53 accumulation, similarly to the behaviour we observed in MCF-7 after double treatment of Nutlin+TNF-α.*

In summary, mathematical modelling provided a robust framework to investigate the perturbations of p53 dynamics due to NF-κB activation. By refining our model and performing data-constrained perturbations on the p53/MDM2 feedback loop model, we observed trends that reproduced the experimental results and supported our hypothesis of an increased p53 synthesis rate driven by NF-κB activation as the cause of the perturbed p53 dynamics observed when NF-κB is activated simultaneously.

3.4. p53 perturbed dynamics by NF-κB and cellular response to stresses.

Our results suggest that the activation of NF-κB via inflammatory cytokines perturbs p53 dynamics, which become more sustained. p53 is well known as the master regulator of cell response to different stresses and its dynamics are important in the transcriptional program that will be activated (Purvis et al. 2012). We next asked what could happen to cell fate and DNA damage repair mechanism with p53 dynamics perturbed by NF-κB activation via TNF-α and IL-1β.

3.4.1. TNF-α is a main driver of MCF-7 cell death induction.

To assess whether a simultaneous activation of p53 and NF-κB, triggered by different stimuli, thus inducing different dynamics, might induce different cell fates we evaluated first the rate of cell death. We performed a Flow Cytometry assay on $NFkB^+$ and $NFkB^-$ cells upon all possible combinations of treatments previously tested, splitting the experimental conditions according to p53 dynamics: sustained (upon Nutlin) and oscillatory (upon γ-irradiation). MCF-7 were treated with TNF-α or IL-1β to activate NF-κB, while also co-stimulated with Nutlin/γ-irradiation. Cells were collected 24 hours after treatments and exposed to TO-PRO-3 stain, which can penetrate damaged membranes, indicative of dead cells. We chose this staining because the dye exhibits far-red fluorescence signal ($\lambda_{exctiation}$ = 642 nm, $\lambda_{emission}$ = 661 nm), so we did not expect crosstalk with p53-GFP and p65-mScarlet signals (see protocol in Materials and Methods **paragraph 5.11.**).

Results from p53 sustained dynamics are reported in **Figure 3.32**. In $NFkB^+$ cells, Nutlin treatment does not induce cell death, as expected. Both TNF-α and Nutlin+TNF-α treatments induce a higher rate of cell death, similar levels to H_2O_2 (positive control). However, IL-1β and Nutlin+IL-1β do not induce cell death since the number of dead cells is similar to untreated condition. We obtained similar trends in $NFkB^-$ cells: only cells treated with TNF-α undergo cell death, while the number of dead cells treated with Nutlin and/or IL-1β is below the threshold.

The same experiment, but in cells in which we triggered p53 oscillatory dynamics with γ-irradiation, produced similar results, as reported in **Figure 3.33**. In both $NFkB^+$ and $NFkB^-$ cells, DNA damage induction does not provoke cell death, while TNF-α and its combination with γ-irradiation leads to a significantly higher rate of cell death. IL-1β, alone or in combination with γ-irradiation, does not induce cell death.

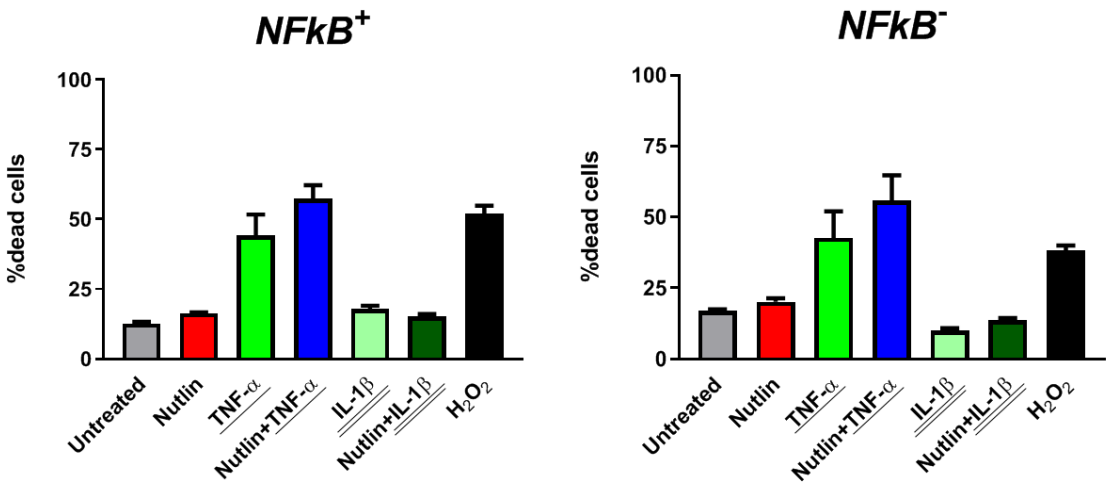

Figure 3.32. Cell death rate upon sustained p53 dynamics. *Quantification of cell death levels from Flow Cytometry experiment. p53 sustained dynamics was triggered with Nutlin; NF-κB pathway was triggered with TNF-α and IL-1β. Error bars: standard deviation of technical replicates (n=3).*

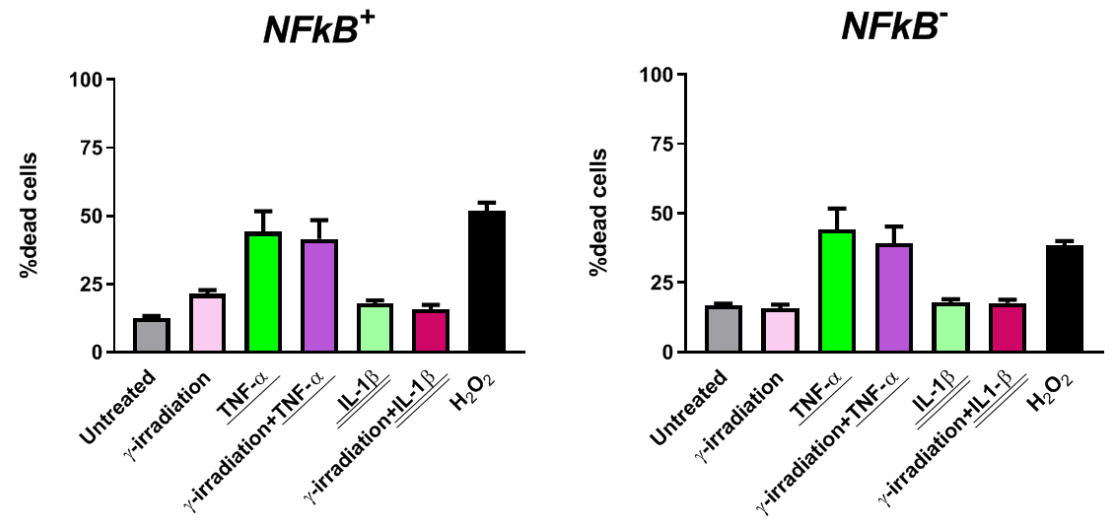

Figure 3.33. Cell death rate upon oscillatory p53 dynamics. *Quantification of cell death levels from Flow Cytometry experiment. p53 oscillatory dynamics was triggered with γ-irradiation; NF-κB pathway was triggered with TNF-α and IL-1β. Error bars: standard deviation of technical replicates (n=3).*

From these results, we can speculate that with these experimental settings, cell death is merely tuned by TNF-α treatment. This result is actually coherent with the model proposed by (Lee et al. 2016), in which treating cells with a single pulse of TNF-α favours the caspase pathway (thus promoting apoptotic transcriptional programs), to the detriment of NF-κB pro-survival activity. However, from these results, different p53 dynamics neither increase nor decrease the induction of cell death, regardless of

the presence of NF-κB. In fact, both NFkB$^+$ and NFkB$^-$ cells do not display different trends in cell death levels upon TNF-α or IL-1β.

3.4.2. NF-κB-perturbed p53 dynamics result in less efficient DNA damage repair.

We next focused our attention on the DNA damage repair mechanism, prompted by a work published in 2022 by the group of Mogens H. Jensen. In the biophysical model proposed by this paper, the DNA damage repair mechanism has higher efficiency with p53 oscillations. In case of perturbations or abolition of p53 oscillations (like with Nutlin or UV light), DNA damage foci will not be properly repaired, due to the Ostwald ripening phenomenon (Houk et al. 2009). With the premises and considerations proposed in that paper, we therefore asked what happens to the DNA damage repair if the oscillatory dynamics of p53 are perturbed by the activation of NF-κB, as we saw from our live-cell imaging experiments (**Figure 3.11** and **Figure 3.22**).

When DSBs occur, histone H2AX undergoes phosphorylation and is subsequently recruited to the damaged sites, where it, in turn, recruits other molecules involved in DNA repair machinery (Kuo & Yang, 2008). To evaluate the efficiency of different p53 dynamics in repairing DNA damage foci, we then quantified the number of γ-H2AX foci in NFkB$^+$ and NFkB$^-$ cells, by immunofluorescence (see analysis procedure in Materials and Methods **paragraph 5.5**). We triggered p53 oscillatory dynamics via γ-irradiation (10 Gy) and then we perturbed its oscillations via Nutlin (10 μM) and TNF-α addition (10 ng/mL). We compared the amount of γ–H2AX foci at 1 hour, when we expect a higher number of foci, since cells are in the acute phase of DNA damage induction, and 24 hours, when DNA damage should have been repaired (Heltberg et al. 2022).

We started by comparing NFkB$^+$ and NFkB$^-$ cells upon γ-irradiation, γ–irradiation+Nutlin (to force p53 sustained dynamics) and γ–irradiation+TNF-α, treatment that perturbs p53 oscillations (**Figure 3.34A**). In **Figure 3.34B** the numbers of γ-H2AX foci, that were quantified at 1 and 24 hours after treatments in NFkB$^+$ cells, are reported. While TNF-α does not induce DNA damage, as expected, γ-irradiation (alone or combined with other stimuli) elicits a high level of damage foci at 1 hour (acute phase) for all the conditions involving γ-irradiation. Overall, this is highly reduced at 24 hours, indicating repair. Interestingly, cells treated with γ–irradiation+Nutlin, where p53 dynamics is sustained, are less efficient in repairing

DNA damage, since we detected a high number of damage foci 24 hours after the treatment. This result is in line with the model proposed by (Heltberg et al. 2022), in which p53 sustained dynamics is less able to effectively repair the induced damage than the oscillatory one. Moreover, cells treated also with TNF-α display a high number of damage foci at 24 hours, at a similar level to cells co-treated with γ-irradiation+Nutlin. This means that NF-κB-perturbed p53 dynamics worsened the efficiency of the DNA damage repair mechanism, similarly to what we observed for γ-irradiation+Nutlin.

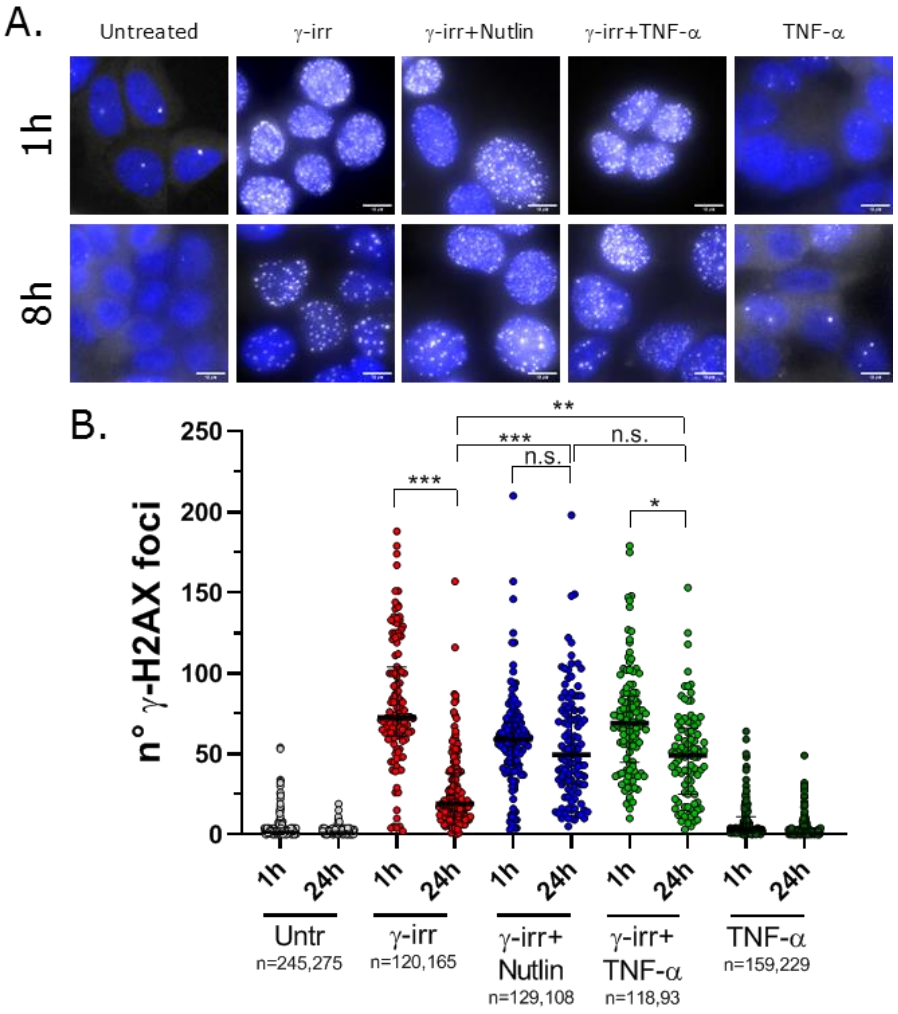

Figure 3.34. Quantification of DNA damage foci upon Nutlin and TNF-α in NFkB⁺ cells. *(A) Immunofluorescence images of γ-H2AX, marker of DNA damage (white signal) in NFkB⁺ cells. Blue signal = Hoechst. Scale bar: 10 μm. (B) Quantification of the number of γ-H2AX foci. N° of biological replicates = 1. N° of analysed cells are reported in each condition. Black bar = median, with interquartile range. Statistical test: Kruskal-Wallis (*p< 0.05, **p< 0.01, ***p< 0.005).*

In NFkB$^-$ cells, we detected similar trends for γ-irradiation and γ-irradiation+Nutlin. While upon the first treatment DNA damage significantly decreases after 24 hours, the second one prevents cells from efficiently repairing DNA damage, as evidenced by a heightened number of damage foci 24 hours post-treatment. Interestingly, in these cells, lacking p53 oscillatory dynamics perturbation by NF-κB activation, the levels of damage upon the co-treatment with TNF-α significantly decreased and DNA damage foci are better repaired, reaching similar levels to γ-irradiation treatment alone (**Figure 3.35**). This further confirms that NF-κB-mediated disruption of p53 oscillations worsens DNA repair.

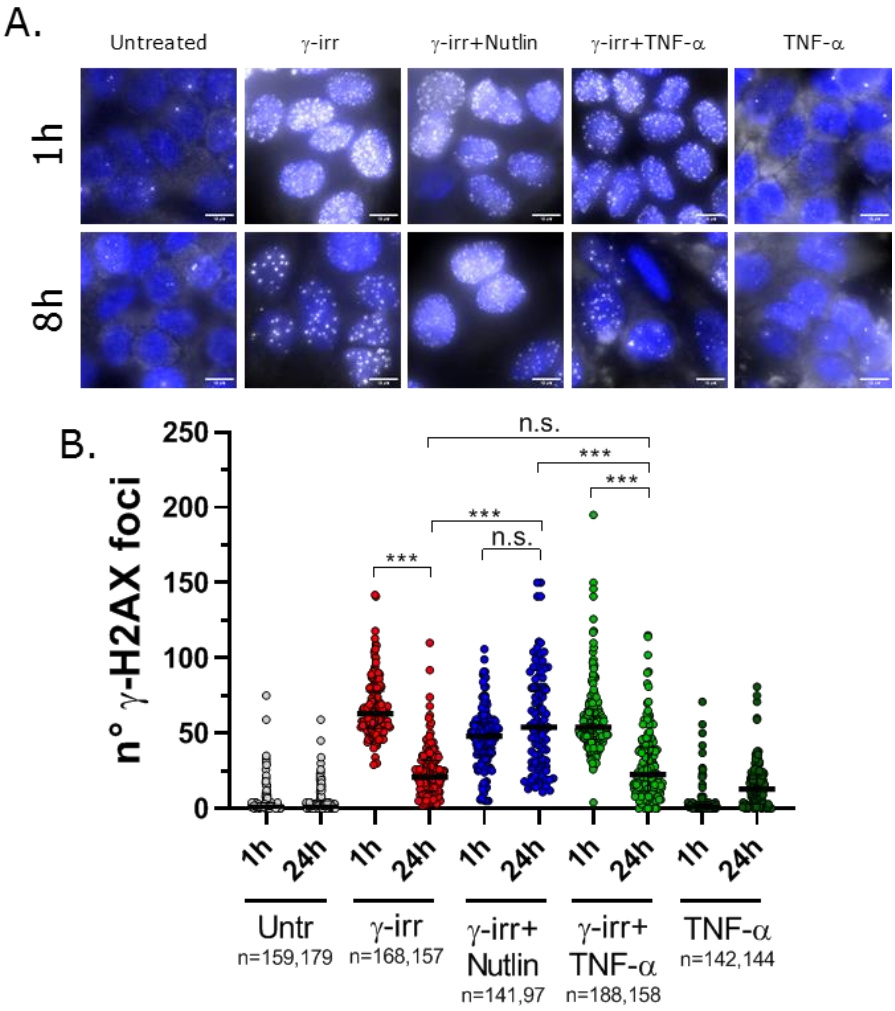

Figure 3.35. Quantification of DNA damage foci upon Nutlin and TNF-α in NFkB$^-$ cells. *(A) Immunofluorescence images of γ-H2AX, marker of DNA damage (white signal) in NFkB$^-$ cells. Blue signal = Hoechst. Scale bar: 10 μm. (B) Quantification of the number of γ-H2AX foci. N° of biological replicates = 1. N° of analysed cells are reported in each condition. Black bar = median, with interquartile range. Statistical test: Kruskal-Wallis (*p< 0.05, **p< 0.01, ***p< 0.005).*

To further confirm these results, we repeated this experiment, but now activating the NF-κB pathway via IL-1β addition (200 ng/mL). Similarly to the previous experiment, NFkB$^+$ cells retain a high number of γ-H2AX foci if p53 oscillations upon γ-irradiation are perturbed with Nutlin. Notably, cells treated with γ-irradiation and IL-1β also display a higher number of damage foci at 24 hours, which is significantly similar to cells co-treated with Nutlin (**Figure 3.36,** left). In NFkB$^-$ cells, instead, while after γ-irradiation DNA damage foci are repaired in 24 hours, we detected a higher number upon co-treatment with Nutlin. Interestingly, without NF-κB pathway activation, the levels of damage significantly decreased upon co-treatment with IL-1β, and DNA damage foci were repaired more effectively, reaching levels similar to those observed with γ-irradiation treatment alone (**Figure 3.36,** right). We can then conclude that also with IL-1β we found a behaviour similar to TNF-α: NF-κB-dependent perturbation of p53 oscillatory dynamics upon DNA damage and IL-1β worsens its efficiency in DNA damage repair.

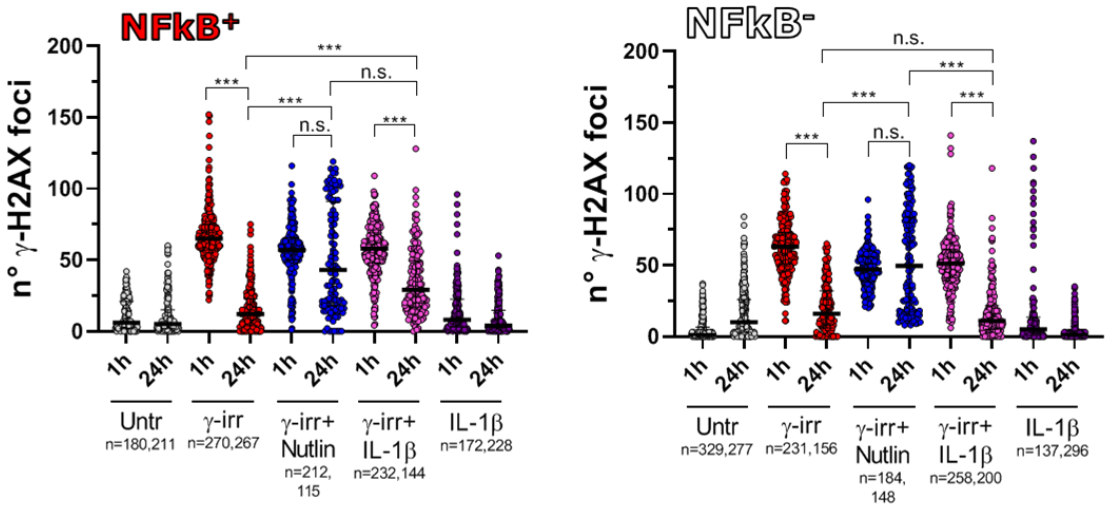

Figure 3.36. Quantification of DNA damage foci upon Nutlin and IL-1β in NFkB$^+$ and NFkB$^-$ cells. *Quantification of the number of γ-H2AX foci upon γ-irradiation and Nutlin/IL-1β treatments in NFkB$^+$ (left) and NFkB$^-$ (right) cells. N° of biological replicates = 1. N° of analysed cells are reported in each condition. Black bar = median, with interquartile range. Statistical test: Kruskal-Wallis (*p< 0.05, **p< 0.01, ***p< 0.005).*

4. DISCUSSION

The identification of the precise mechanism of how p53 and NF-κB mediate cell life/death decisions after stresses is crucial in tuning appropriate therapies to trigger apoptosis in cancer cells. These TFs are often dysregulated in cancer and a reciprocal influence between each other has been proven to be related to different cellular processes (Carrà et al. 2020). Since their pro-apoptotic and pro-survival roles, p53 and NF-κB have often been described as antagonists, but how their crosstalk works is still debated and not completely understood. In an *in vivo* scenario, cancer cells are subjected to stimuli coming from the tumour's inflammatory microenvironment and therapy-induced DNA damage. This suggests that the activation of p53 and NF-κB pathways, and the cell's response to stress, consequently, depends on the interplay between these pathways. However, previous studies have mostly focused on overexpression of one TF to counterbalance the other or the use of novel small molecules that might cause off-target confounding effects, potentially masking the real interplay between them.

A further level of complexity arises from the fact that both TFs display a dynamic behaviour. Their dynamics are pivotal in orchestrating cellular responses to different stimuli and controlling gene expression (Purvis et al. 2012) (Bacher et al. 2021). These intricate dynamics ensure precise timing and coordination of cellular decisions, such as cell cycle arrest, apoptosis, or inflammation. However, TFs dynamics have never been investigated in the context of p53/NF-κB crosstalk since in the literature most studies investigated the crosstalk with a static approach, without considering p53 and NF-κB temporal evolutions.

In this work, we investigated p53/NF-κB crosstalk, by either removing or tagging endogenous proteins and avoiding over-expressions. We find that the crosstalk between p53 and NF-κB is reflected in their dynamics, which are perturbed upon their simultaneous activation, which in turn affects target gene expression and DNA damage repair mechanism. Our findings emphasize the importance of studying the interaction between transcriptional pathways from a dynamic standpoint and at the single-cell level. By following at the same time both p53 and NF-κB dynamics via live-cell fluorescence microscopy, we showed that a simultaneous activation of p53 and NF-κB pathways perturb p53 response after a triggering stimulus. This was the case when inducing different p53 dynamics: both oscillatory upon DNA damage and sustained upon Nutlin treatment. Sustained p53 nuclear accumulation upon Nutlin was indeed enhanced by NF-κB activation via TNF-α or IL-1β treatments. p53

oscillations after DNA damage induction become accelerated and more sustained in time upon NF-κB activation with TNF-α. These results are in contrast with a paper by (Konrath et al. 2020), where they observed acceleration, but not enhancement in p53 oscillations upon a co-stimulation of γ-irradiation and TNF-α. A possible explanation for this difference may lie in the fact that, given the same extent of damage and quantity of TNF-α, (Konrath et al. 2020) used lung carcinoma cells with over-expressed fluorescently tagged p53 under the control of a different promoter (without an NF-κB binding site, contrarily to the endogenous one). Importantly, by knocking-out NF-κB from our cells, we did not observe enhancement nor perturbation in p53 oscillations and p53 accumulation dynamics upon the same stimuli triggering NF-κB. These data suggest that NF-κB is directly involved in p53 dynamics perturbation.

To deepen our observations, we then focused on single-cell p53 and NF-κB responses. By separating cell population according to the level of NF-κB response, we saw that those cells in which NF-κB nuclear levels over time were higher displayed a higher amount of nuclear p53. By using smFISH, we detected a similar correlation between *CDKN1A* and *NFKBIA* expression levels, target genes of p53 and NF-κB, respectively. With the same technique, we probed *TP53* mature mRNAs, obtaining a higher level of mature transcripts both upon TNF-α and Nutlin+TNF-α treatments. These results highlight that the NF-κB-derived perturbations of p53 dynamics that we detected via live-cell imaging may be due to a direct NF-κB-mediated transcription of the *TP53* gene by NF-κB when it gets activated. Mathematical modelling of the p53-MDM2 feedback loop further sustained our hypothesis: by increasing the p53 synthesis rate, its response to perturbation simulating Nutlin was enhanced, and its oscillations upon the simulation of DNA damage were accelerated and turned into a sustained accumulation, closely resembling our experimental data.

These results were quite surprising, because, with few exceptions (O'Prey et al. 2010) (Lowe et al. 2014), p53 and NF-κB are usually described as antagonists, with one inhibiting the activity of the other and vice versa (Cooks et al. 2014) (Shi & Jiang, 2021). In our cells, instead, a simultaneous activation of both TFs leads to an enhancement in p53 nuclear accumulation and its target gene expression. To investigate the effects of NF-κB-driven p53 dynamics perturbation, we focused on DNA damage repair mechanism, prompted by a recent biophysical model, proposing that p53 oscillations can stabilize the repair foci, avoiding the Oswald ripening phenomenon and leading to an efficient repair (Heltberg et al. 2022). We then tested the hypothesis made by this model in cells in which p53 dynamics was perturbed by

NF-κB activation and our results seemed to be in line with one of their assumptions. In fact, our data suggest that while unperturbed p53 oscillations efficiently repaired DNA damage, their perturbation upon Nutlin treatment or NF-κB pathway activation led to a persistent level of DNA damage foci.

Our data thus suggest a novel insight of the crosstalk between p53 and NF-κB. Indeed, in our MCF-7 breast cancer cells this crosstalk appears to be synergic at the molecular level (since NF-κB activation stimulates the expression of p53), but antagonistic at a functional level, since the perturbed p53 dynamics induced by NF-κB activation lead to delayed DNA damage repair.

This impairment in DNA damage repair could play a double-edged sword role in a scenario where cells are subjected to anti-cancer treatments. The perturbed p53 sustained dynamics could trigger transcriptional programs leading to apoptosis or senescence (Friedel & Loewer, 2022), but chronic DNA damage may activate other molecular pathways that instead promote cell survival (Clementi et al. 2020). Persistent DNA damage has also the potential to give rise to a variety of mutations and to induce genomic instability, which serves as the principal catalyst for cancer progression and chemoresistance (Zhang, 2020) (Moon et al. 2023). Moreover, it has been shown that anti-cancer treatments based on DNA damage efficiently induced apoptosis in proliferating cells, while quiescent cancer cells can overcome the damage and develop chemoresistance (Wu et al. 2017) (Lindell et al. 2023). It would be very interesting to investigate how p53 dynamics behave when perturbed by NF-κB activity in these two populations. Moreover, it will be necessary to also investigate if and how mutp53 protein dynamics can be perturbed by NF-κB in cancers characterized by p53 mutations (Mantovani et al. 2019) (Chen et al. 2022).

Our current results pose intriguing and significant questions that we aim to address in the future. A comprehensive understanding of the biological outcome of such p53 dynamics perturbations upon NF-κB activation requires deeper investigation. In our experiments, NF-κB was triggered with a single pulse of TNF-α; this acute inflammatory stimulus was sufficient to trigger cell death programs, as we detected a high number of dying cells via FACS. Our findings on MCF-7 cell fate are consistent with previous studies (Lee et al. 2016), but how p53 dynamics can be modulated in case of chronic inflammation needs to be further investigated. In future experiments, we address modulating NF-κB dynamics by applying to cells pulses of TNF-α with specific microfluidic devices (Zambrano et al. 2016). In this way, we will be able to further correlate multiple features of TFs dynamics, enhancing our comprehension of

how p53 and NF-κB dynamics are entangled in the temporal scale, even for prolonged and pre-existing inflammatory signals.

By smFISH and mathematical modelling of the p53/MDM2 feedback loop, we showed how perturbations in p53 dynamics might be attributed to NF-κB's direct transcription of the *TP53* gene. To further validate these data, we planned to perform ChIP (Chromatin Immunoprecipitation), in order to assess more deeply whether NF-κB binds the promoter of p53 and of its target genes occurs after TNF-α/IL-1β treatment.

We focused our attention in studying p53/NF-κB crosstalk in breast cancer cells, but it is worth investigating if we can generalize our results in other cancer settings. Regulating p53 and NF-κB dynamics to control tumour response might be particularly relevant in colorectal cancer (CRC), which is characterized by a resistant phenotype with high metastatic capacity after chemotherapy (Solé et al. 2022) and a persistent NF-κB-derived inflammatory status (Hai Ping et al. 2016). Despite some clues on p53/NF-κB crosstalk in CRC (Wagner et al. 2015), a simultaneous characterization of both TFs dynamics has never been performed. Osteosarcoma is another valid target for studying p53/NF-κB crosstalk. In this malignant bone tumour, while WT p53 form is present, but its functions are impaired by MDM2 overexpression (Senturk et al. 2017) (Ho et al. 2021), NF-κB was found to be involved in tumour initiation and progression (Avnet et al. 2021). We actually performed a pilot experiment on osteosarcoma U2OS cells, detecting a similar trend to that found in MCF-7: we quantified a higher nuclear abundance in p53 nuclear levels upon simultaneous activation of p53 and NF-κB with Nutlin and TNF-α, respectively, via immunofluorescence and Western Blot. In the future, we plan to introduce fluorescently tagged versions of our TFs in the HCT116 CRC cell line and U2OS osteosarcoma cell line, so we will be able to follow their dynamics with a live-cell imaging approach.

A further level of complexity relies on the entanglement in p53/NF-κB crosstalk **(Figure 1.8**). Other molecular players are involved in reciprocal interactions between p53 and NF-κB, such as MDM2, IκBα and IKK (Tergaonkar et al. 2002) (Carrà et al. 2016) (Konrath et al. 2020). In this work, we have shown how the dynamics of p53 are perturbed by NF-κB, but their negative regulators also follow dynamics related to the TF they regulate, being part of the feedback loop. A future evolution of this work will include the study of MDM2 and IκBα dynamics upon NF-κB-driven p53 dynamics perturbation, by tagging these two with different fluorescent molecules. Moreover, both p53 and NF-κB have been demonstrated to directly bind to IκBα and MDM2,

respectively (Carrà et al. 2016) (Cheney et al. 2008). However, it is currently not clear whether these interactions are modulated during TFs oscillations. Future studies will address this topic by using Fluorescence Cross-Correlation Spectroscopy (Bacia et al. 2006): from fluctuating fluorescence signals, a cross-correlation function is computed and used to measure the degree of binding or co-localization between two molecules.

Finally, there is accumulating evidence that both p53 and NF-κB dynamics are predictors of the response to chemotherapy and anti-cancer drugs of cells cultured in 2D, but these models inevitably mimic only partially the physical and chemical environment of in vivo highly complex tumours (Valkenburg et al. 2018). For this reason, a realistic characterization of p53/NF-κB dynamics should be done employing a configuration that resembles the tumour microenvironment, such as three-dimensional tumour spheroids and organoids, a powerful and realistic tool to study tissue genesis, development and disease (Tang et al. 2022), thus reducing the cell-to-organ gap, intrinsic in traditional cell cultures systems. Pilot experiments are already ongoing in this direction: we are currently setting up technical and experimental conditions to perform live-cell imaging of p53 and NF-κB dynamics on spheroids generated from our MCF-7 lines.

Taken together our data point out the importance of using a dynamic point of view to understand the crosstalk between p53 and NF-κB dynamics from their crosstalk. Our data offer novel insights on the interaction providing a more nuanced view on the proposed "antagonism" between these two TFs. We think that our approach could be extended to understand the interaction of different transcriptional networks with similar structures. We believe that single-cell quantitative characterization of p53/NF-κB dynamic crosstalk could shed new light in resulting cell fate decisions in response to anti-cancer treatments and inflammatory micro-environmental signals.

5. MATERIALS AND METHODS

5.1. Cell culture.

MCF-7 cells and derived clonal populations were cultured in RPMI medium (Thermo-Fisher, cat 11835105), supplemented with 10% of heat-inactivated Fetal Bovin Serum (FBS, Thermo-Fisher, cat 10270106), 100 units/mL penicillin-streptomycin (Thermo-Fisher, cat. 15140122) and 2 mM L-Glutamine (Gibco, Thermo-Fisher, cat. 25030081). Cells were cultured at 37°C in a humidified incubator with 5% CO_2. For regular maintenance, cells were split every 3-4 days through trypsinization (Thermo-Fisher, cat 11835105), seeded into 75 cm flasks or p100 dishes, and subjected to weekly testing for mycoplasma contamination using a PCR-based assay.

5.2. Treatments for p53 and NF-κB activation.

To trigger p53 oscillatory dynamics, MCF-7 cells were exposed to γ-irradiation (10 Gy), with a 137Cs source (Biobeam 2000), thus inducing DSBs. To trigger p53 sustained dynamics, MCF-7 cells were treated with Nutlin-3a (10 μM, Sigma-Aldrich, SML0580), a small molecule that blocks p53 interactions with its negative regulator MDM2. To trigger NF-κB cytosolic-to-nuclear translocation, cells were treated with either TNF-α (10 ng/mL, DBA, cat 11835105) or IL-1β (200 ng/mL, DBA, cat 200-01B). Both cytokines bind to a specific transmembrane protein, which in turn activates a reaction cascade inducing IκBα phosphorylation and NF-κB release.

5.3. Plasmids production and lentiviral infection of p65-mScarlet.

Federica Colombo and Alessandra Agresti kindly shared plasmids and protocol for p65-mScarlet lentiviral infection. Plasmids were produced via bacterial transformation. Each plasmid was diluted to a final concentration of 2-5 ng/mL in H_2O and the quantity used for each transformation was 15 ng. Each solution was added to the "top 10" bacteria (Thermo-Fisher, cat C404003), and then left in ice for 30 minutes. Bacteria were then subjected to heat-shock (2 minutes, 42°C) and let them recover in ice for 10 minutes. 1 mL of Lysogeny broth (LB, without antibiotic) was added to bacteria, incubated then for 1 hour, while mildly shaking (300 rpm) at 37°C. Tubes were then centrifuged at 4000 rpm for 5 minutes, the supernatant was discarded and the bacteria pellet was suspended in 400 μL of LB. 200 μL were then spread with a spatula on a plate coated with Ampicillin-resistant LB-agar. Plates were then left upside down overnight at 37°C. The day after, one bacterial colony from the

plate was added to a beuta containing 120 mL of LB with 1:1000 diluted Ampicillin, and then left on a stirring platform overnight at 37°C. The following day, MIDI-Prep protocol (NucleoBond Xtra EF plasmid purification, Carlo Erba, cat FC140420L) was performed to extract plasmids, that were then quantified via UV spectrophotometry.

Paola Falletta shared HEK 293T cells, necessary for virus production. $3x10^6$ HEK 293T cells, cultured in DMEM supplemented with 10% FBS, 1x L-glutamine and 1x pen/strep, were seeded in a p100 dish the day before transfection. The following day, the medium was replaced 2 hours before transfection with 9 mL of DMEM and plasmids, HBS 2X (used volume for p100 plate = 500 μL) and $CaCl_2$ (2.5 M, used volume for p100 plate = 50 μL) were thawed before transfection. The protocol relies on three plasmids: p65-mScarlet construct (12000 ng) (**Figure 5.1**), VSV-G (7000 ng, Addgene, cat 8454) and psPAX2 (11000 ng, Addgene, cat 12260). Each plasmid was added at the working concentration in H_2O. After 5 minutes at room temperature (RT), $CaCl_2$ was added to the master mix. After 5 minutes at RT, HBS is added dropwise, while bubbling the master mix with a 2 mL pipette. The mix was then added dropwise to the plate with HEK 293T cells. The medium was replaced 14 hours after transfection and the supernatant containing the virus was collected, filtered with a 0.22 μm syringe filter and added to MCF-7 cells 30 hours after the medium change. Infected cells were incubated at 37°C and 5% CO_2 and were passaged 3-4 times with BSL 2 laboratory procedures for at least 2 weeks, after which the virus became inactivated.

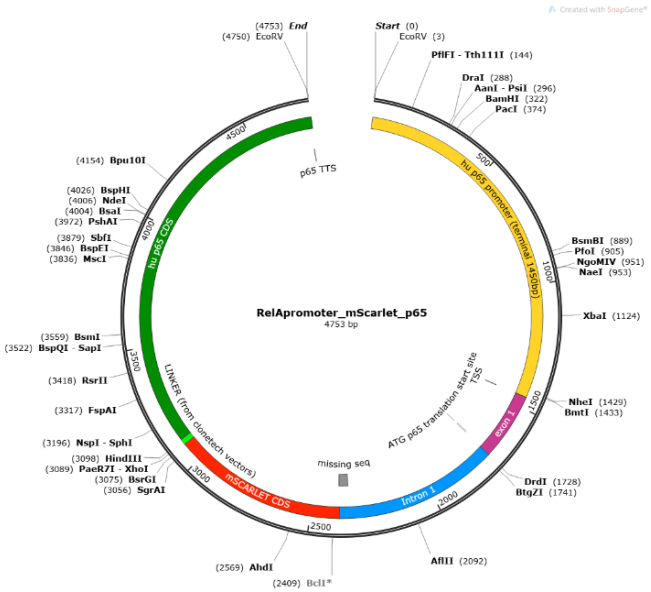

Figure 5.1. mScarlet-p65 vector used for lentiviral infection of MCF-7. *Construct used to infect MCF-7 p53-GFP line and derived clonal populations. Image created with SnapGene.*

5.4. Generation of clonal cell population.

MCF-7 cells were harvested by 1x Trypsin and counted. A final concentration of 1 cell/100 μL was achieved by serial dilutions and 100 μL were pipetted from a reservoir to a 96-well plate. The plate was screened for single colonies in the following weeks and growing colonies were then expanded.

5.5. Immunofluorescence and image analysis.

MCF-7 cells were seeded on coverslips and grown up to 80% of confluency. Cells were treated according to the experimental settings (γ-irradiation/Nutlin/TNF-α/IL-1β), washed once in PBS and fixed in 4% paraformaldehyde (PFA) for 10 minutes at RT. After fixation, cells underwent quenching with 50 mM NH_4Cl to reduce background, permeabilization with 0.1% Triton X-100 (Sigma Aldrich) and blocking at RT for 45 minutes in PBS supplemented with 20% FBS, 0.05% Tween 20 (Sigma Aldrich, cat. P2287) and 5% BSA (Sigma Aldrich, cat. A7906). Next, cells were incubated for 1 hour at RT with primary antibodies (diluted in 2% BSA) to detect p53 (mouse monoclonal antibody, Santa Cruz cat sc-126, 1:200 dilution), NF-κB (rabbit monoclonal antibody, Cell-Signalling/Euroclone, cat BK8242S, 1:100 dilution) or the DNA damage marker γ-H2AX (rabbit polyclonal γ-H2AX antibody, Abcam cat ab11174, 1:200 dilution). After three PBS washes, cells were incubated with secondary antibodies 1:1000 diluted in 2% BSA (anti-mouse IgG Alexa Fluor 488, Thermo-Fisher, cat A11029; anti-rabbit IgG Alexa Fluor 546, Thermo-Fisher, cat A11035; anti-rabbit IgG Alexa Fluor 647, Thermo-Fisher, cat A32733), for 1 hour at RT in the dark. Cells were washed three times in PBS and incubated in the dark with a DNA staining solution (Hoechst 33342, Thermo-Fisher, cat. H3570, 1:5000 dilution in PBS), for 10 min at RT. After two washes with PBS, coverslips were mounted with Vectashield (Vector Laboratories) and sealed. Images were collected with a widefield microscope (Olympus IX-81), equipped with a sCMOS camera (physical pixel size = 108.3 nm) and a 60x 1.49 N.A. oil-immersion objective (Olympus Life science, Segrate, IT) (UV led exposure: 100 ms; Blue led exposure: 500 ms; Yellow led exposure = 500 ms).

Images were then analysed with custom-written ImageJ/FIJI and MATLAB routines. Cells nuclei and entire profiles were automatically segmented via the Cellpose tool (Stringer et al. 2021). To quantify p53 nuclear abundance and NF-κB N.C.R., both raw data, nuclei and cytoplasms masks were loaded in MATLAB. Each nuclear mask is associated with its cytoplasm mask according to the level of superimposition

between the two masks. Cells detected at the boundary of the image were excluded. p53 mean fluorescence intensity was computed from single-cell nuclear masks, while NF-κB N.C.R. was computed as follows. The code quantifies the area of both the nucleus and the entire cell (A_{nucl}, A_{cell}), with respective fluorescence intensities (I_{nucl}, I_{cell}). Cytoplasm's fluorescence intensity is computed as: $I_{cytopl} = {(A_{cell} * I_{cell} - A_{nucl} * I_{nucl})}/{(A_{cell} - A_{nucl})}$. N.C.R. is then calculated as I_{nucl} / I_{cytopl}. Data from single images were then grouped according to the treatment.

To quantify the number of γ-H2AX foci, z-stack images were collected with a z-step of 0.5 μm (UV led exposure = 20 ms; Yellow led exposure = 250 ms). We then used the ThunderSTROM ImageJ plugin (Ovesný et al. 2014) to automatically detect and quantify spots of DNA damage (camera setup parameters: offset = 100; photoelectrons per A/D counts = 0.22; basal level = 100; connectivity = 8; threshold for spot detection = 4*std(Wavelet filter) with local maximum method). The algorithm generated a table with the positions of single spots. Cell nuclei were segmented through Cellpose (Stringer et al. 2021). Masks and tables with spots positions were loaded in MATLAB, where a custom-written routine assigned each spot to the respective nucleus and quantified the number of spots per cell. Cells detected at the boundary of the image were excluded.

5.6. Western Blot.

Cells were cultured on 10 cm dishes up to 80-90% of confluency. According to experimental time-points, dishes were washed once with PBS and lysed in 140 μL RIPA buffer (25 mM Tris HCl pH 7.6, 150 mM NaCl, 1% Sodium deoxycholate, 1% Triton X-100, 2 mM EDTA dihydrate) supplemented with protease inhibitors (Sigma-Aldrich, cat. 4693124001). Samples were next incubated at 4 °C for 15 min under constant rotation, centrifuged at 13000 rcf at 4°C and the supernatants were then collected into new vials. Lysates were then quantified via the BCA assay (Thermo-Fisher, cat. 23225). Single lysates were prepared in order to load from 25 to 40 μg of proteins, thus adding H_2O and 4x Laemmli protein sample buffer (Biorad, cat 1610747, supplemented with 10% of β-mercaptoethanol) up to the final volume. Lysates were then loaded into an 8% SDS-polyacrylamide gels (Lower gel: 4.7 mL H_2O, 2.5 mL Resolving Buffer, 6.6 mL Acrylamide, 100 μL ammonium persulfate, 10 μL TEMED; Stacking gel: 2.862 mL H_2O, 2.5 mL Upper Buffer, 833 μL Acrylamide, 50 μL ammonium persulfate, 5 μL TEMED); electrophoresis ran at 100 Volts for ~2-3

hours. Proteins were then transferred to nitrocellulose membranes in cold transfer buffer (25 mM Tris, 192 mM glycine, 20% methanol) through run at 100 Volts for 2 hours (or at 15 Volts, overnight) at 4°C. Membranes were then exposed to Ponceau solution, washed with TBS-T solution (0.1% Tween20 in TBS: 20 mM Tris base, 137 mM sodium chloride, pH 7.6) and blocked in 5% non-fat dried milk in TBS-T solution for 1 hour at RT on oscillating platform. Membranes were then incubated overnight at 4°C with primary antibodies, all diluted in 5% non-fat dried milk in TBS-T solution (anti-p53 mouse monoclonal antibody, Santa Cruz cat sc-126, 1:3000 dilution; anti-NF-κB rabbit monoclonal antibody, Cell-Signalling/Euroclone, cat BK8242S, 1:2000 dilution; anti-GAPDH rabbit monoclonal Abcam, cat. ab128915, 1:40000 dilution; anti-vinculin mouse monoclonal, Thermo-Fisher, cat. MA5-11690, 1:4000 dilution). Next, membranes were washed three times in TBS-T, 5 min each wash at RT, while shaking, and then incubated for 1 hour at RT with peroxidase-conjugated secondary antibodies (anti-mouse IgG, Cell Signalling, cat. 7076; anti-rabbit IgG, Cell Signalling, cat. 7074) diluted 1:5000 in 5% non-fat dried milk in TBS-T solution. Membranes were then developed using an ECL substrate (Bio Rad, cat. 1705061) and images were acquired with a CCD camera via ChemiDoc MP imaging system. Bands intensity was quantified via ImageLab software.

5.7. smFISH and image analysis.

Cells were seeded on coverslips and cultured up to 80% of confluency. After treatments, cells were fixed in 4% PFA (10 min at RT), and washed with 135 mM Glycine in PBS for 10 min at RT. smFISH protocol changed according to the probe. For *CDKN1A* and *NFKBIA* probes (*Design Ready Stellaris*), cells were incubated with a washing buffer I, composed of 10% saline sodium citrate (SSC) in nuclease-free water (Sigma-Aldrich, cat 95284), for 5 minutes at RT. Then, cells were incubated with a washing buffer II, composed of 10% SSC and 20% deionized formamide in nuclease-free water, for 5 minutes at RT. Next, cells underwent hybridization, by placing coverslips onto a drop (80 μL) of hybridization solution (1 μL of probe in 100 μL of 10% SSC, 10% dextran sulphate and 20% deionized formamide in nuclease-free water) and left over-night in a humidified chamber (37°C). The following day, cells were washed twice with buffer I (30 min per wash, at 37 °C in the dark), once in 10% SCC-20×, and then incubated with a DNA staining solution (Hoechst 33342, 1:10000 diluted in PBS) for 10 min at RT in the dark.

For *TP53* probe (*HuluFISH*), cells were washed twice with HuluWash buffer (2x SSC, 2M Urea) for 10 minutes each at RT. Cells were then hybridized into a humidified chamber (30°C) by placing the coverslips onto a drop of hybridization solution (0.5 μL of *TP53* probe diluted into 50 μL of 2x SSC, 2M Urea, 10% dextran sulphate, 5x Denhardt's solution). The following day, cells were washed twice in HuluWash buffer (30 minutes per wash, at 37 °C in the dark) and then incubated with a DNA staining solution (Hoechst 33342, 1:10000 in PBS) for 10 min at RT in the dark. Coverslips were mounted on glass slides with Vectashield (Vector Laboratories) and sealed. 3D z-stack images were collected with the widefield microscope (Olympus IX-81) used also for immunofluorescence (see **paragraph 5.5**) (z-step = 0.3 μm; UV led exposure: 20 ms; Yellow led exposure (*CDKN1A*): 500 ms; Red led exposure = 500 ms (*NFKBIA*), 100 ms (*TP53*)).

Images were then processed with custom-written routines and FISH-Quant (Mueller et al. 2013). Nuclei and single-cell profiles were segmented via Cellpose and then transformed into FISH-Quant regions-of-interest (ROI) by Python routines written by Tom Fillot. With FISH-Quant, the amount of mature RNA molecules per cell was detected as 3D Gaussian spots exhibiting peak intensity levels above a predetermined threshold, which was kept constant for each analysed image. The threshold was differently set according to the analysed probe (*TP53*, *CDKN1A*, and *NFKBIA*).

5.8. RNA extraction and RT-qPCR.

Cells were cultured on 10 cm dishes up to 80-90% of confluency. According to experimental time-points, cells were lysed in 500 μL of TRIzol reagent (Thermo-Fisher, cat. 15596018) to extract the total RNA. Lysates were then purified using silica membrane columns (NucleoSpin RNA Plus, Machery-Nagel, Carlo Erba, cat FC140955N), thus extracting the RNA that was quantified and tested for purity by NanoDrop fluorometer (Thermo-Fisher). For each sample, 2 μg of RNA underwent reverse transcription to cDNA using the High-Capacity cDNA Reverse Transcription Kit (Thermo-Fisher cat. 4368814). Real-time qPCR analysis was then performed to assess the expression of p53/NF-κB target genes. The reaction solution was prepared as follows: 8 μl of cDNA solution (5 μL of cDNA 1:100 diluted + 3 μL of nuclease-free H_2O) and 5 μL of Oligo Solution, composed by 10 μL of SYBR Green mix (Roche, LightCycler 480 I Master) and 2 mL of primer mix (100 μM of forward and reverse primers). GAPDH was used as an internal standard for cDNA normalization.

5.9. Live-cell confocal imaging and data analysis.

Cells were seeded and cultured onto µ-Slide 8-Well Glass Bottom supports (Ibidi, cat 80827), in order to reach 60-70% confluency on the day of the live-cell imaging experiment. Before imaging, cells were incubated with nuclei staining (Hoechst 33342, 1:10000 in RPMI), for 10 minutes at 37°C and 5% CO_2; then the medium was replaced with 150 µL of fresh medium. Treatments were prepared at double concentration and 150 µL were directly added to the respective well. We used both a Leica TCS SP5 and SP8 confocal microscopes, with an incubation system where cells were stably maintained at 37°C in 5% CO_2. We used a 20x, 0.5 NA objective, open pinhole (Airy = 3) and 400 Hz of acquisition frequency. p53-GFP and p65-mScarlet were imaged with the 488 nm and 546 nm Argon lasers, respectively, in the SP5 microscope and with a White Light Laser in the SP8 microscope. Hoechst 33342 stained nuclei were imaged with the low energy 405 nm UV diode laser (power = 5-10%). Images were acquired as 16-bit, 1024×1024, thus returning a single LIF file containing all TIFF x-y-t stacks. The frequency of acquisition was decided according to the experimental conditions that we were testing and the number of fields of view per condition: to acquire the fast NF-κB dynamics on multiple fields and to avoid oversampling, the acquisition frequency was set between 6-8 minutes.

Time-courses were processed and analysed via semi-automatic custom-written ImageJ/FIJI macros and MATLAB scripts. From the global LIF file, single TIFFs, corresponding to the single fields of view, were grouped into separate stacks. Each frame of the stack was then segmented via Cellpose, to have masks of both nuclei and entire cell profiles, that were subsequently grouped into new stacks. In MATLAB, each stack was processed one at a time. Each nucleus was associated with its "cytoplasm" according to the level of superimposition between the two masks. Cells detected at the boundary of the image were excluded. p53 and NF-κB mean fluorescence intensity was computed from nuclear masks, while NF-κB N.C.R. was computed as reported in **Paragraph 5.5**. Each mask was then tracked along the time-course with the Hungarian linker algorithm (Jaqaman et al. 2008) (Careccia et al. 2019). Single-cell profiles were then grouped in several matrices according to the measured entity: p53 nuclear intensity, NF-κB nuclear intensity and N.C.R., nuclei and cytoplasms areas and x-y coordinates in the field of view. Matrices were then concatenated according to the respective treatment and profiles were smoothed with the *smoothdata* MATLAB function (method = Gaussian, window size for p53 = 7 (Konrath et al. 2020), window size for NF-κB = 4). Single-cell profiles that do not reach 2/3 of the length of the acquisition and that do not start from the first frame

were excluded. AUC of p53 and NF-κB profiles (after removing the basal level) were calculated as the integral in the time interval considered, normalized by the actual length of each profile. Peaks of oscillations of p53 dynamics were computed using the *islocalmax* MATLAB function, thus considering the two peaks with higher prominence. To investigate the relationship between p53 and NF-κB nuclear responses at the single-cell level, we measured the area under the curve (AUC) of nuclear NF-κB as a way to quantify the extent of NF-κB translocation, instead of relying on N.C.R. profiles.

5.10. Mathematical modelling.

The model we used was proposed by (Hunziker et al. 2010). We started from the set of parameters proposed by the paper, described in **Table 1** (3rd column). Before each simulation, parameters were randomized allowing a maximal fold change around the original value in an interval of ±5. The system equilibration up to 72 hours was tested. The starting values of P, M, R and C in ODEs (**Figure 3.29**) were set at 0, 60, 0, and 0, respectively (Azam et al. 2018). ODEs were resolved by the *ode23tb*

Parameter	Description	Original Value (Hunziker et al. 2010)	Used in our model	Units
σ_p	p53 synthesis rate	1000	720.5	$nM*h^{-1}$
α	MDM2-independent degradation of p53	0.1	0.018	h^{-1}
γ	MDM2 degradation	0.2	0.042	h^{-1}
k_b	p53-MDM2 complex dissociation	7200	7536	h^{-1}
$k_f = k_b/r$	p53-MDM2 dissociation constant	5000	6645	$nM^{-1}*h^{-1}$
r		1.44	1.134	-
K_{trs}	MDM2 transcription rate	0.03	0.008	$nM^{-1}*h^{-1}$
β	MDM2 mRNA degradation rate	0.6	0.428	h^{-1}
K_{trd}	MDM2 translation rate	1.4	0.2	h^{-1}
δ	MDM2-dependent degradation of p53	11	0.9	h^{-1}

Table 1. Parameters of the mathematical model. *Parameters of p53-MDM2 feedback loop proposed by Hunziker et al. (3rd column) and used in our model (4th column) are reported (in resting condition) with respective description, value and unit.*

function in MATLAB, with an absolute tolerance error of 10^{-3}. Simulations of DNA damage and Nutlin treatments were performed according to parameters modifications proposed by (Hunziker et al. 2010). Simulations were run to assess how p53-MDM2 feedback loop might evolve in 24h.

We reported the best parameters able to reproduce p53 oscillations and sustained dynamics observed in the experiments in the 4th column of **Table 1**. To simulate DNA damage, parameters have been modified in this way: γ (MDM2 degradation rate) was increased by a factor of 2.5; δ (MDM2-dependent degradation of p53) was decreased by a factor of 5.5; k_f was decreased, by increasing *r* by a factor of 10.

To simulate Nutlin, we employed an approach inspired by the delayed effect of Nutlin proposed by (Purvis et al. 2012). We applied to the parameter k_f a time-dependent reduction from k_f (at t=0) to k_f/R (for large t), according to the following formula: $k_f(t) = k_f \cdot 1/(1 + N(t) \cdot (R - 1))$. The formula relies on the normalized effect of Nutlin (*N(t)*) that in turn reproduces different types of pharmacokinetics. In particular, we found an accumulation of p53 similar to the one observed in our experiments if *R* (maximum fold change reduction)=500 and $N(t) = t^n/(t_{\frac{1}{2}}^n + t^n)$ with $t_{1/2}$ (time of half-maximum)=24 h, n=3.

To simulate the increase in p53 protein synthesis, which would be directly proportional to the rise in mature mRNA from the same gene, we applied a time-dependent linear function to scale the parameter $\sigma_p(t)$ according to different fold changes, between 6 (baseline) and 20.

5.11. Flow Cytometry analysis.

Cells were seeded in a 6-wells plate and the experiment was performed when cells reached 70–80% of confluency. According to the respective timings of treatments, cells were washed in PBS, trypsinized and resuspended in 250 mL of staining solution, composed of 5% FBS, and TO-PRO-3 iodide (642/661) 1 μM for 5 minutes to allow TO-PRO-3 incorporation in the dead cells fraction. Cells were then washed, centrifuged, and resuspended in 50 μl of staining solution for analysis. Levels of cell death were measured by FACS on a BD FACS Canto II (BD Biosciences), and data were analysed using FlowJo software.

5.12. Statistical analysis.

All the statistical tests that have been used and the number of experimental replicates are described in figures captions. The threshold of significance was set to p-value=0.05. In the scatter dot plots, the median is shown as a line within the interquartile range.

6. BIBLIOGRAPHY

Ahmed, Aftab, e Erik I. Verriest. 2017. «Modeling & Analysis of Gene Expression as a Nonlinear Feedback Problem With State-Dependent Delay». *IFAC-PapersOnLine* 50 (1): 12679–84. https://doi.org/10.1016/j.ifacol.2017.08.2248.

Ak, Prashanth, e Arnold J. Levine. 2010. «P53 and NF-κB: Different Strategies for Responding to Stress Lead to a Functional Antagonism». *The FASEB Journal* 24 (10): 3643–52. https://doi.org/10.1096/fj.10-160549.

Allegra, Alessandro, Antonio Speciale, Maria Sofia Molonia, Letterio Guglielmo, Caterina Musolino, Guido Ferlazzo, Gregorio Costa, Antonella Saija, e Francesco Cimino. 2018. «Curcumin Ameliorates the in Vitro Efficacy of Carfilzomib in Human Multiple Myeloma U266 Cells Targeting P53 and NF-κB Pathways». *Toxicology in Vitro* 47 (marzo): 186–94. https://doi.org/10.1016/j.tiv.2017.12.001.

Alon, Uri. 2007. «Network Motifs: Theory and Experimental Approaches». *Nature Reviews Genetics* 8 (6): 450–61. https://doi.org/10.1038/nrg2102.

An, Won G., Meera Kanekal, M. Celeste Simon, Emin Maltepe, Mikhail V. Blagosklonny, e Leonard M. Neckers. 1998. «Stabilization of Wild-Type P53 by Hypoxia-Inducible Factor 1α». *Nature* 392 (6674): 405–8. https://doi.org/10.1038/32925.

Ankers, John M, Raheela Awais, Nicholas A Jones, James Boyd, Sheila Ryan, Antony D Adamson, Claire V Harper, et al. 2016. «Dynamic NF-κB and E2F Interactions Control the Priority and Timing of Inflammatory Signalling and Cell Proliferation». *eLife* 5 (maggio): e10473. https://doi.org/10.7554/eLife.10473.

Armstrong, Michael B., Xin Bian, Yihong Liu, Chitra Subramanian, Anthony B. Ratanaproeksa, Feng Shao, Victor C. Yu, Roland P.S. Kwok, Anthony W. Opipari, e Valerie P. Castle. 2006. «Signaling from P53 to NF-κB Determines the Chemotherapy Responsiveness of Neuroblastoma». *Neoplasia* 8 (11): 967–77. https://doi.org/10.1593/neo.06574.

Ashall, Louise, Caroline A. Horton, David E. Nelson, Pawel Paszek, Claire V. Harper, Kate Sillitoe, Sheila Ryan, et al. 2009. «Pulsatile Stimulation Determines Timing and Specificity of NF-κB-Dependent Transcription». *Science* 324 (5924): 242–46. https://doi.org/10.1126/science.1164860.

Avnet, Sofia, Silvia Lemma, Margherita Cortini, Gemma Di Pompo, Francesca Perut, Maria Veronica Lipreri, Laura Roncuzzi, et al. 2021. «The Release of Inflammatory Mediators from Acid-Stimulated Mesenchymal Stromal Cells Favours Tumour Invasiveness and Metastasis in Osteosarcoma». *Cancers* 13 (22): 5855. https://doi.org/10.3390/cancers13225855.

Azam, Muhammad Rizwan, Sahar Fazal, Mukhtar Ullah, e Aamer I. Bhatti. 2018. «System-based Strategies for P53 Recovery». *IET Systems Biology* 12 (3): 101–7. https://doi.org/10.1049/iet-syb.2017.0025.

Aziz, M H, H Shen, e C G Maki. 2011. «Acquisition of P53 Mutations in Response to the Non-Genotoxic P53 Activator Nutlin-3». *Oncogene* 30 (46): 4678–86. https://doi.org/10.1038/onc.2011.185.

Bacher, Susanne, Johanna Meier-Soelch, Michael Kracht, e M. Lienhard Schmitz. 2021. «Regulation of Transcription Factor NF-κB in Its Natural Habitat: The Nucleus». *Cells* 10 (4): 753. https://doi.org/10.3390/cells10040753.

Bacia, Kirsten, Sally A Kim, e Petra Schwille. 2006. «Fluorescence Cross-Correlation Spectroscopy in Living Cells». *Nature Methods* 3 (2): 83–89. https://doi.org/10.1038/nmeth822.

Barnes, Sarah E, Ying Wang, Luqiu Chen, Luciana L Molinero, Thomas F Gajewski, Cesar Evaristo, e Maria-Luisa Alegre. 2015. «T Cell-NF-κB Activation Is Required for Tumor Control in Vivo». *Journal for ImmunoTherapy of Cancer* 3 (1): 1. https://doi.org/10.1186/s40425-014-0045-x.

Bartfeld, Sina, Simone Hess, Bianca Bauer, Nikolaus Machuy, Lesley A Ogilvie, Johannes Schuchhardt, e Thomas F Meyer. 2010. «High-Throughput and Single-Cell Imaging of NF-κB Oscillations Using Monoclonal Cell Lines». *BMC Cell Biology* 11 (1): 21. https://doi.org/10.1186/1471-2121-11-21.

Basu, Ashis. 2018. «DNA Damage, Mutagenesis and Cancer». *International Journal of Molecular Sciences* 19 (4): 970. https://doi.org/10.3390/ijms19040970.

Batchelor, Eric, Alexander Loewer, Caroline Mock, e Galit Lahav. 2011. «Stimulus-dependent Dynamics of P53 in Single Cells». *Molecular Systems Biology* 7 (1): 488. https://doi.org/10.1038/msb.2011.20.

Ben-Neriah, Yinon, e Michael Karin. 2011. «Inflammation Meets Cancer, with NF-κB as the Matchmaker». *Nature Immunology* 12 (8): 715–23. https://doi.org/10.1038/ni.2060.

Bessho, Yasumasa, Hiromi Hirata, Yoshito Masamizu, e Ryoichiro Kageyama. 2003. «Periodic Repression by the bHLH Factor Hes7 Is an Essential Mechanism for the Somite Segmentation Clock». *Genes & Development* 17 (12): 1451–56. https://doi.org/10.1101/gad.1092303.

Bhattacharyya, Sumit, Alip Borthakur, Pradeep K. Dudeja, e Joanne K. Tobacman. 2010. «Lipopolysaccharide-Induced Activation of NF-κB Non-Canonical Pathway Requires BCL10 Serine 138 and NIK Phosphorylations». *Experimental Cell Research* 316 (19): 3317–27. https://doi.org/10.1016/j.yexcr.2010.05.004.

Busuttil, Valere, Nathalie Droin, Laura McCormick, Francesca Bernassola, Eleonora Candi, Gerry Melino, e Douglas R. Green. 2010. «NF-κB Inhibits T-Cell Activation-Induced, P73-Dependent Cell Death by Induction of MDM2». *Proceedings of the National Academy of Sciences* 107 (42): 18061–66. https://doi.org/10.1073/pnas.1006163107.

Canman, Christine E., Dae-Sik Lim, Karlene A. Cimprich, Yoichi Taya, Katsuyuki Tamai, Kazuyasu Sakaguchi, Ettore Appella, Michael B. Kastan, e Janet D. Siliciano. 1998. «Activation of the ATM Kinase by Ionizing Radiation and Phosphorylation of P53». *Science* 281 (5383): 1677–79. https://doi.org/10.1126/science.281.5383.1677.

Careccia, Giorgia, Federica Colombo, Mario Tirone, Alessandra Agresti, Marco E. Bianchi, Samuel Zambrano, e Emilie Vénéreau. 2019. «Exploiting Live Imaging to Track Nuclei During Myoblast Differentiation and Fusion». *Journal of Visualized Experiments*, fasc. 146 (aprile): 58888. https://doi.org/10.3791/58888.

Carrà, Giovanna, Sabrina Crivellaro, Riccardo Taulli, Angelo Guerrasio, Giuseppe Saglio, e Alessandro Morotti. 2016. «Mechanisms of P53 Functional De-Regulation: Role of the IκB-α/P53 Complex». *International Journal of Molecular Sciences* 17 (12): 1997. https://doi.org/10.3390/ijms17121997.

Carrà, Giovanna, Marcello Francesco Lingua, Beatrice Maffeo, Riccardo Taulli, e Alessandro Morotti. 2020. «P53 vs NF-κB: The Role of Nuclear Factor-Kappa B in the Regulation of P53 Activity and Vice Versa». *Cellular and Molecular Life Sciences* 77 (22): 4449–58. https://doi.org/10.1007/s00018-020-03524-9.

Chang, Nan-Shan. 2002. «The Non-Ankyrin C Terminus of IκBα Physically Interacts with P53 in Vivo and Dissociates in Response to Apoptotic Stress, Hypoxia, DNA Damage, and Transforming Growth Factor-B1-Mediated Growth Suppression». *Journal of Biological Chemistry* 277 (12): 10323–31. https://doi.org/10.1074/jbc.M106607200.

Chen, Xiaohua, Taotao Zhang, Wei Su, Zhihui Dou, Dapeng Zhao, Xiaodong Jin, Huiwen Lei, et al. 2022. «Mutant P53 in Cancer: From Molecular Mechanism to Therapeutic Modulation». *Cell Death & Disease* 13 (11): 974. https://doi.org/10.1038/s41419-022-05408-1.

Cheney, Misty D., Pamela P. McKenzie, Erin L. Volk, Liying Fan, e Linda C. Harris. 2008. «MDM2 Displays Differential Activities Dependent upon the Activation Status of NFκB». *Cancer Biology & Therapy* 7 (1): 38–44. https://doi.org/10.4161/cbt.7.1.5125.

Cheng, Qian, e Jiandong Chen. 2010. «Mechanism of P53 Stabilization by ATM after DNA Damage». *Cell Cycle* 9 (3): 472–78. https://doi.org/10.4161/cc.9.3.10556.

Cheng, Quen J., Sho Ohta, Katherine M. Sheu, Roberto Spreafico, Adewunmi Adelaja, Brooks Taylor, e Alexander Hoffmann. 2021. «NF-κB Dynamics Determine the Stimulus Specificity of Epigenomic Reprogramming in Macrophages». *Science* 372 (6548): 1349–53. https://doi.org/10.1126/science.abc0269.

Chien, Yuchen, Claudio Scuoppo, Xiaowo Wang, Xueping Fang, Brian Balgley, Jessica E. Bolden, Prem Premsrirut, et al. 2011. «Control of the Senescence-Associated Secretory Phenotype by NF-κB Promotes Senescence and Enhances Chemosensitivity». *Genes & Development* 25 (20): 2125–36. https://doi.org/10.1101/gad.17276711.

Clementi, Elena, Larissa Inglin, Erin Beebe, Corina Gsell, Zuzana Garajova, e Enni Markkanen. 2020. «Persistent DNA Damage Triggers Activation of the Integrated Stress Response to Promote Cell Survival under Nutrient Restriction». *BMC Biology* 18 (1): 36. https://doi.org/10.1186/s12915-020-00771-x.

Colombo, Federica, Samuel Zambrano, e Alessandra Agresti. 2018. «NF-κB, the Importance of Being Dynamic: Role and Insights in Cancer». *Biomedicines* 6 (2): 45. https://doi.org/10.3390/biomedicines6020045.

Cooks, Tomer, Curtis C. Harris, e Moshe Oren. 2014. «Caught in the Cross Fire: P53 in Inflammation». *Carcinogenesis* 35 (8): 1680–90. https://doi.org/10.1093/carcin/bgu134.

Cooks, Tomer, Ioannis S. Pateras, Ohad Tarcic, Hilla Solomon, Aaron J. Schetter, Sylvia Wilder, Guillermina Lozano, et al. 2013. «Mutant P53 Prolongs NF-κB Activation and Promotes Chronic Inflammation and Inflammation-Associated Colorectal Cancer». *Cancer Cell* 23 (5): 634–46. https://doi.org/10.1016/j.ccr.2013.03.022.

Crivellaro, Sabrina, Cristina Panuzzo, Giovanna Carrà, Alessandro Volpengo, Francesca Crasto, Enrico Gottardi, Ubaldo Familiari, et al. 2015. «Non Genomic Loss of Function of Tumor Suppressors in CML: BCR-ABL Promotes IκBα Mediated P53 Nuclear Exclusion». *Oncotarget* 6 (28): 25217–25. https://doi.org/10.18632/oncotarget.4611.

Dajee, Maya, Mirella Lazarov, Jennifer Y. Zhang, Ti Cai, Cheryl L. Green, Alan J. Russell, M. Peter Marinkovich, et al. 2003. «NF-κB Blockade and Oncogenic Ras Trigger Invasive Human Epidermal Neoplasia». *Nature* 421 (6923): 639–43. https://doi.org/10.1038/nature01283.

DeLeo, A B, G Jay, E Appella, G C Dubois, L W Law, e L J Old. 1979. «Detection of a Transformation-Related Antigen in Chemically Induced Sarcomas and Other Transformed Cells of the Mouse.» *Proceedings of the National Academy of Sciences* 76 (5): 2420–24. https://doi.org/10.1073/pnas.76.5.2420.

Dey, Anwesha, Vinay Tergaonkar, e David P. Lane. 2008. «Double-Edged Swords as Cancer Therapeutics: Simultaneously Targeting P53 and NF-κB Pathways». *Nature Reviews Drug Discovery* 7 (12): 1031–40. https://doi.org/10.1038/nrd2759.

Diep, Sydney, Mahita Maddukuri, Stephanie Yamauchi, Ganamee Geshow, e Nikki A. Delk. 2022. «Interleukin-1 and Nuclear Factor Kappa B Signaling Promote Breast Cancer Progression and Treatment Resistance». *Cells* 11 (10): 1673. https://doi.org/10.3390/cells11101673.

Dreyfus, David H, Masayuki Nagasawa, Erwin W Gelfand, e Lucy Y Ghoda. 2005. «Modulation of P53 Activity by Iκ Bα : Evidence Suggesting a Common Phylogeny between NF-κ B and P53 Transcription Factors». *BMC Immunology* 6 (1): 12. https://doi.org/10.1186/1471-2172-6-12.

Droin, Colas, Eric R. Paquet, e Felix Naef. 2019. «Low-Dimensional Dynamics of Two Coupled Biological Oscillators». *Nature Physics* 15 (10): 1086–94. https://doi.org/10.1038/s41567-019-0598-1.

E. Tamura, R., J. F. De Vasconcellos, D. Sarkar, T. A. Libermann, P. B. Fisher, e L. F. Zerbini. 2012. «GADD45 Proteins: Central Players in Tumorigenesis». *Current Molecular Medicine* 12 (5): 634–51. https://doi.org/10.2174/156652412800619978.

Eliaš, Ján, e Cicely K. Macnamara. 2021. «Mathematical Modelling of P53 Signalling during DNA Damage Response: A Survey». *International Journal of Molecular Sciences* 22 (19): 10590. https://doi.org/10.3390/ijms221910590.

Erl, Wolfgang, Göran K. Hansson, Rainer De Martin, Georg Draude, Kim S. C. Weber, e Christian Weber. 1999. «Nuclear Factor-κB Regulates Induction of Apoptosis and Inhibitor of Apoptosis Protein-1 Expression in Vascular Smooth Muscle Cells». *Circulation Research* 84 (6): 668–77. https://doi.org/10.1161/01.RES.84.6.668.

Fei, Peiwen, Eric J. Bernhard, e Wafik S. El-Deiry. 2002. «Tissue-Specific Induction of P53 Targets in Vivo». *Cancer Research* 62 (24): 7316–27.

Feng, Jianhua, Rastislav Tamaskovic, Zhongzhou Yang, Derek P. Brazil, Adrian Merlo, Daniel Hess, e Brian A. Hemmings. 2004. «Stabilization of Mdm2 via Decreased Ubiquitination Is Mediated by Protein Kinase B/Akt-Dependent Phosphorylation». *Journal of Biological Chemistry* 279 (34): 35510–17. https://doi.org/10.1074/jbc.M404936200.

Fiore, Alessandra, Stefano Ugel, Francesco De Sanctis, Sara Sandri, Giulio Fracasso, Rosalinda Trovato, Silvia Sartoris, et al. 2018. «Induction of Immunosuppressive Functions and NF-κB by FLIP in Monocytes». *Nature Communications* 9 (1): 5193. https://doi.org/10.1038/s41467-018-07654-4.

Fischer, M. 2017. «Census and Evaluation of P53 Target Genes». *Oncogene* 36 (28): 3943–56. https://doi.org/10.1038/onc.2016.502.

Franklin, J. Matthew, Rajarshi P. Ghosh, Quanming Shi, Michael P. Reddick, e Jan T. Liphardt. 2020. «Concerted Localization-Resets Precede YAP-Dependent Transcription». *Nature Communications* 11 (1): 4581. https://doi.org/10.1038/s41467-020-18368-x.

Friedel, Laura, e Alexander Loewer. 2022. «The Guardian's Choice: How P53 Enables Context-specific Decision-making in Individual Cells». *The FEBS Journal* 289 (1): 40–52. https://doi.org/10.1111/febs.15767.

Gasparian, Alexander V., Catherine A. Burkhart, Andrei A. Purmal, Leonid Brodsky, Mahadeb Pal, Madhi Saranadasa, Dmitry A. Bosykh, et al. 2011. «Curaxins: Anticancer Compounds That Simultaneously Suppress NF-κB and Activate P53 by Targeting FACT». *Science Translational Medicine* 3 (95). https://doi.org/10.1126/scitranslmed.3002530.

Geva-Zatorsky, Naama, Erez Dekel, Eric Batchelor, Galit Lahav, e Uri Alon. 2010. «Fourier Analysis and Systems Identification of the P53 Feedback Loop». *Proceedings of the National Academy of Sciences* 107 (30): 13550–55. https://doi.org/10.1073/pnas.1001107107.

Geva-Zatorsky, Naama, Nitzan Rosenfeld, Shalev Itzkovitz, Ron Milo, Alex Sigal, Erez Dekel, Talia Yarnitzky, et al. 2006. «Oscillations and Variability in the P53 System». *Molecular Systems Biology* 2 (1): 2006.0033. https://doi.org/10.1038/msb4100068.

Ghosh, Supratit, Meghna Bhattacharjee, e Nandan Kumar Jana. 2022. «Gene Regulation by p53 in Human Cancer System». *Asian Pacific Journal of Cancer Biology* 7 (1): 97–109. https://doi.org/10.31557/apjcb.2022.7.1.97-109.

Gilmore, T D. 2006. «Introduction to NF-κB: Players, Pathways, Perspectives». *Oncogene* 25 (51): 6680–84. https://doi.org/10.1038/sj.onc.1209954.

Greten, Florian R., Lars Eckmann, Tim F. Greten, Jin Mo Park, Zhi-Wei Li, Laurence J. Egan, Martin F. Kagnoff, e Michael Karin. 2004. «IKKβ Links Inflammation and Tumorigenesis in a Mouse Model of Colitis-Associated Cancer». *Cell* 118 (3): 285–96. https://doi.org/10.1016/j.cell.2004.07.013.

Gudkov, A. V., K. V. Gurova, e E. A. Komarova. 2011. «Inflammation and P53: A Tale of Two Stresses». *Genes & Cancer* 2 (4): 503–16. https://doi.org/10.1177/1947601911409747.

Gurova, Katerina V., Jason E. Hill, Canhui Guo, Anatoly Prokvolit, Lyudmila G. Burdelya, Eugenia Samoylova, Anna V. Khodyakova, et al. 2005. «Small Molecules That Reactivate P53 in Renal Cell Carcinoma Reveal a NF-κB-Dependent Mechanism of P53 Suppression in Tumors». *Proceedings of the National Academy of Sciences* 102 (48): 17448–53. https://doi.org/10.1073/pnas.0508888102.

Hafner, Antonina, Martha L. Bulyk, Ashwini Jambhekar, e Galit Lahav. 2019. «The Multiple Mechanisms That Regulate P53 Activity and Cell Fate». *Nature Reviews Molecular Cell Biology* 20 (4): 199–210. https://doi.org/10.1038/s41580-019-0110-x.

Hafner, Antonina, José Reyes, Jacob Stewart-Ornstein, Michael Tsabar, Ashwini Jambhekar, e Galit Lahav. 2020. «Quantifying the Central Dogma in the P53 Pathway in Live Single Cells». *Cell Systems* 10 (6): 495-505.e4. https://doi.org/10.1016/j.cels.2020.05.001.

Hafner, Antonina, Jacob Stewart-Ornstein, Jeremy E Purvis, William C Forrester, Martha L Bulyk, e Galit Lahav. 2017. «P53 Pulses Lead to Distinct Patterns of Gene Expression Albeit Similar DNA-Binding Dynamics». *Nature Structural & Molecular Biology* 24 (10): 840–47. https://doi.org/10.1038/nsmb.3452.

Hai Ping, Pei, Tan Feng Bo, Liu Li, Yu Nan Hui, e Zhu Hong. 2016. «IL-1β/NF-Kb Signaling Promotes Colorectal Cancer Cell Growth through miR-181a/PTEN Axis». *Archives of Biochemistry and Biophysics* 604 (agosto): 20–26. https://doi.org/10.1016/j.abb.2016.06.001.

Hanson, Ryan L., e Eric Batchelor. 2020. «Rucaparib Treatment Alters P53 Oscillations in Single Cells to Enhance DNA-Double-Strand-Break-Induced Cell Cycle Arrest». *Cell Reports* 33 (2): 108240. https://doi.org/10.1016/j.celrep.2020.108240.

Harima, Yukiko, Yoshiki Takashima, Yuriko Ueda, Toshiyuki Ohtsuka, e Ryoichiro Kageyama. 2013. «Accelerating the Tempo of the Segmentation Clock by Reducing the Number of Introns in the Hes7 Gene». *Cell Reports* 3 (1): 1–7. https://doi.org/10.1016/j.celrep.2012.11.012.

Haronikova, Lucia, Ondrej Bonczek, Pavlina Zatloukalova, Filip Kokas-Zavadil, Martina Kucerikova, Philip J. Coates, Robin Fahraeus, e Borivoj Vojtesek. 2021. «Resistance Mechanisms to Inhibitors of P53-MDM2 Interactions in Cancer Therapy: Can We Overcome Them?» *Cellular & Molecular Biology Letters* 26 (1): 53. https://doi.org/10.1186/s11658-021-00293-6.

Harton, Marie D, Woo Seuk Koh, Amie D Bunker, Abhyudai Singh, e Eric Batchelor. 2019. «P53 Pulse Modulation Differentially Regulates Target Gene Promoters to Regulate Cell Fate Decisions». *Molecular Systems Biology* 15 (9). https://doi.org/10.15252/msb.20188685.

Hayden, Matthew S., e Sankar Ghosh. 2008. «Shared Principles in NF-κB Signaling». *Cell* 132 (3): 344–62. https://doi.org/10.1016/j.cell.2008.01.020.

Heltberg, Mathias S., Alessandra Lucchetti, Feng-Shu Hsieh, Duy Pham Minh Nguyen, Sheng-hong Chen, e Mogens H. Jensen. 2022. «Enhanced DNA Repair through Droplet Formation and P53 Oscillations». *Cell* 185 (23): 4394-4408.e10. https://doi.org/10.1016/j.cell.2022.10.004.

Heyne, Kristina, Christine Winter, Fabian Gerten, Christina Schmidt, e Klaus Roemer. 2013. «A Novel Mechanism of Crosstalk between the P53 and NFκB Pathways: MDM2 Binds and Inhibits p65RelA». *Cell Cycle* 12 (15): 2479–92. https://doi.org/10.4161/cc.25495.

Ho, Cheng-Jung, Huey-Jiun Ko, Tzu-Shao Liao, Xiang-Ren Zheng, Po-Hsu Chou, Li-Ting Wang, Ru-Wei Lin, Chung-Hwan Chen, e Chihuei Wang. 2021. «Severe Cellular Stress Activates Apoptosis Independently of P53 in Osteosarcoma». *Cell Death Discovery* 7 (1): 275. https://doi.org/10.1038/s41420-021-00658-y.

Hoffmann, Alexander, Andre Levchenko, Martin L. Scott, e David Baltimore. 2002. «The IκB-NF-κB Signaling Module: Temporal Control and Selective Gene Activation». *Science* 298 (5596): 1241–45. https://doi.org/10.1126/science.1071914.

Hou, Helei, Dantong Sun, e Xiaochun Zhang. 2019. «The Role of MDM2 Amplification and Overexpression in Therapeutic Resistance of Malignant Tumors». *Cancer Cell International* 19 (1): 216. https://doi.org/10.1186/s12935-019-0937-4.

Houk, Levi R., Sivakumar R. Challa, Benjamin Grayson, Paul Fanson, e Abhaya K. Datye. 2009. «The Definition of "Critical Radius" for a Collection of Nanoparticles Undergoing Ostwald Ripening». *Langmuir* 25 (19): 11225–27. https://doi.org/10.1021/la902263s.

Hsu, Shu-Ching, Mikhail A. Gavrilin, Hsiu-Hsiang Lee, Chia-Cheng Wu, Shou- Hwa Han, e Ming-Zong Lai. 1999. «NF-κB-Dependent Fas Ligand Expression». *European Journal of Immunology* 29 (9): 2948–56. https://doi.org/10.1002/(SICI)1521-4141(199909)29:09<2948::AID-IMMU2948>3.0.CO;2-0.

Hu, W., Z. Feng, e A. J. Levine. 2012. «The Regulation of Multiple P53 Stress Responses Is Mediated through MDM2». *Genes & Cancer* 3 (3–4): 199–208. https://doi.org/10.1177/1947601912454734.

Huang, Wei-Chien, Tsai-Kai Ju, Mien-Chie Hung, e Ching-Chow Chen. 2007. «Phosphorylation of CBP by IKKα Promotes Cell Growth by Switching the Binding Preference of CBP from P53 to NF-κB». *Molecular Cell* 26 (1): 75–87. https://doi.org/10.1016/j.molcel.2007.02.019.

Humpton, Timothy J., e Karen H. Vousden. 2016. «Regulation of Cellular Metabolism and Hypoxia by P53». *Cold Spring Harbor Perspectives in Medicine* 6 (7): a026146. https://doi.org/10.1101/cshperspect.a026146.

Hunziker, Alexander, Mogens H Jensen, e Sandeep Krishna. 2010. «Stress-Specific Response of the P53-Mdm2 Feedback Loop». *BMC Systems Biology* 4 (1): 94. https://doi.org/10.1186/1752-0509-4-94.

Hutti, Jessica E., Benjamin E. Turk, John M. Asara, Averil Ma, Lewis C. Cantley, e Derek W. Abbott. 2007. «IκB Kinase β Phosphorylates the K63 Deubiquitinase A20 To Cause Feedback Inhibition of the NF-κB Pathway». *Molecular and Cellular Biology* 27 (21): 7451–61. https://doi.org/10.1128/MCB.01101-07.

Ikeda, Akiko, Xiangao Sun, Yan Li, Yong-kang Zhang, Richard Eckner, Takahiro S. Doi, Toshitada Takahashi, Yuichi Obata, Katsuji Yoshioka, e Ken-ichi Yamamoto. 2000. «P300/CBP-Dependent and -Independent Transcriptional Interference between NF-κB RelA and P53». *Biochemical and Biophysical Research Communications* 272 (2): 375–79. https://doi.org/10.1006/bbrc.2000.2786.

Imbert, Arthur, Wei Ouyang, Adham Safieddine, Emeline Coleno, Christophe Zimmer, Edouard Bertrand, Thomas Walter, e Florian Mueller. 2021. «FISH-Quant v2: A Scalable and Modular Analysis Tool for smFISH Image Analysis». Preprint. Bioinformatics. https://doi.org/10.1101/2021.07.20.453024.

Jaqaman, Khuloud, Dinah Loerke, Marcel Mettlen, Hirotaka Kuwata, Sergio Grinstein, Sandra L Schmid, e Gaudenz Danuser. 2008. «Robust Single-Particle Tracking in Live-Cell Time-Lapse Sequences». *Nature Methods* 5 (8): 695–702. https://doi.org/10.1038/nmeth.1237.

Jentsch, Marcel, Petra Snyder, Caibin Sheng, Elena Cristiano, e Alexander Loewer. 2020. «P53 Dynamics in Single Cells Are Temperature-Sensitive». *Scientific Reports* 10 (1): 1481. https://doi.org/10.1038/s41598-020-58267-1.

Jiménez, Alba, Dan Lu, Marian Kalocsay, Matthew J Berberich, Petra Balbi, Ashwini Jambhekar, e Galit Lahav. 2022. «Time-series Transcriptomics and Proteomics Reveal Alternative Modes to Decode P53 Oscillations». *Molecular Systems Biology* 18 (3): e10588. https://doi.org/10.15252/msb.202110588.

Jones, Russell G., David R. Plas, Sara Kubek, Monica Buzzai, James Mu, Yang Xu, Morris J. Birnbaum, e Craig B. Thompson. 2005. «AMP-Activated Protein Kinase Induces a P53-Dependent Metabolic Checkpoint». *Molecular Cell* 18 (3): 283–93. https://doi.org/10.1016/j.molcel.2005.03.027.

Kageyama, Ryoichiro, Hiromi Shimojo, e Itaru Imayoshi. 2015. «Dynamic Expression and Roles of Hes Factors in Neural Development». *Cell and Tissue Research* 359 (1): 125–33. https://doi.org/10.1007/s00441-014-1888-7.

Karamouzis, Michalis V, Panagiotis A Konstantinopoulos, e Athanasios G Papavassiliou. 2007. «Roles of CREB-Binding Protein (CBP)/P300 in Respiratory Epithelium Tumorigenesis». *Cell Research* 17 (4): 324–32. https://doi.org/10.1038/cr.2007.10.

Karin, Michael, Yixue Cao, Florian R. Greten, e Zhi-Wei Li. 2002. «NF-κB in Cancer: From Innocent Bystander to Major Culprit». *Nature Reviews Cancer* 2 (4): 301–10. https://doi.org/10.1038/nrc780.

Karin, Michael, e Florian R. Greten. 2005. «NF-κB: Linking Inflammation and Immunity to Cancer Development and Progression». *Nature Reviews Immunology* 5 (10): 749–59. https://doi.org/10.1038/nri1703.

Kashatus, David, Patricia Cogswell, e Albert S. Baldwin. 2006. «Expression of the Bcl-3 Proto-Oncogene Suppresses P53 Activation». *Genes & Development* 20 (2): 225–35. https://doi.org/10.1101/gad.1352206.

Kaur, Parminder, Shiv Verma, Prem Prakash Kushwaha, e Sanjay Gupta. 2023. «EZH2 and NF-κB: A Context-Dependent Crosstalk and Transcriptional Regulation in Cancer». *Cancer Letters* 560 (aprile): 216143. https://doi.org/10.1016/j.canlet.2023.216143.

Kawai, Taro, e Shizuo Akira. 2010. «The Role of Pattern-Recognition Receptors in Innate Immunity: Update on Toll-like Receptors». *Nature Immunology* 11 (5): 373–84. https://doi.org/10.1038/ni.1863.

Kawauchi, Keiko, Keigo Araki, Kei Tobiume, e Nobuyuki Tanaka. 2008. «Activated P53 Induces NF-κB DNA Binding but Suppresses Its Transcriptional Activation». *Biochemical and Biophysical Research Communications* 372 (1): 137–41. https://doi.org/10.1016/j.bbrc.2008.05.021.

Kellogg, Ryan A, Chengzhe Tian, Tomasz Lipniacki, Stephen R Quake, e Savaş Tay. 2015. «Digital Signaling Decouples Activation Probability and Population Heterogeneity». *eLife* 4 (ottobre): e08931. https://doi.org/10.7554/eLife.08931.

Kellogg, Ryan A., e Savaş Tay. 2015. «Noise Facilitates Transcriptional Control under Dynamic Inputs». *Cell* 160 (3): 381–92. https://doi.org/10.1016/j.cell.2015.01.013.

Khoshnan, Ali, Charles Tindell, Isett Laux, David Bae, Brydon Bennett, e Andre E. Nel. 2000. «The NF-κB Cascade Is Important in Bcl-xL Expression and for the Anti-Apoptotic Effects of the CD28 Receptor in Primary Human CD4+ Lymphocytes». *The Journal of Immunology* 165 (4): 1743–54. https://doi.org/10.4049/jimmunol.165.4.1743.

Kizilirmak, Cise, Marco E. Bianchi, e Samuel Zambrano. 2022. «Insights on the NF-κB System Using Live Cell Imaging: Recent Developments and Future Perspectives». *Frontiers in Immunology* 13 (giugno): 886127. https://doi.org/10.3389/fimmu.2022.886127.

Kizilirmak, Cise, Emanuele Monteleone, José Manuel García-Manteiga, Francesca Brambilla, Alessandra Agresti, Marco E. Bianchi, e Samuel Zambrano. 2021. «Small Transcriptional Differences Lead to Distinct NF- *κ* B Dynamics in Quasi-Identical Cells». Preprint. Systems Biology. https://doi.org/10.1101/2021.12.07.471485.

Konrath, Fabian, Anna Mittermeier, Elena Cristiano, Jana Wolf, e Alexander Loewer. 2020. «A Systematic Approach to Decipher Crosstalk in the P53 Signaling Pathway Using Single Cell Dynamics». A cura di Kathryn Miller-Jensen. *PLOS Computational Biology* 16 (6): e1007901. https://doi.org/10.1371/journal.pcbi.1007901.

Kortlever, Roderik M., Paul J. Higgins, e René Bernards. 2006. «Plasminogen Activator Inhibitor-1 Is a Critical Downstream Target of P53 in the Induction of Replicative Senescence». *Nature Cell Biology* 8 (8): 877–84. https://doi.org/10.1038/ncb1448.

Koushki, Newsha, Ajinkya Ghagre, Luv Kishore Srivastava, Clayton Molter, e Allen J. Ehrlicher. 2023. «Nuclear Compression Regulates YAP Spatiotemporal Fluctuations in Living Cells». *Proceedings of the National Academy of Sciences* 120 (28): e2301285120. https://doi.org/10.1073/pnas.2301285120.

Kracikova, M, G Akiri, A George, R Sachidanandam, e S A Aaronson. 2013. «A Threshold Mechanism Mediates P53 Cell Fate Decision between Growth Arrest and Apoptosis». *Cell Death & Differentiation* 20 (4): 576–88. https://doi.org/10.1038/cdd.2012.155.

Kuo, Linda J., e Li-Xi Yang. 2008. «Gamma-H2AX - a Novel Biomarker for DNA Double-Strand Breaks». *In Vivo (Athens, Greece)* 22 (3): 305–9.

Kussie, Paul H., Svetlana Gorina, Vincent Marechal, Brian Elenbaas, Jacque Moreau, Arnold J. Levine, e Nikola P. Pavletich. 1996. «Structure of the MDM2 Oncoprotein Bound to the P53 Tumor Suppressor Transactivation Domain». *Science* 274 (5289): 948–53. https://doi.org/10.1126/science.274.5289.948.

Lahav, Galit, Nitzan Rosenfeld, Alex Sigal, Naama Geva-Zatorsky, Arnold J Levine, Michael B Elowitz, e Uri Alon. 2004. «Dynamics of the P53-Mdm2 Feedback Loop in Individual Cells». *Nature Genetics* 36 (2): 147–50. https://doi.org/10.1038/ng1293.

Lane, Brian R., Jianguo Liu, Paul J. Bock, Dominique Schols, Michael J. Coffey, Robert M. Strieter, Peter J. Polverini, e David M. Markovitz. 2002. «Interleukin-8 and Growth-Regulated Oncogene Alpha Mediate Angiogenesis in Kaposi's Sarcoma». *Journal of Virology* 76 (22): 11570–83. https://doi.org/10.1128/JVI.76.22.11570-11583.2002.

Lane, D. P. 1992. «P53, Guardian of the Genome». *Nature* 358 (6381): 15–16. https://doi.org/10.1038/358015a0.

Lane, D. P., e L. V. Crawford. 1979. «T Antigen Is Bound to a Host Protein in SY40-Transformed Cells». *Nature* 278 (5701): 261–63. https://doi.org/10.1038/278261a0.

Lavin, Martin F., e Sergei Kozlov. 2007. «ATM Activation and DNA Damage Response». *Cell Cycle* 6 (8): 931–42. https://doi.org/10.4161/cc.6.8.4180.

Lawrence, T. 2009. «The Nuclear Factor NF- B Pathway in Inflammation». *Cold Spring Harbor Perspectives in Biology* 1 (6): a001651–a001651. https://doi.org/10.1101/cshperspect.a001651.

Lee, Robin E. C., Mohammad A. Qasaimeh, Xianfang Xia, David Juncker, e Suzanne Gaudet. 2016. «NF-κB Signalling and Cell Fate Decisions in Response to a Short Pulse of Tumour Necrosis Factor». *Scientific Reports* 6 (1): 39519. https://doi.org/10.1038/srep39519.

Lee, Robin E.C., Sarah R. Walker, Kate Savery, David A. Frank, e Suzanne Gaudet. 2014. «Fold Change of Nuclear NF-κB Determines TNF-Induced Transcription in Single Cells». *Molecular Cell* 53 (6): 867–79. https://doi.org/10.1016/j.molcel.2014.01.026.

Lee, Timothy K, e Markus W Covert. 2010. «High-Throughput, Single-Cell NF-κB Dynamics». *Current Opinion in Genetics & Development* 20 (6): 677–83. https://doi.org/10.1016/j.gde.2010.08.005.

Lee, Tong Ihn, Nicola J. Rinaldi, François Robert, Duncan T. Odom, Ziv Bar-Joseph, Georg K. Gerber, Nancy M. Hannett, et al. 2002. «Transcriptional Regulatory Networks in *Saccharomyces Cerevisiae*». *Science* 298 (5594): 799–804. https://doi.org/10.1126/science.1075090.

Leibowitz, Saskia M., e Jun Yan. 2016. «NF-κB Pathways in the Pathogenesis of Multiple Sclerosis and the Therapeutic Implications». *Frontiers in Molecular Neuroscience* 9 (settembre). https://doi.org/10.3389/fnmol.2016.00084.

Lev Bar-Or, Ruth, Ruth Maya, Lee A. Segel, Uri Alon, Arnold J. Levine, e Moshe Oren. 2000. «Generation of Oscillations by the P53-Mdm2 Feedback Loop: A Theoretical and Experimental Study». *Proceedings of the National Academy of Sciences* 97 (21): 11250–55. https://doi.org/10.1073/pnas.210171597.

Levine, Arnold J., e Moshe Oren. 2009. «The First 30 Years of P53: Growing Ever More Complex». *Nature Reviews Cancer* 9 (10): 749–58. https://doi.org/10.1038/nrc2723.

Li, Qin, e Guillermina Lozano. 2013. «Molecular Pathways: Targeting Mdm2 and Mdm4 in Cancer Therapy». *Clinical Cancer Research* 19 (1): 34–41. https://doi.org/10.1158/1078-0432.CCR-12-0053.

Li, Xian. 2006. «Effects of IκBα and Its Mutants on NF-κB and P53 Signaling Pathways». *World Journal of Gastroenterology* 12 (41): 6658. https://doi.org/10.3748/wjg.v12.i41.6658.

Lindell, Emma, Lei Zhong, e Xiaonan Zhang. 2023. «Quiescent Cancer Cells—A Potential Therapeutic Target to Overcome Tumor Resistance and Relapse». *International Journal of Molecular Sciences* 24 (4): 3762. https://doi.org/10.3390/ijms24043762.

Liu, Fei, Yifeng Xia, Aaron S. Parker, e Inder M. Verma. 2012. «IKK Biology». *Immunological Reviews* 246 (1): 239–53. https://doi.org/10.1111/j.1600-065X.2012.01107.x.

Liu, Ting, Lingyun Zhang, Donghyun Joo, e Shao-Cong Sun. 2017. «NF-κB Signaling in Inflammation». *Signal Transduction and Targeted Therapy* 2 (1): 17023. https://doi.org/10.1038/sigtrans.2017.23.

Lloyd-Lewis, Bethan, Philippos Mourikis, e Silvia Fre. 2019. «Notch Signalling: Sensor and Instructor of the Microenvironment to Coordinate Cell Fate and Organ Morphogenesis». *Current Opinion in Cell Biology* 61 (dicembre): 16–23. https://doi.org/10.1016/j.ceb.2019.06.003.

Loewer, Alexander, Eric Batchelor, Giorgio Gaglia, e Galit Lahav. 2010. «Basal Dynamics of P53 Reveal Transcriptionally Attenuated Pulses in Cycling Cells». *Cell* 142 (1): 89–100. https://doi.org/10.1016/j.cell.2010.05.031.

Loughery, Jayne, Miranda Cox, Linda M. Smith, e David W. Meek. 2014. «Critical Role for P53-Serine 15 Phosphorylation in Stimulating Transactivation at P53-Responsive Promoters». *Nucleic Acids Research* 42 (12): 7666–80. https://doi.org/10.1093/nar/gku501.

Lowe, Julie M., Daniel Menendez, Pierre R. Bushel, Maria Shatz, Erin L. Kirk, Melissa A. Troester, Stavros Garantziotis, Michael B. Fessler, e Michael A. Resnick. 2014. «P53 and NF-κB Coregulate Proinflammatory Gene Responses in Human Macrophages». *Cancer Research* 74 (8): 2182–92. https://doi.org/10.1158/0008-5472.CAN-13-1070.

Lowrey, Phillip L., e Joseph S. Takahashi. 2004. «MAMMALIAN CIRCADIAN BIOLOGY: Elucidating Genome-Wide Levels of Temporal Organization». *Annual Review of Genomics and Human Genetics* 5 (1): 407–41. https://doi.org/10.1146/annurev.genom.5.061903.175925.

Lu, Xiongbin, Thuy-Ai Nguyen, e Lawrence A. Donehower. 2005. «Reversal of the ATM/ATR-Mediated DNA Damage Response by the Oncogenic Phosphatase PPM1D». *Cell Cycle* 4 (8): 4060–64. https://doi.org/10.4161/cc.4.8.1876.

Luo, Qingyin, Jill Beaver, Yuan Liu, e Zunzhen Zhang. 2017. «Dynamics of P53: A Master Decider of Cell Fate». *Genes* 8 (2): 66. https://doi.org/10.3390/genes8020066.

Magné, Nicolas, Robert-Alain Toillon, Virginie Bottero, Céline Didelot, Paul Van Houtte, Jean-Pierre Gérard, e Jean-François Peyron. 2006. «NF-κB Modulation and Ionizing Radiation: Mechanisms and Future Directions for Cancer Treatment». *Cancer Letters* 231 (2): 158–68. https://doi.org/10.1016/j.canlet.2005.01.022.

Mah, L-J, A El-Osta, e T C Karagiannis. 2010. «γH2AX: A Sensitive Molecular Marker of DNA Damage and Repair». *Leukemia* 24 (4): 679–86. https://doi.org/10.1038/leu.2010.6.

Mantovani, Fiamma, Licio Collavin, e Giannino Del Sal. 2019. «Mutant P53 as a Guardian of the Cancer Cell». *Cell Death & Differentiation* 26 (2): 199–212. https://doi.org/10.1038/s41418-018-0246-9.

Marechal, A., e L. Zou. 2013. «DNA Damage Sensing by the ATM and ATR Kinases». *Cold Spring Harbor Perspectives in Biology* 5 (9): a012716–a012716. https://doi.org/10.1101/cshperspect.a012716.

Maroto, Miguel, Robert A. Bone, e J. Kim Dale. 2012. «Somitogenesis». *Development* 139 (14): 2453–56. https://doi.org/10.1242/dev.069310.

Martinez, Fernando Oneissi. 2008. «Macrophage Activation and Polarization». *Frontiers in Bioscience* 13 (13): 453. https://doi.org/10.2741/2692.

Matsuda, Mitsuhiro, Hanako Hayashi, Jordi Garcia-Ojalvo, Kumiko Yoshioka-Kobayashi, Ryoichiro Kageyama, Yoshihiro Yamanaka, Makoto Ikeya, Junya Toguchida, Cantas Alev, e Miki Ebisuya. 2020. «Species-Specific Segmentation Clock Periods Are Due to Differential Biochemical Reaction Speeds». *Science* 369 (6510): 1450–55. https://doi.org/10.1126/science.aba7668.

Maya, Ruth, Moshe Balass, Seong-Tae Kim, Dganit Shkedy, Juan-Fernando Martinez Leal, Ohad Shifman, Miri Moas, et al. 2001. «ATM-Dependent Phosphorylation of Mdm2 on Serine 395: Role in P53 Activation by DNA Damage». *Genes & Development* 15 (9): 1067–77. https://doi.org/10.1101/gad.886901.

Mayo, Lindsey D., e David B. Donner. 2001. «A Phosphatidylinositol 3-Kinase/Akt Pathway Promotes Translocation of Mdm2 from the Cytoplasm to the Nucleus». *Proceedings of the National Academy of Sciences* 98 (20): 11598–603. https://doi.org/10.1073/pnas.181181198.

Mengel, Benedicte, Alexander Hunziker, Lykke Pedersen, Ala Trusina, Mogens H Jensen, e Sandeep Krishna. 2010. «Modeling Oscillatory Control in NF-κB, P53 and Wnt Signaling». *Current Opinion in Genetics & Development* 20 (6): 656–64. https://doi.org/10.1016/j.gde.2010.08.008.

Meyer, Kirstin, Nicholas C. Lammers, Lukasz J. Bugaj, Hernan G. Garcia, e Orion D. Weiner. 2022. «Decoding of YAP Levels and Dynamics by Pluripotency Factors». Preprint. Cell Biology. https://doi.org/10.1101/2022.10.17.512504.

Michaelis, M, F Rothweiler, S Barth, J Cinatl, M Van Rikxoort, N Löschmann, Y Voges, et al. 2011. «Adaptation of Cancer Cells from Different Entities to the MDM2 Inhibitor Nutlin-3 Results in the Emergence of P53-Mutated Multi-Drug-Resistant Cancer Cells». *Cell Death & Disease* 2 (12): e243–e243. https://doi.org/10.1038/cddis.2011.129.

Milne, D.M., D.G. Campbell, F.B. Caudwell, e D.W. Meek. 1994. «Phosphorylation of the Tumor Suppressor Protein P53 by Mitogen-Activated Protein Kinases.» *Journal of Biological Chemistry* 269 (12): 9253–60. https://doi.org/10.1016/S0021-9258(17)37101-6.

Miné-Hattab, Judith, Siyu Liu, e Angela Taddei. 2022. «Repair Foci as Liquid Phase Separation: Evidence and Limitations». *Genes* 13 (10): 1846. https://doi.org/10.3390/genes13101846.

Mirza-Aghazadeh-Attari, Mohammad, Amir Mohammadzadeh, Bahman Yousefi, Ainaz Mihanfar, Ansar Karimian, e Maryam Majidinia. 2019. «53BP1: A Key Player of DNA Damage Response with Critical Functions in Cancer». *DNA Repair* 73 (gennaio): 110–19. https://doi.org/10.1016/j.dnarep.2018.11.008.

Mirzoeva, Olga K., e John H. J. Petrini. 2001. «DNA Damage-Dependent Nuclear Dynamics of the Mre11 Complex». *Molecular and Cellular Biology* 21 (1): 281–88. https://doi.org/10.1128/MCB.21.1.281-288.2001.

Mitrophanov, Alexander Y., e Eduardo A. Groisman. 2008. «Positive Feedback in Cellular Control Systems». *BioEssays* 30 (6): 542–55. https://doi.org/10.1002/bies.20769.

Moll, Ute M., e Oleksi Petrenko. 2003. «The MDM2-P53 Interaction». *Molecular Cancer Research: MCR* 1 (14): 1001–8.

Monk, Nicholas A.M. 2003. «Oscillatory Expression of Hes1, P53, and NF-κB Driven by Transcriptional Time Delays». *Current Biology* 13 (16): 1409–13. https://doi.org/10.1016/S0960-9822(03)00494-9.

Moon, Jaeyoung, Ichiwa Kitty, Kusuma Renata, Sisi Qin, Fei Zhao, e Wootae Kim. 2023. «DNA Damage and Its Role in Cancer Therapeutics». *International Journal of Molecular Sciences* 24 (5): 4741. https://doi.org/10.3390/ijms24054741.

Moroishi, Toshiro, Carsten Gram Hansen, e Kun-Liang Guan. 2015. «The Emerging Roles of YAP and TAZ in Cancer». *Nature Reviews Cancer* 15 (2): 73–79. https://doi.org/10.1038/nrc3876.

Mortezaee, Keywan, Masoud Najafi, Bagher Farhood, Amirhossein Ahmadi, Yaiza Potes, Dheyauldeen Shabeeb, e Ahmed Eleojo Musa. 2019. «Modulation of Apoptosis by Melatonin for Improving Cancer Treatment Efficiency: An Updated Review». *Life Sciences* 228 (luglio): 228–41. https://doi.org/10.1016/j.lfs.2019.05.009.

Mosser, David M. 2003. «The Many Faces of Macrophage Activation». *Journal of Leukocyte Biology* 73 (2): 209–12. https://doi.org/10.1189/jlb.0602325.

Mueller, Florian, Adrien Senecal, Katjana Tantale, Hervé Marie-Nelly, Nathalie Ly, Olivier Collin, Eugenia Basyuk, Edouard Bertrand, Xavier Darzacq, e Christophe Zimmer. 2013. «FISH-Quant: Automatic Counting of Transcripts in 3D FISH Images». *Nature Methods* 10 (4): 277–78. https://doi.org/10.1038/nmeth.2406.

Mulay, Shrikant R., Dana Thomasova, Mi Ryu, e Hans-Joachim Anders. 2012. «MDM2 (Murine Double Minute-2) Links Inflammation and Tubular Cell Healing during Acute Kidney Injury in Mice». *Kidney International* 81 (12): 1199–1211. https://doi.org/10.1038/ki.2011.482.

Müller, Markus, Alessandro Morotti, e Carola Ponzetto. 2002. «Activation of NF-κB Is Essential for Hepatocyte Growth Factor-Mediated Proliferation and Tubulogenesis». *Molecular and Cellular Biology* 22 (4): 1060–72. https://doi.org/10.1128/MCB.22.4.1060-1072.2002.

Murphy, Samantha H., Kotaro Suzuki, Michael Downes, Genevieve L. Welch, Paul De Jesus, Loren J. Miraglia, Anthony P. Orth, Sumit K. Chanda, Ronald M. Evans, e Inder M. Verma. 2011. «Tumor Suppressor Protein (p)53, Is a Regulator of NF-κB Repression by the Glucocorticoid Receptor». *Proceedings of the National Academy of Sciences* 108 (41): 17117–22. https://doi.org/10.1073/pnas.1114420108.

Murray-Zmijewski, Fiona, Elizabeth A. Slee, e Xin Lu. 2008a. «A Complex Barcode Underlies the Heterogeneous Response of P53 to Stress». *Nature Reviews Molecular Cell Biology* 9 (9): 702–12. https://doi.org/10.1038/nrm2451.

Fiona Murray-Zmijewski, Elizabeth A. Slee and Xin Lu. 2008b. «A Complex Barcode Underlies the Heterogeneous Response of P53 to Stress». *Nature Reviews Molecular Cell Biology* 9 (9): 702–12. https://doi.org/10.1038/nrm2451.

Nakano, Katsunori, e Karen H Vousden. 2001. «PUMA, a Novel Proapoptotic Gene, Is Induced by P53». *Molecular Cell* 7 (3): 683–94. https://doi.org/10.1016/S1097-2765(01)00214-3.

Nelson, D. E., A. E. C. Ihekwaba, M. Elliott, J. R. Johnson, C. A. Gibney, B. E. Foreman, G. Nelson, et al. 2004. «Oscillations in NF-κB Signaling Control the Dynamics of Gene Expression». *Science* 306 (5696): 704–8. https://doi.org/10.1126/science.1099962.

Novák, Béla, e John J. Tyson. 2008. «Design Principles of Biochemical Oscillators». *Nature Reviews Molecular Cell Biology* 9 (12): 981–91. https://doi.org/10.1038/nrm2530.

Oeckinghaus, A., e S. Ghosh. 2009. «The NF- B Family of Transcription Factors and Its Regulation». *Cold Spring Harbor Perspectives in Biology* 1 (4): a000034–a000034. https://doi.org/10.1101/cshperspect.a000034.

Oliner, Jonathan D., Anne Y. Saiki, e Sean Caenepeel. 2016. «The Role of MDM2 Amplification and Overexpression in Tumorigenesis». *Cold Spring Harbor Perspectives in Medicine* 6 (6): a026336. https://doi.org/10.1101/cshperspect.a026336.

O'Prey, Jim, Diane Crighton, Angel G. Martin, Karen H. Vousden, Howard O. Fearnhead, e Kevin M. Ryan. 2010. «P53-Mediated Induction of Noxa and p53AIP1 Requires NFκB». *Cell Cycle* 9 (5): 947–52. https://doi.org/10.4161/cc.9.5.10872.

Ortega, Ángel, Ivana Vera, Maria Diaz, Carla Navarro, Milagros Rojas, Wheeler Torres, Heliana Parra, Juan Salazar, Juan De Sanctis, e Valmore Bermúdez. 2021. «The YAP/TAZ Signaling Pathway in the Tumor Microenvironment and Carcinogenesis: Current Knowledge and Therapeutic Promises». *International Journal of Molecular Sciences* 23 (1): 430. https://doi.org/10.3390/ijms23010430.

Osborn, Daniel P.S., Kuoyu Li, Yaniv Hinits, e Simon M. Hughes. 2011. «Cdkn1c Drives Muscle Differentiation through a Positive Feedback Loop with Myod». *Developmental Biology* 350 (2): 464–75. https://doi.org/10.1016/j.ydbio.2010.12.010.

Ovesný, Martin, Pavel Křížek, Josef Borkovec, Zdeněk Švindrych, e Guy M. Hagen. 2014. «ThunderSTORM: A Comprehensive ImageJ Plug-in for PALM and STORM Data Analysis and Super-Resolution Imaging». *Bioinformatics* 30 (16): 2389–90. https://doi.org/10.1093/bioinformatics/btu202.

Paek, Andrew L., Julia C. Liu, Alexander Loewer, William C. Forrester, e Galit Lahav. 2016. «Cell-to-Cell Variation in P53 Dynamics Leads to Fractional Killing». *Cell* 165 (3): 631–42. https://doi.org/10.1016/j.cell.2016.03.025.

Pahl, Heike L. 1999. «Activators and Target Genes of Rel/NF-κB Transcription Factors». *Oncogene* 18 (49): 6853–66. https://doi.org/10.1038/sj.onc.1203239.

Pan, Duojia. 2010. «The Hippo Signaling Pathway in Development and Cancer». *Developmental Cell* 19 (4): 491–505. https://doi.org/10.1016/j.devcel.2010.09.011.

Panciera, Tito, Luca Azzolin, Michelangelo Cordenonsi, e Stefano Piccolo. 2017. «Mechanobiology of YAP and TAZ in Physiology and Disease». *Nature Reviews Molecular Cell Biology* 18 (12): 758–70. https://doi.org/10.1038/nrm.2017.87.

Papa, Anselmo, Davide Caruso, Martina Strudel, Silverio Tomao, e Federica Tomao. 2016. «Update on Poly-ADP-Ribose Polymerase Inhibition for Ovarian Cancer Treatment». *Journal of Translational Medicine* 14 (1): 267. https://doi.org/10.1186/s12967-016-1027-1.

Park, Mi, e Jin Hong. 2016. «Roles of NF-κB in Cancer and Inflammatory Diseases and Their Therapeutic Approaches». *Cells* 5 (2): 15. https://doi.org/10.3390/cells5020015.

Partch, Carrie L., Carla B. Green, e Joseph S. Takahashi. 2014. «Molecular Architecture of the Mammalian Circadian Clock». *Trends in Cell Biology* 24 (2): 90–99. https://doi.org/10.1016/j.tcb.2013.07.002.

Paszek, Pawel, Sheila Ryan, Louise Ashall, Kate Sillitoe, Claire V. Harper, David G. Spiller, David A. Rand, e Michael R. H. White. 2010. «Population Robustness Arising from Cellular Heterogeneity». *Proceedings of the National Academy of Sciences* 107 (25): 11644–49. https://doi.org/10.1073/pnas.0913798107.

Pavlakis, Evangelos, e Thorsten Stiewe. 2020. «P53's Extended Reach: The Mutant P53 Secretome». *Biomolecules* 10 (2): 307. https://doi.org/10.3390/biom10020307.

Perkins, Neil D. 2007. «Integrating Cell-Signalling Pathways with NF-κB and IKK Function». *Nature Reviews Molecular Cell Biology* 8 (1): 49–62. https://doi.org/10.1038/nrm2083.

Porter, Joshua R., Brian E. Fisher, e Eric Batchelor. 2016. «P53 Pulses Diversify Target Gene Expression Dynamics in an mRNA Half-Life-Dependent Manner and Delineate Co-Regulated Target Gene Subnetworks». *Cell Systems* 2 (4): 272–82. https://doi.org/10.1016/j.cels.2016.03.006.

Prasad, Sahdeo, Jayaraj Ravindran, e Bharat B. Aggarwal. 2010. «NF-κB and Cancer: How Intimate Is This Relationship». *Molecular and Cellular Biochemistry* 336 (1–2): 25–37. https://doi.org/10.1007/s11010-009-0267-2.

Purvis, Jeremy E., Kyle W. Karhohs, Caroline Mock, Eric Batchelor, Alexander Loewer, e Galit Lahav. 2012. «P53 Dynamics Control Cell Fate». *Science* 336 (6087): 1440–44. https://doi.org/10.1126/science.1218351.

Purvis, Jeremy E., e Galit Lahav. 2013. «Encoding and Decoding Cellular Information through Signaling Dynamics». *Cell* 152 (5): 945–56. https://doi.org/10.1016/j.cell.2013.02.005.

Rasmi, Rajan Radha, Kunnathur Murugesan Sakthivel, e Chandrasekaran Guruvayoorappan. 2020. «NF-κB Inhibitors in Treatment and Prevention of Lung Cancer». *Biomedicine & Pharmacotherapy* 130 (ottobre): 110569. https://doi.org/10.1016/j.biopha.2020.110569.

Ravi, R., B. Mookerjee, Y. van Hensbergen, G. C. Bedi, A. Giordano, W. S. El-Deiry, E. J. Fuchs, e A. Bedi. 1998. «P53-Mediated Repression of Nuclear Factor-kappaB RelA via the Transcriptional Integrator P300». *Cancer Research* 58 (20): 4531–36.

Richards, Jacob, e Michelle L. Gumz. 2013. «Mechanism of the Circadian Clock in Physiology». *American Journal of Physiology-Regulatory, Integrative and Comparative Physiology* 304 (12): R1053–64. https://doi.org/10.1152/ajpregu.00066.2013.

Riley, M. F., e G. Lozano. 2012. «The Many Faces of MDM2 Binding Partners». *Genes & Cancer* 3 (3–4): 226–39. https://doi.org/10.1177/1947601912455322.

Riley, Todd, Eduardo Sontag, Patricia Chen, e Arnold Levine. 2008. «Transcriptional Control of Human P53-Regulated Genes». *Nature Reviews Molecular Cell Biology* 9 (5): 402–12. https://doi.org/10.1038/nrm2395.

Roe, Jae-Seok, Hyungsoo Kim, Soon-Min Lee, Sung-Tae Kim, Eun-Jung Cho, e Hong-Duk Youn. 2006. «P53 Stabilization and Transactivation by a von Hippel-Lindau Protein». *Molecular Cell* 22 (3): 395–405. https://doi.org/10.1016/j.molcel.2006.04.006.

Rosenfeld, Nitzan, Michael B Elowitz, e Uri Alon. 2002. «Negative Autoregulation Speeds the Response Times of Transcription Networks». *Journal of Molecular Biology* 323 (5): 785–93. https://doi.org/10.1016/S0022-2836(02)00994-4.

Ryan, Kevin M., Mary K. Ernst, Nancy R. Rice, e Karen H. Vousden. 2000. «Role of NF-κB in P53-Mediated Programmed Cell Death». *Nature* 404 (6780): 892–97. https://doi.org/10.1038/35009130.

Sabio, Guadalupe, e Roger J. Davis. 2014. «TNF and MAP Kinase Signalling Pathways». *Seminars in Immunology* 26 (3): 237–45. https://doi.org/10.1016/j.smim.2014.02.009.

Schneider, Günter, e Oliver H. Krämer. 2011a. «NFκB/P53 Crosstalk—a Promising New Therapeutic Target». *Biochimica et Biophysica Acta (BBA) - Reviews on Cancer* 1815 (1): 90–103. https://doi.org/10.1016/j.bbcan.2010.10.003.

Günter Schneider, Oliver H. Krämer. 2011b. «NFκB/P53 Crosstalk—a Promising New Therapeutic Target». *Biochimica et Biophysica Acta (BBA) - Reviews on Cancer* 1815 (1): 90–103. https://doi.org/10.1016/j.bbcan.2010.10.003.

Schumm, Katie, Sonia Rocha, Jorge Caamano, e Neil D Perkins. 2006. «Regulation of p53 tumour suppressor target gene expression by the p52 NF-κB subunit». *The EMBO Journal* 25 (20): 4820–32. https://doi.org/10.1038/sj.emboj.7601343.

Sen, Ranjan, e David Baltimore. 1986. «Multiple Nuclear Factors Interact with the Immunoglobulin Enhancer Sequences». *Cell* 46 (5): 705–16. https://doi.org/10.1016/0092-8674(86)90346-6.

Senturk, J C, S Bohlman, e J J Manfredi. 2017. «Mdm2 Selectively Suppresses DNA Damage Arising from Inhibition of Topoisomerase II Independent of P53». *Oncogene* 36 (44): 6085–96. https://doi.org/10.1038/onc.2017.229.

Serasanambati, Mamatha, e Shanmuga Reddy Chilakapati. 2016. «Function of Nuclear Factor Kappa B (NF-kB) in Human Diseases-A Review». *South Indian Journal of Biological Sciences* 2 (4): 368. https://doi.org/10.22205/sijbs/2016/v2/i4/103443.

Shangary, Sanjeev, e Shaomeng Wang. 2008. «Targeting the MDM2-P53 Interaction for Cancer Therapy». *Clinical Cancer Research* 14 (17): 5318–24. https://doi.org/10.1158/1078-0432.CCR-07-5136.

Shankar, Eswar, Ailin Zhang, Daniel Franco, e Sanjay Gupta. 2017. «Betulinic Acid-Mediated Apoptosis in Human Prostate Cancer Cells Involves P53 and Nuclear Factor-Kappa B (NF-κB) Pathways». *Molecules* 22 (2): 264. https://doi.org/10.3390/molecules22020264.

Shen, Hong, Diarmuid M. Moran, e Carl G. Maki. 2008. «Transient Nutlin-3a Treatment Promotes Endoreduplication and the Generation of Therapy-Resistant Tetraploid Cells». *Cancer Research* 68 (20): 8260–68. https://doi.org/10.1158/0008-5472.CAN-08-1901.

Shen-Orr, Shai S., Ron Milo, Shmoolik Mangan, e Uri Alon. 2002. «Network Motifs in the Transcriptional Regulation Network of Escherichia Coli». *Nature Genetics* 31 (1): 64–68. https://doi.org/10.1038/ng881.

Shi, Di, e Peng Jiang. 2021. «A Different Facet of p53 Function: Regulation of Immunity and Inflammation During Tumor Development». *Frontiers in Cell and Developmental Biology* 9 (ottobre): 762651. https://doi.org/10.3389/fcell.2021.762651.

Shou, Yan, Nianyu Li, Li Li, Joseph L. Borowitz, e Gary E. Isom. 2002. «NF-κB-Mediated up-Regulation of Bcl-XS and Bax Contributes to Cytochrome c Release in Cyanide-Induced Apoptosis: Bcl-2 Proteins in Cyanide-Induced Apoptosis». *Journal of Neurochemistry* 81 (4): 842–52. https://doi.org/10.1046/j.1471-4159.2002.00880.x.

Skalniak, Lukasz, Justyna Kocik, Justyna Polak, Anna Skalniak, Monika Rak, Agnieszka Wolnicka-Glubisz, e Tad Holak. 2018. «Prolonged Idasanutlin (RG7388) Treatment Leads to the Generation of P53-Mutated Cells». *Cancers* 10 (11): 396. https://doi.org/10.3390/cancers10110396.

Solan, Nancie J., Hiroko Miyoshi, Eva M. Carmona, Gary D. Bren, e Carlos V. Paya. 2002. «RelB Cellular Regulation and Transcriptional Activity Are Regulated by P100». *Journal of Biological Chemistry* 277 (2): 1405–18. https://doi.org/10.1074/jbc.M109619200.

Solé, Laura, Teresa Lobo-Jarne, Daniel Álvarez-Villanueva, Josune Alonso-Marañón, Yolanda Guillén, Marta Guix, Irene Sangrador, et al. 2022. «P53 Wild-Type Colorectal Cancer Cells That Express a Fetal Gene Signature Are Associated with Metastasis and Poor Prognosis». *Nature Communications* 13 (1): 2866. https://doi.org/10.1038/s41467-022-30382-9.

Son, Deok-Soo, Syder M. Kabir, Yuan-Lin Dong, Eunsook Lee, e Samuel E. Adunyah. 2012. «Inhibitory Effect of Tumor Suppressor P53 on Proinflammatory Chemokine Expression in Ovarian Cancer Cells by Reducing Proteasomal Degradation of IκB». A cura di Ashok Kumar. *PLoS ONE* 7 (12): e51116. https://doi.org/10.1371/journal.pone.0051116.

Sonnen, Katharina F., Volker M. Lauschke, Julia Uraji, Henning J. Falk, Yvonne Petersen, Maja C. Funk, Mathias Beaupeux, Paul François, Christoph A. Merten, e Alexander Aulehla. 2018. «Modulation of Phase Shift between Wnt and Notch Signaling Oscillations Controls Mesoderm Segmentation». *Cell* 172 (5): 1079-1090.e12. https://doi.org/10.1016/j.cell.2018.01.026.

Stehlik, Christian, Rainer De Martin, Bernd R. Binder, e Joachim Lipp. 1998. «Cytokine Induced Expression of Porcine Inhibitor of Apoptosis Protein (Iap) Family Member Is Regulated by NF-κB». *Biochemical and Biophysical Research Communications* 243 (3): 827–32. https://doi.org/10.1006/bbrc.1998.8185.

Stewart-Ornstein, Jacob, Ho Wa (Jacky) Cheng, e Galit Lahav. 2017. «Conservation and Divergence of P53 Oscillation Dynamics across Species». *Cell Systems* 5 (4): 410-417.e4. https://doi.org/10.1016/j.cels.2017.09.012.

Stewart-Ornstein, Jacob, Yoshiko Iwamoto, Miles A. Miller, Mark A. Prytyskach, Stephane Ferretti, Philipp Holzer, Joerg Kallen, et al. 2021. «P53 Dynamics Vary between Tissues and Are Linked with Radiation Sensitivity». *Nature Communications* 12 (1): 898. https://doi.org/10.1038/s41467-021-21145-z.

Strickland, I, e S Ghosh. 2006. «Use of Cell Permeable NBD Peptides for Suppression of Inflammation». *Annals of the Rheumatic Diseases* 65 (suppl_3): iii75–82. https://doi.org/10.1136/ard.2006.058438.

Stringer, Carsen, Tim Wang, Michalis Michaelos, e Marius Pachitariu. 2021. «Cellpose: A Generalist Algorithm for Cellular Segmentation». *Nature Methods* 18 (1): 100–106. https://doi.org/10.1038/s41592-020-01018-x.

Sun, Shao-Cong. 2017. «The Non-Canonical NF-κB Pathway in Immunity and Inflammation». *Nature Reviews Immunology* 17 (9): 545–58. https://doi.org/10.1038/nri.2017.52.

Sung, Myong-Hee, Luigi Salvatore, Rossana De Lorenzi, Anindya Indrawan, Manolis Pasparakis, Gordon L. Hager, Marco E. Bianchi, e Alessandra Agresti. 2009. «Sustained Oscillations of NF-κB Produce Distinct Genome Scanning and Gene Expression Profiles». A cura di Gustavo Stolovitzky. *PLoS ONE* 4 (9): e7163. https://doi.org/10.1371/journal.pone.0007163.

Szołtysek, Katarzyna, Patryk Janus, Gracjana Zając, Tomasz Stokowy, Anna Walaszczyk, Wiesława Widłak, Bartosz Wojtaś, et al. 2018. «RRAD, IL4I1, CDKN1A, and SERPINE1 Genes Are Potentially Co-Regulated by NF-κB and P53 Transcription Factors in Cells Exposed to High Doses of Ionizing Radiation». *BMC Genomics* 19 (1): 813. https://doi.org/10.1186/s12864-018-5211-y.

Tak, Paul P., e Gary S. Firestein. 2001. «NF-κB: A Key Role in Inflammatory Diseases». *Journal of Clinical Investigation* 107 (1): 7–11. https://doi.org/10.1172/JCI11830.

Takashima, Yoshiki, Toshiyuki Ohtsuka, Aitor González, Hitoshi Miyachi, e Ryoichiro Kageyama. 2011. «Intronic Delay Is Essential for Oscillatory Expression in the Segmentation Clock». *Proceedings of the National Academy of Sciences* 108 (8): 3300–3305. https://doi.org/10.1073/pnas.1014418108.

Tang, Xiao-Yan, Shanshan Wu, Da Wang, Chu Chu, Yuan Hong, Mengdan Tao, Hao Hu, Min Xu, Xing Guo, e Yan Liu. 2022. «Human Organoids in Basic Research and Clinical Applications». *Signal Transduction and Targeted Therapy* 7 (1): 168. https://doi.org/10.1038/s41392-022-01024-9.

Taniguchi, Koji, e Michael Karin. 2018. «NF-κB, Inflammation, Immunity and Cancer: Coming of Age». *Nature Reviews Immunology* 18 (5): 309–24. https://doi.org/10.1038/nri.2017.142.

Tao, Weikang, e Arnold J. Levine. 1999. «P19 ^{ARF} Stabilizes P53 by Blocking Nucleo-Cytoplasmic Shuttling of Mdm2». *Proceedings of the National Academy of Sciences* 96 (12): 6937–41. https://doi.org/10.1073/pnas.96.12.6937.

Tay, Savaş, Jacob J. Hughey, Timothy K. Lee, Tomasz Lipniacki, Stephen R. Quake, e Markus W. Covert. 2010. «Single-Cell NF-κB Dynamics Reveal Digital Activation and Analogue Information Processing». *Nature* 466 (7303): 267–71. https://doi.org/10.1038/nature09145.

Tergaonkar, Vinay, Matthew Pando, Omid Vafa, Geoffrey Wahl, e Inder Verma. 2002. «P53 Stabilization Is Decreased upon NFκB Activation». *Cancer Cell* 1 (5): 493–503. https://doi.org/10.1016/S1535-6108(02)00068-5.

Tergaonkar, Vinay, e Neil D. Perkins. 2007. «P53 and NF-κB Crosstalk: IKKα Tips the Balance». *Molecular Cell* 26 (2): 158–59. https://doi.org/10.1016/j.molcel.2007.04.006.

Tilstra, Jeremy S, Cheryl L Clauson, Laura J Niedernhofer, e Paul D Robbins. 2011. «NF-□B in Aging and Disease». *Aging and Disease* 2 (6).

Toshiyuki, Miyashita, e John C Reed. 1995. «Tumor Suppressor P53 Is a Direct Transcriptional Activator of the Human Bax Gene». *Cell* 80 (2): 293–99. https://doi.org/10.1016/0092-8674(95)90412-3.

Tunnacliffe, Edward, e Jonathan R. Chubb. 2020. «What Is a Transcriptional Burst?» *Trends in Genetics* 36 (4): 288–97. https://doi.org/10.1016/j.tig.2020.01.003.

Valkenburg, Kenneth C., Amber E. de Groot, e Kenneth J. Pienta. 2018. «Targeting the Tumour Stroma to Improve Cancer Therapy». *Nature Reviews Clinical Oncology* 15 (6): 366–81. https://doi.org/10.1038/s41571-018-0007-1.

Vassilev, Lyubomir T. 2007. «MDM2 Inhibitors for Cancer Therapy». *Trends in Molecular Medicine* 13 (1): 23–31. https://doi.org/10.1016/j.molmed.2006.11.002.

Vassilev, Lyubomir T., Binh T. Vu, Bradford Graves, Daisy Carvajal, Frank Podlaski, Zoran Filipovic, Norman Kong, et al. 2004. «In Vivo Activation of the P53 Pathway by Small-Molecule Antagonists of MDM2». *Science* 303 (5659): 844–48. https://doi.org/10.1126/science.1092472.

Venturelli, Ophelia S., Hana El-Samad, e Richard M. Murray. 2012. «Synergistic Dual Positive Feedback Loops Established by Molecular Sequestration Generate Robust Bimodal Response». *Proceedings of the National Academy of Sciences* 109 (48). https://doi.org/10.1073/pnas.1211902109.

Wagner, Tobias, Nicole Kiweler, Katharina Wolff, Shirley K. Knauer, André Brandl, Peter Hemmerich, Jan-Hermen Dannenberg, Thorsten Heinzel, Günter Schneider, e Oliver H. Krämer. 2015. «Sumoylation of HDAC2 Promotes NF-κB-Dependent Gene Expression». *Oncotarget* 6 (9): 7123–35. https://doi.org/10.18632/oncotarget.3344.

Wang, Nan, Hongwei Liang, e Ke Zen. 2014. «Molecular Mechanisms That Influence the Macrophage M1â€“M2 Polarization Balance». *Frontiers in Immunology* 5 (novembre). https://doi.org/10.3389/fimmu.2014.00614.

Wang, Ping, Hang-Yu Wang, Xing-Jie Gao, Hua-Xia Zhu, Xiao-Peng Zhang, Feng Liu, e Wei Wang. 2023. «Encoding and Decoding of P53 Dynamics in Cellular Response to Stresses». *Cells* 12 (3): 490. https://doi.org/10.3390/cells12030490.

Wang, Yu-Hsiu, Teresa L. F. Ho, Anushya Hariharan, Hui Chin Goh, Yao Liang Wong, Nicole S. Verkaik, May Yin Lee, et al. 2022. «Rapid Recruitment of P53 to DNA Damage Sites Directs DNA Repair Choice and Integrity». *Proceedings of the National Academy of Sciences* 119 (10): e2113233119. https://doi.org/10.1073/pnas.2113233119.

Webster, Gill A., e Neil D. Perkins. 1999. «Transcriptional Cross Talk between NF-κB and P53». *Molecular and Cellular Biology* 19 (5): 3485–95. https://doi.org/10.1128/MCB.19.5.3485.

Weinberg, Richard L., Dmitry B. Veprintsev, Mark Bycroft, e Alan R. Fersht. 2005. «Comparative Binding of P53 to Its Promoter and DNA Recognition Elements». *Journal of Molecular Biology* 348 (3): 589–96. https://doi.org/10.1016/j.jmb.2005.03.014.

Weisz, Lilach, Alexander Damalas, Michalis Liontos, Panagiotis Karakaidos, Giulia Fontemaggi, Revital Maor-Aloni, Marina Kalis, et al. 2007. «Mutant P53 Enhances Nuclear Factor κB Activation by Tumor Necrosis Factor α in Cancer Cells». *Cancer Research* 67 (6): 2396–2401. https://doi.org/10.1158/0008-5472.CAN-06-2425.

Werner, Shannon L., Jeffrey D. Kearns, Victoria Zadorozhnaya, Candace Lynch, Ellen O'Dea, Mark P. Boldin, Averil Ma, David Baltimore, e Alexander Hoffmann. 2008. «Encoding NF-κB Temporal Control in Response to TNF: Distinct Roles for the Negative Regulators IκBα and A20». *Genes & Development* 22 (15): 2093–2101. https://doi.org/10.1101/gad.1680708.

Wu, H., e G. Lozano. 1994. «NF-Kappa B Activation of P53. A Potential Mechanism for Suppressing Cell Growth in Response to Stress.» *Journal of Biological Chemistry* 269 (31): 20067–74. https://doi.org/10.1016/S0021-9258(17)32128-2.

Wu, Xiao, Meng-Yao Wu, Min Jiang, Qiaoming Zhi, Xiaojie Bian, Meng-Dan Xu, Fei-Ran Gong, et al. 2017. «TNF-α Sensitizes Chemotherapy and Radiotherapy against Breast Cancer Cells». *Cancer Cell International* 17 (1): 13. https://doi.org/10.1186/s12935-017-0382-1.

Wu, Zhao-Hui, Yuling Shi, Randal S. Tibbetts, e Shigeki Miyamoto. 2006. «Molecular Linkage Between the Kinase ATM and NF-κB Signaling in Response to Genotoxic Stimuli». *Science* 311 (5764): 1141–46. https://doi.org/10.1126/science.1121513.

Xia, Yifeng, Roanna C. Padre, Tatiana Hurtado De Mendoza, Virginie Bottero, Vinay B. Tergaonkar, e Inder M. Verma. 2009. «Phosphorylation of P53 by IκB Kinase 2 Promotes Its Degradation by β-TrCP». *Proceedings of the National Academy of Sciences* 106 (8): 2629–34. https://doi.org/10.1073/pnas.0812256106.

Xie, Jun, Lichun Zhang, Bodong Liu, Xiao Liang, e Jue Shi. 2022. «Single-Cell Analysis of P53 Transitional Dynamics Unravels Stimulus- and Cell Type-Dependent Signaling Output Motifs». *BMC Biology* 20 (1): 85. https://doi.org/10.1186/s12915-022-01290-7.

Yamashita, Masayuki, e Emmanuelle Passegué. 2019. «TNF-α Coordinates Hematopoietic Stem Cell Survival and Myeloid Regeneration». *Cell Stem Cell* 25 (3): 357-372.e7. https://doi.org/10.1016/j.stem.2019.05.019.

Yang, Nanfei, Tingzhe Sun, e Pingping Shen. 2020. «Deciphering P53 Dynamics and Cell Fate in DNA Damage Response Using Mathematical Modeling». *Genome Instability & Disease* 1 (5): 265–77. https://doi.org/10.1007/s42764-020-00019-6.

Yang, Pei-Ming, Wei-Chien Huang, Yi-Chu Lin, Wen-Yu Huang, Hui-Ann Wu, Wei-Lun Chen, Yu-Fan Chang, et al. 2009. «Loss of IKKβ Activity Increases P53 Stability and P21 Expression Leading to Cell Cycle Arrest and Apoptosis». *Journal of Cellular and Molecular Medicine*, febbraio. https://doi.org/10.1111/j.1582-4934.2009.00712.x.

Yang, Ruizhen, Bo Huang, Yanting Zhu, Yang Li, Feng Liu, e Jue Shi. 2018. «Cell Type–Dependent Bimodal P53 Activation Engenders a Dynamic Mechanism of Chemoresistance». *Science Advances* 4 (12): eaat5077. https://doi.org/10.1126/sciadv.aat5077.

Zajkowicz, Artur, Małgorzata Krześniak, Iwona Matuszczyk, Magdalena Głowala-Kosińska, Dorota Butkiewicz, e Marek Rusin. 2013. «Nutlin-3a, an MDM2 Antagonist and P53 Activator, Helps to Preserve the Replicative Potential of Cancer Cells Treated with a Genotoxic Dose of Resveratrol». *Molecular Biology Reports* 40 (8): 5013–26. https://doi.org/10.1007/s11033-013-2602-7.

Zambrano, Samuel, Marco E. Bianchi, e Alessandra Agresti. 2014. «High-Throughput Analysis of NF-κB Dynamics in Single Cells Reveals Basal Nuclear Localization of NF-κB and Spontaneous Activation of Oscillations». A cura di Michael A. Mancini. *PLoS ONE* 9 (3): e90104. https://doi.org/10.1371/journal.pone.0090104.

Zambrano, Samuel, Ilario De Toma, Arianna Piffer, Marco E Bianchi, e Alessandra Agresti. 2016. «NF-κB Oscillations Translate into Functionally Related Patterns of Gene Expression». *eLife* 5 (gennaio): e09100. https://doi.org/10.7554/eLife.09100.

Zambrano, Samuel, Alessia Loffreda, Elena Carelli, Giacomo Stefanelli, Federica Colombo, Edouard Bertrand, Carlo Tacchetti, et al. 2020. «First Responders Shape a Prompt and Sharp NF-κB-Mediated Transcriptional Response to TNF-α». *iScience* 23 (9): 101529. https://doi.org/10.1016/j.isci.2020.101529.

Zhang, Huidong. 2020. «Mechanisms of Mutagenesis Induced by DNA Lesions: Multiple Factors Affect Mutations in Translesion DNA Synthesis». *Critical Reviews in Biochemistry and Molecular Biology* 55 (3): 219–51. https://doi.org/10.1080/10409238.2020.1768205.

Zhang, Qiuhong, Sanjana Gupta, David L. Schipper, Gabriel J. Kowalczyk, Allison E. Mancini, James R. Faeder, e Robin E.C. Lee. 2017. «NF-κB Dynamics Discriminate between TNF Doses in Single Cells». *Cell Systems* 5 (6): 638-645.e5. https://doi.org/10.1016/j.cels.2017.10.011.

Zhou, Bin-Bing S., e Stephen J. Elledge. 2000. «The DNA Damage Response: Putting Checkpoints in Perspective». *Nature* 408 (6811): 433–39. https://doi.org/10.1038/35044005.

Zhou, Muxiang, Lubing Gu, Ningxi Zhu, William G Woods, e Harry W Findley. 2003. «Transfection of a Dominant-Negative Mutant NF-kB Inhibitor (IkBm) Represses P53-Dependent Apoptosis in Acute Lymphoblastic Leukemia Cells: Interaction of IkBm and P53». *Oncogene* 22 (50): 8137–44. https://doi.org/10.1038/sj.onc.1206911.

Zhu, Haohao, Hui Gao, Yingying Ji, Qin Zhou, Zhiqiang Du, Lin Tian, Ying Jiang, Kun Yao, e Zhenhe Zhou. 2022. «Targeting P53–MDM2 Interaction by Small-Molecule Inhibitors: Learning from MDM2 Inhibitors in Clinical Trials». *Journal of Hematology & Oncology* 15 (1): 91. https://doi.org/10.1186/s13045-022-01314-3.